

Stony Brook University



OFFICIAL COPY

The official electronic file of this thesis or dissertation is maintained by the University Libraries on behalf of The Graduate School at Stony Brook University.

© All Rights Reserved by Author.

**Functional Genomic Identification of Multiple Targets for
Inhibiting Tumor-Promoting Fibroblasts**

A Dissertation Presented

by

Megha Rajaram

to

The Graduate School

in Partial Fulfillment of the

Requirements

for the Degree of

Doctor of Philosophy

in

Genetics

Stony Brook University

May 2012

Stony Brook University
The Graduate School

Megha Rajaram

We, the dissertation committee for the above candidate for the
Doctor of Philosophy degree, hereby recommend
acceptance of this dissertation.

Scott Powers - Dissertation Advisor
Associate Professor, Cold Spring Harbor Laboratory

Howard Crawford - Chairperson of Defense
Associate Professor, Pharmacological Sciences

Mikala Egeblad
Assistant Professor, Cold Spring Harbor Laboratory

Michael Wigler
Professor, Cold Spring Harbor Laboratory

Vivek Mittal
Associate Professor, Weill Cornell Medical College

This dissertation is accepted by the Graduate School

Charles Taber
Interim Dean of the Graduate School

Abstract of the Dissertation

Functional genomic identification of multiple targets for inhibiting tumor-promoting fibroblasts

by

Megha Rajaram

Doctor of Philosophy

in

Genetics

Stony Brook University

2012

There is increasing evidence that cancers develop as aberrant tissues with co-evolving tumor and surrounding non-malignant cells rather than from a single aberrant cell that has undergone multiple genetic alterations. As a result, different cellular components of the tumor mass are involved in a highly complex molecular crosstalk. However, all of the underlying molecular mechanisms of these interactions are not fully identified. Here, I have used genome-wide analysis to identify genes that mediate functional interactions between breast cancer cells and fibroblasts using a model system that allows for both genomic analysis and genetic manipulation of epithelial and stromal compartments. I've established through extensive bioinformatics analysis that this system reflects stromal alterations that occur in human primary breast cancers. RNAi analyses and a co-injection tumorigenicity assay were used to functionally validate genes involved in breast epithelial-stromal fibroblast interactions. I found that the majority of the genes surveyed mediated significant yet diverse roles in promoting cancer *in vivo*. Previous functional analyses have emphasized single genes or single processes as being the key players in tumor-promoting properties of fibroblasts but did not take a systematic genome-wide approach. Our results indicate there are instead multiple genes and processes involved in fibroblast promotion of breast cancer, providing multiple targets for therapeutic inhibition.

Table of Contents

Abstract.....	iii
Table of Contents	iv
List of Figures.....	vi
List of Tables	viii
List of Abbreviations	ix
Acknowledgements.....	xi
Chapter I. Microenvironmental paradigm of cancer progression	1
Introduction	2
History	4
Components of the tumor microenvironment	5
Fibroblasts as components of the microenvironment.....	8
Fibroblasts and their role in cancer	10
Origins of carcinoma-associated fibroblasts	10
Functions of carcinoma-associated fibroblasts	13
Breast cancer and the tumor microenvironment	22
Classification of breast cancers	24
Microenvironmental regulation of breast cancer	25
Molecular mediators of tumor-stromal interactions in breast cancer.....	25
Genomic analysis of tumor-stromal interactions	26
Aims of this study	28
Chapter II. Identification of candidates for functional analysis	30
Introduction	30
Results	33
Discussion	62
Chapter III. Role of fibroblast secreted AREG in breast tumor-stromal fibroblast interactions	66
Introduction	66
Results	70
Discussion	93
Chapter IV. Functional roles of fibroblast secreted CCL2, CCL7and CCL8 in breast tumor-fibroblast interactions.....	97
Introduction	97

Results	102
Discussion	129
Chapter V. Conclusions and future perspectives.....	134
Chapter VI. Materials and methods.....	140
Bibliography	150
Appendix.....	173
Introduction	169
Results	170
Discussion	170
References	173

List of Figures

Figure 1.1	Microenvironment of solid tumors	3
Figure 1.2	Cellular components of breast microenvironment	23
Figure 2.1	Effect of co-injected fibroblasts on JIMT-1 tumorigenicity	35
Figure 2.2	Effect of co-injected fibroblasts on HCC1954 tumorigenicity	36
Figure 2.3	Effect of co-injected fibroblasts on Cal51 tumorigenicity	37
Figure 2.4	Effect of co-injected fibroblasts on Cal51 tumorigenicity	39
Figure 2.5	Incorporation of HFFF2 fibroblasts from Cal51 tumors	43
Figure 2.6	Tumor-promoting activities of co-injected fibroblasts	44
Figure 2.7	Experimental schema to identify candidate genes	48
Figure 2.8	Heatmap of relative expression of the 320 genes in monocultured and co-cultured fibroblasts	49
Figure 2.9	Ligand induction and receptor expression in pro-tumorigenic fibroblasts and breast cancer cells	54
Figure 2.10	320 gene signature distinguishes cancer stroma from normal stroma; expression of candidate genes in primary human cancer stroma.	57
Figure 2.11	Co-culture tumor supporting fibroblast gene expression in human breast cancer	61
Figure 3.1	Representation of gene and protein domains of human AREG	68
Figure 3.2	Amphiregulin is induced in CC-TSF	72
Figure 3.3	shRNA silencing of amphiregulin expression in HFFF2 fibroblasts	73
Figure 3.4	RNAi suppression of amphiregulin restricts pro-tumorigenic effect of tumor-supportive fibroblasts	76
Figure 3.5	Amphiregulin does not cause proliferation <i>in vitro</i> or <i>in vivo</i>	78
Figure 3.6	Amphiregulin silencing causes necrosis	81
Figure 3.7	Amphiregulin silencing in fibroblasts affects phosphorylation of EGFR	82
Figure 3.8	Amphiregulin silencing in fibroblasts does not affect immune cell recruitment	84
Figure 3.9	Amphiregulin silencing in fibroblasts affects recruitment of host fibroblasts	85
Figure 3.10	Amphiregulin upregulates α -SMA expression in tumor-supportive fibroblasts	87
Figure 3.11	Amphiregulin affects migration of fibroblasts (SWHA)	89
Figure 3.12	Amphiregulin affects migration of fibroblasts (BMA)	91
Figure 3.13	Mode of amphiregulin action	96
Figure 4.1	CCL2, CCL7 and CCL8 are induced in membrane separated co-cultures of tumor-supportive fibroblasts and breast cancer cell lines	103
Figure 4.2	shRNAs targeting CCL2, CCL7 and CCL8 efficiently silence expression and are growth neutral	105
Figure 4.3	RNAi suppression of CCL2 restricts protumorigenic ability of tumor-supportive fibroblasts	109

Figure 4.4	RNAi suppression of CCL7 restricts protumorigenic ability of tumor-supportive fibroblasts	111
Figure 4.5	RNAi suppression of CCL8 has a minor effect on the protumorigenic ability of tumor-supportive fibroblasts	113
Figure 4.6	CCL2.CCL7 and CCL8 do not affect proliferation of breast cancer cells <i>in vitro</i>	115
Figure 4.7	In vivo effects of silencing fibroblast secreted CCL2	117
Figure 4.8	In vivo effects of silencing fibroblast produced CCL7 and CCL8	119
Figure 4.9	shRNAs targeting CCR1 efficiently silence expression in breast cancer cells	123
Figure 4.10	CCR1 silencing on breast cancer cells affects tumor growth in the presence of fibroblasts	125
Figure 4.11	Silencing CCR1 on breast cancer cells affects recruitment of immune cells and proliferation	127
Figure A.1:	Fibroblast secreted STC1 does not have a functional role in tumor-promoting ability of tumor-supportive fibroblasts	175

List of Tables

Table 1.1	Cell types in the tumor microenvironment	7
Table 1.2	Factors produced by CAFs	19
Table 2.1	Characteristics of breast cancer cell lines	34
Table 2.2	List of upregulated secreted molecules	52
Table 4.1	Modes of action of CCL2,CCL7,CCL8 and CCR1	133
Table 6.1	A list of primary antibodies used in this study	148
Table 6.2	A list of shRNA targeting sequences used in this study	149

List of commonly used abbreviations

ACVR2A:	Activin A receptor, type IIA
ADAM:	A disintegrin and metalloproteinase domain
ADAMTS:	A disintegrin and metalloproteinase domain with thrombospondin motif
AREG	Amphiregulin
bFGF:	Fibroblast growth factor, basic; FGF2
BDNF:	Brain derived neurotropic factor
BM-hMSC	Bone marrow-derived human mesenchymal stem cells
BMP:	Bone morphogenetic protein
BRCA1:	Breast cancer 1, gene
CAF:	Carcinoma associated fibroblasts
CC-TSF:	Co-culture tumor supporting fibroblasts
CCL:	Chemokine, CC motif, ligand
CCR:	Chemokine, CC motif, receptor
CD31:	Cluster of differentiation 31; PECAM1
COX2:	Cyclooxygenase 2; Prostaglandin-endoperoxide synthase 2
CTGF:	Connective tissue growth factor
CX3C:	Chemokine, CX3C motif
CXC:	Chemokine, CXC motif
CXCL:	Chemokine, CXC motif, ligand
CXCR:	Chemokine, CXC motif, receptor
DCIS:	Ductal carcinoma, <i>in situ</i>
ECM:	Extracellular matrix
EGF:	Epidermal growth factor
EMT:	Epithelial to mesenchyme transition
EMMPRIN:	Extracellular matrix metalloproteinase inducer (CD147)
EnDMT:	Endothelial to mesenchymal transition
ER:	Estrogen receptor
Erb-B2:	see HER2
FACS	Fluorescence-activated cell sorting
FGF:	Fibroblast growth factor
FSP:	Fibroblast specific protein
GEMM:	Genetically engineered mouse models
GFP:	Green fluorescent protein
GM-CSF	Granulocyte-macrophage colony stimulating factor
HB-EGF:	Heparin binding EGF-like growth factor
HER2:	v-ERB-B2 avian erythroblastic leukemia viral oncogene homolog 2
HFFF2:	Human fetal foreskin fibroblast 2
HGF:	Hepatocyte growth factor
hMSC:	human mesenchymal stem cells

ICAM:	Intercellular cell adhesion molecule
IFN- γ :	Interferon-gamma
IGF:	Insulin-like growth factor
IL-1:	Interleukin 1
IL-8:	Interleukin 8
KGF:	Keratinocyte growth factor
LCM:	Laser capture microdissection
Met:	Hepatocyte growth factor; Met protooncogene
MCP-1:	Monocyte chemotactic protein
MMP:	Matrix metalloproteinase
MTT:	3-(4,5-dimethylthiazol-2-yl)-2,5-diphenyltetrazolium bromide
NK:	Natural Killer
NRG:	Neuregulin
NSF:	Non-supportive fibroblasts
p65:	see RelA
PAI1:	Plasminogen activator inhibitor type 1
PDGF:	Platelet derived growth factor
pEGFR:	phosphorylated EGF receptor
PECAM1:	Platelet-endothelial cell adhesion molecule 1
PR:	Progesterone receptor
ps20:	Prostate secreted protein 20
qRT-PCR:	quantitative reverse transcriptase polymerase chain reaction
RANTES:	Regulated upon Activation, Normally T-Expressed, and presumably Secreted; also called CCL5
RelA:	v-Rel avian reticuloendotheliosis viral oncogene A; also called p65
RNAi:	interfering RNA
ROS:	Reactive oxygen species
RSV:	Raus Sarcoma Virus
SDC-1:	Syndecan 1
SDF-1:	Stromal-cell derived factor
SFRP-1:	secreted frizzled-related protein
shAREG:	short hairpin; AREG targeted
shN.T.:	short hairpin; Non-targeting
siRNA:	Short interfering RNA
SMA:	Smooth muscle actin
SPP1:	Secreted phosphoprotein 1; Osteopontin
STC1:	Stanniocalcin 1
TGF- α :	Transforming growth factor alpha
TGF- β :	Transforming growth factor beta
TIMP:	Tissue inhibitor of metalloproteinase

TNF- α : Tumor necrosis factor-alpha
TSF: Tumor supportive fibroblasts

Wnt: Wingless-type MMTV Integration site family
WT-MEF: Wild-type mouse embryonic fibroblasts

VCAM: Vascular cell adhesion molecule
VEGF: Vascular endothelial growth factor

Acknowledgements

There are a lot of people who have made my journey through graduate school an excellent experience and I wish to thank them. My mentor, Scott Powers, is definitely on top of that list. Finding an advisor whose scientific philosophy closely matches a student's is rare. When it does happen, as in my case, learning becomes a truly fun experience. Through the last five years, I have learned a great deal from him and that has shaped the way I think about science. I am really grateful for this opportunity afforded to me and want to thank him from the bottom of my heart.

I also want to thank my committee, including Mikala Egeblad, Howard Crawford, Mike Wigler and Vivek Mittal. Mikala, the resident microenvironment expert at CSHL, offered valuable suggestions and advice on critical aspects of experimental design. Howard Crawford gave guidance and support as the chairperson of the committee. Whereas, Mike Wigler and Vivek Mittal provided encouragement and helpful comments.

The past five years have been fun in part due to the atmosphere in the Powers Lab. The lab has been a second family and provided a support network that is more than I could ever ask for. A special thanks to my lab-sisters Cheryl, Ada and Kate for patiently reading my dissertation and for the countless happy hours at Nissen Sushi. Additionally, I would also like to thank Jinyu Li, whose efforts have made most of the genomic analysis in this study possible, and to former Powers lab members- David Mu and Maia Chanrion.

A large part of this work would not have been possible without the help of the Cold Spring Harbor shared resources community. This includes Lisa Bianco and her team for mouse work, Raya Puzis for the immunohistochemistry and Pam Moody for help with the FACS experiments. I would like to acknowledge the immeasurable support provided by the Genetics Graduate program administrators and directors at Stony Brook University, including Kate Bell, Jerry Thomsen and Turhan Canli.

To my parents, Lalitha and Rajaram have been a wonderful resource for support and love. Without their support I would not be where I am today. They continue to inspire me every single day. To my darling sister, Misha, a biostatistician, who never refused to make a heatmap or explain a statistical test to me. To my grandparents, Natarajan and Sundari, who are full of love and shower me with it. To my aunt and uncle, Uma and Ravi Swami, who provided me a warm, loving home away from home. My parents-in-law Jim and Cheryl, who are my biggest admirers. To Sylvia, for teaching me a thing or two about friendship, and life and to all my friends for making graduate school unforgettable.

Lastly, to my husband Ryan, I couldn't have done this without his love and support. Our life together is an amazing journey that has only just begun!

CHAPTER I

Microenvironmental paradigm of cancer progression

The classical view of tumorigenesis as a cell-autonomous process has been largely supplanted by a model in which cells of the surrounding non-malignant microenvironment cooperate with malignant cells to promote tumor growth (Hu and Polyak, 2008a). Fibroblasts often represent the majority of the stromal cells in carcinomas (Orimo and Weinberg, 2006) and have been shown to promote tumor progression by inducing proliferation, angiogenesis and remodeling of the extracellular matrix (ECM). In some cases, fibroblasts can even mediate resistance to therapy (Allinen et al., 2004; Crawford et al., 2009; Olumi et al., 1999; Orimo et al., 2005). Although several molecules that mediate pro-tumorigenic interactions between tumor cells and stromal fibroblasts have been identified, they have been identified individually in widely different tumor types and model systems. It is still not clear how many functionally important fibroblast-derived pro-tumorigenic factors there are for a given human cancer type such as breast cancer, nor is it exactly clear how to best devise strategies for therapeutic intervention (Ostman and Augsten, 2009).

The three major goals of my thesis project were to (1) develop a model system of fibroblast-breast cancer cell interactions that mimics what occurs in primary breast cancers, (2) determine how many secreted factors are induced in fibroblasts by breast cancer cells, and (3) determine how many of the secreted factors play a role in promoting tumorigenicity. In this chapter, I review the history and current status of tumor microenvironment with a special emphasis on carcinoma associated fibroblasts. In addition, I review the literature for known molecules contributing to breast epithelial-stromal fibroblast interactions focusing on

previous studies that have used genome-wide approaches. Finally, I present the specific aims of the study and the rationale for the experimental design.

Introduction

Understanding the molecular events that drive cancer progression has been a hotbed of cancer research for several decades. Since the discovery of the first oncogene over thirty years ago (Varmus et al., 1975) cancer research has progressed rapidly with significant advances in several areas including the discovery of causative genetic aberrations in human cancer, understanding the signaling pathways that are impinged upon by these genetic aberrations, and in some cases successful development of therapies that target genetic aberrations. However, there are processes we still don't fully understand. One of which being how the surrounding non-malignant cells interact with cancer cells during cancer progression.

Cancer progression was once considered a cell-autonomous process. The prevailing thought was that it depended solely on activation of oncogenes and deletion of tumor suppressor genes in cancer cells. However, this ignored the interactions of cancer cells with their surroundings, which is a feature of any organ or tissue in eukaryotic systems. However it has become clear that tumors aren't just a mass of abnormal cancer cells, but instead an aberrant tissue composed of several different cell types that are in constant communication with each other. The tumor microenvironment is the term that has come to be used most often in the literature to describe this network of cancer cells, the surrounding normal cells, the extracellular matrix (ECM), blood vessels, and the homo and heterotypic interactions between them (Figure 1.1)

Figure 1.1

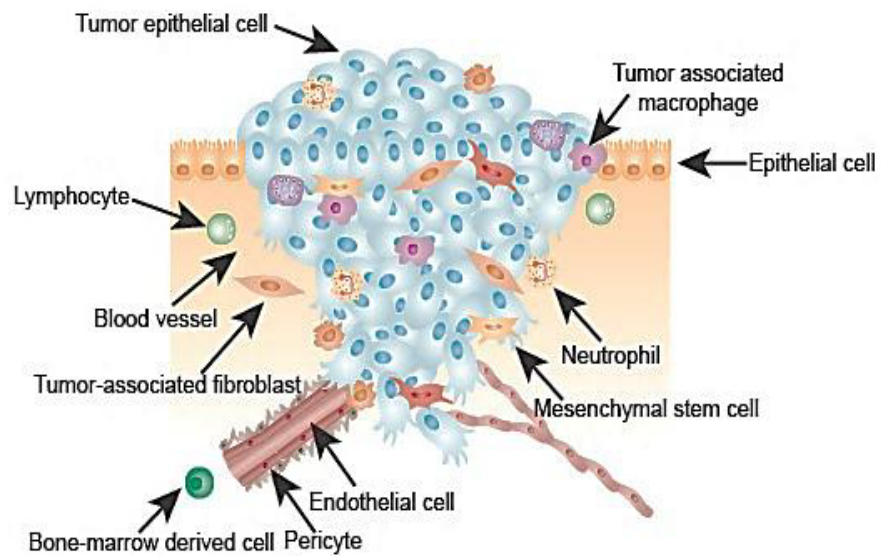


Figure 1.1: Schematic representation of the tumor microenvironment at the primary tumor site of solid cancers such as breast, prostate or lung cancers. The microenvironment is composed of normal and tumor epithelial cells, fibroblasts, vascular cells, immune cells and mesenchymal stem cells. Composition of cell types and proportions varies with a specific cancer type. Adapted from Joyce and Pollard, 2009.

History

The idea that the microenvironment plays an important role in cancer progression dates back to when Stephen Paget proposed his famous “seed and soil hypothesis” in 1889 (Paget, 1889). Paget speculated that cancer cells (the seed) receive critical cues from the microenvironment (the soil) that result in their growth, survival and metastasis.

Pathologists observed the human cancer-associated modification of the stroma relative to normal stroma that was an apparent reaction to the tumor cells in several different types of cancer (Debenzon, 1951; Haller, 1951; Le Melletier et al., 1952; Von Numers, 1953). It is for this reason they termed it “reactive”. Later on, in animal model systems, investigators analyzed the reactive stroma in more detail and found that it had increased proliferation, thickening and number of immune cells (Todorutiu and Simu, 1965).

Subsequently, Dr. Folkman observed that tumors engage endothelial cells in order to form blood vessels to support their rapid growth (Folkman et al., 1971). Extensive research based on this concept has led to the discovery of vascular endothelial growth factor (VEGF) and therapeutic antibodies that neutralize it are used in the clinic today (Ferrara et al., 2004; Kim et al., 1993; Leung et al., 1989).

Mintz and Illmensee in the 1970s demonstrated that the development of tumors can depend on the tissue structures surrounding the tumor cells. Teratocarcinomas injected subcutaneously formed tumors, but mouse blastocysts injected with teratocarcinoma cells did not. Surprisingly, in the latter case the injected blastocysts could result in the birth of seemingly “normal” mice. Moreover, the injected cancer cells even contributed to “normal” organ structures (Mintz and Illmensee, 1975). This ground-breaking work inspired Dr. Bissell and her colleagues to perform experiments that conclusively established the role of the microenvironment in tumor progression.

Dr. Bissell's group showed that the ability of the Rous Sarcoma Virus (RSV) to transform cells was context dependent. In these experiments, they injected RSV into 4-day-old embryos and no tumors were produced despite the expression of active v-src throughout the embryo. In contrast, the virus was able to transform cells under cell culture conditions (Dolberg and Bissell, 1984). The development of tumors was clearly context dependent but what were the conditions that made it possible for the tumors to grow and what were the circumstances under which tumors were inhibited? Subsequently, it was established that several microenvironmental processes influenced the development of tumors. For example, wounding was shown to be important to this process (Dolberg et al., 1985). The identification of specific genes followed, with TGF- β being the first (Sieweke et al., 1990) and soluble cytokines and extracellular matrix components followed (reviewed in (Bissell and Hines, 2011)).

Components of the tumor microenvironment

In order to study the interactions between tumor cells and components of the microenvironment, it was first necessary to define the composition of the microenvironment. Most solid epithelial tumors such as breast, pancreatic, prostate and lung have highly complex microenvironments composed of several types of stromal cells and the ECM.

The ECM consists of a complex network of protein based structures providing a structural framework for tumor growth. It also provides signals that contribute to its growth and metastasis. Major components of the ECM are proteoglycans, hyaluronic acid, collagen, fibronectin and laminin (Egeblad et al., 2010). The basement membrane is an ECM structure which in normal tissues serves as a barrier between the epithelial cells and the stroma. Cells of the epithelium and stroma receive structural as well as biochemical cues from the ECM (Lu et al., 2012). Stromal cells include mesenchymal cells, cells of the vasculature and

immune cells. Mesenchymal cells are composed of fibroblasts, myofibroblasts, adipocytes and mesenchymal stem cells.

The cells of the vasculature are composed of endothelial cells and surrounding pericytes (Fakhrejahani and Toi, 2012; Folkman et al., 1971). Immune cells of the tumor microenvironment are the most diverse group of cells and perform both tumor-promoting and tumor-inhibiting activities. Immune cells include those from the innate immune system such as myeloid cells as well as lymphocytes from the adaptive immune system. Immune cells of either type can promote or inhibit tumorigenicity. In general, tumor-promoting cells can include helper T-cells, regulatory T cells, B cells, myeloid-derived suppressor cells, M2 macrophages, N2 neutrophils, platelets and mast cells. Inhibitory cells include dendritic cells, N1 neutrophils, M1 macrophages, and cytotoxic T-cells (Egeblad et al., 2010; Hanahan and Coussens, 2012). Table 1.1 lists the most prominent components of tumor microenvironments along with their effects on tumor progression.

Table 1.1: Prominent cell types in the tumor microenvironment with effects on tumor progression (Adapted from Egeblad et al, 2010)

Cell type	Tumor promoting?	Functions affected
Non-vascular, non-immune		
Normal epithelial cells	No	growth
Myoepithelial cells	No	invasion, growth
Fibroblasts	Yes	growth, invasion,
		migration, angiogenesis
Mesenchymal stem cells	Yes	growth, metastasis
Adipocytes	Yes	growth, survival, angiogenesis
Vascular		
Endothelial cells	Yes	angiogenesis
Perivascular cells	Yes	angiogenesis
	No	metastasis
Bone marrow-derived cells	Yes	growth, angiogenesis, invasion
Immune		
Dendritic cells	No	antitumor-immunity
Myeloid derived suppressor and immature myeloid cells	Yes	metastasis, angiogenesis
		reduce antitumor immunity
Macrophages, M1-like	No	
Macrophages, M2-like	Yes	invasion, angiogenesis
Mast cells	Yes	angiogenesis
Neutrophils, N1	No	increase antitumor immunity
Neutrophils, N2	Yes	angiogenesis,
		reduce antitumor immunity
T cells, CD4+, T helper 2	Yes	metastasis
T cells, CD8+, cytotoxic	No	kill tumor cells
T cells, CD4+CD25+	Yes	reduce antitumor immunity
T cells, gamma/delta	No	increase antitumor immunity
T cells, Th17	Yes	angiogenesis, growth
	No	increase antitumor immunity
B cells	Yes	reduce antitumor immunity
B cells, Immunoglobulins	Yes	inflammation
Platelets	Yes	metastasis

Fibroblasts as components of the microenvironment

Fibroblasts are cells of mesenchymal origin and were first described as components of connective tissues in the late 19th century (Mueller and Fusenig, 2004; Tarin and Croft, 1969). Fibroblasts secrete structural components of the ECM such as collagens, fibronectin and laminin. Fibroblasts are key players in ECM remodeling through their ability to secrete matrix-metalloproteinases (MMPs) under normal physiological conditions, and also during cancer progression (Kalluri and Zeisberg, 2006). Fibroblasts also induce epithelial cell differentiation in the mammary tissue (Kuperwasser et al., 2004).

The tumor microenvironment resembles wounding. Wounding involves immune cells, blood vessels, epithelial cells and fibroblasts. Upon wounding, fibroblasts receive molecular cues from the injured tissue or surrounding immune cells and begin to migrate and secrete growth factors (Steffensen et al., 2001). Though molecular events leading to this activation of fibroblasts in this situation are not fully understood, some molecules have been identified. Fibroblast growth factor-2 (FGF-2) and transforming growth factor- β 2 (TGF- β 2) are the best studied stimuli and are thought to originate in the injured epithelium (Kalluri and Zeisberg, 2006). Immune cell derived proteins like cell adhesion molecules ICAM1 and VCAM1 or reactive oxygen species (ROS) also play roles in fibroblast activation (Sanz-Moreno et al., 2008; Zeisberg et al., 2000). Activated fibroblasts appear more elongated, more contractile, have a large nucleus and a prominent Golgi apparatus (Simian et al., 2001) compared to non-activated fibroblasts.

While all cells of the fibroblastic lineage express vimentin and fibroblast specific protein-1 (FSP-1), only activated fibroblasts express α -smooth muscle actin (α -SMA) (Kalluri and Zeisberg, 2006). Activated fibroblasts produce higher levels of growth factors, cytokines and matrix-metalloproteinases compared to normal resident fibroblasts. For example, they produce higher levels of hepatocyte growth factor (HGF), insulin-like growth

factor-1 (IGF-1) and epidermal growth factor (EGF) family members, interleukin-1 (IL-1) and monocyte chemoattractant protein-1 (MCP-1/CCL2) (Bhowmick et al., 2004; Strieter et al., 1989) and MMP2 , MMP3 and MMP9 (Sternlicht et al., 1999). Growth factors cause proliferation of epithelial cells (Ankrapp and Bevan, 1993; Panos et al., 1993), cytokines modulate immune responses by recruiting inflammatory cells (Qian et al., 2011b) and matrix metalloproteinases mediate invasion and remodeling of the ECM (Sternlicht et al., 1999).

Fibroblasts and their role in cancer

Fibroblasts within tumors have an elongated appearance, produce more collagen and proliferate faster than their counterparts from normal tissues (Tlsty and Hein, 2001).

Carcinoma associated fibroblasts (CAFs) are largely responsible for the hardening of the tissue that accompanies cancer progression known as desmoplasia (Tlsty and Hein, 2001).

More direct evidence that stromal fibroblasts play a functional role in cancer comes from reports that co-injection of human tumor cells with human fibroblasts can accelerate tumor growth (Camps et al., 1990; Noel et al., 1993). Subsequent reports showed that carcinoma associated fibroblasts are more potent accelerators than fibroblasts derived from normal tissue (Olumi et al., 1999; Orimo et al., 2005).

Origins of carcinoma associated fibroblasts

The sources and origin of CAFs is a subject of intense debate. This is partly because unlike other stromal cells, CAFs don't have well-defined cellular markers. CAFs are commonly identified by α -SMA expression (Kalluri and Zeisberg, 2006) but recent studies have identified subsets of CAFs that don't express α -SMA (Erez et al., 2010; Rudnick et al., 2011) making it complicated to identify them accurately. Moreover, studies show that there may be several parental cells that give rise to CAFs making them heterogeneous in origin.

The most common hypothesis of CAF origin is that they arise through activation of normal fibroblasts of the resident tissue (Ronnov-Jessen et al., 1992). Mouse models and other experimental approaches have backed up this hypothesis (Kojima et al., 2010; Mueller et al., 2007). Subsequent studies have shown that cancer cells "train" the resident fibroblasts of the host tissue to become CAF-like through the secretion of cytokines like TGF- β and IL-1 β (Erez et al., 2010; Kojima et al., 2010).

Another hypothesis is that CAFs are generated through cancer cells undergoing epithelial to mesenchymal Transition (EMT). This is based on the observation that cells isolated from breast tumors that epithelial markers but otherwise behave like fibroblasts (Petersen et al., 2003). A related concept, endothelial to mesenchymal transition (EnDMT) has been described as a source for CAFs in spontaneous models of pancreatic cancer and melanoma (Zeisberg et al., 2007).

Yet another hypothesis is that CAF-like precursor cells might reside in normal tissues and predispose the patient to develop invasive lesions (Schor et al., 1994). This is distinct from cancer cells “training” resident fibroblasts in that cells with CAF-like properties are present in tissues even before cancers develop. Another speculation is that stroma-specific mutations arise in fibroblasts to give rise to CAFs (Kurose et al., 2002; Moinfar et al., 2000). Recent studies have argued against this theory due to lack of mutations in the stromal compartment (Campbell et al., 2009 ;Hosein et al., 2010). Lastly, differentiation of bone marrow derived human mesenchymal stem cells (BM-hMSCs) has been suggested as a source for CAFs. In a study by Mishra and colleagues, conditioned medium from epithelial carcinoma cells led to the differentiation of hMSCs into CAFs *in vitro*. CAFs were identified by increased expression of CAF markers such as SDF-1/CXCL12 (Mishra et al., 2008). In a mouse model of inflammatory gastric cancer, the authors used lineage tracing to show that roughly 20% CAFs in the tumor were bone marrow derived (Quante et al., 2011).

It is possible that some or all these theories are true depending on the stage or type of cancer studied. In the only study that has used lineage tracing to establish the origin of CAFs, ~20% CAFs were bone-marrow derived (Quante et al., 2011). Based on this, in my opinion, there are likely to be multiple cells of origins for CAFs. Also, it is unlikely that there is a mutational origin of CAFs since certain studies have identified stromal-specific mutations, but many others have failed to do so. In fact, groups have shown that mutations detected in

the stroma can be caused by poor experimental technique (Campbell et al., 2009a). Also it is becoming increasingly clear that CAFs are modified epigenetically to perform cancer-associated functions and thus there is no theoretical need to hypothesize mutations (Allinen et al., 2004; Hu et al., 2005).

Whatever the source and mode of activation, CAFs appear to promote tumor progression through increased proliferation, angiogenesis, remodeling the ECM, mediating inflammation, invasion, and migration. Understanding the molecular mediators of these functions is key to restricting the ability of CAFs to promote tumorigenicity. Roles of some important CAF secreted mediators are discussed in the following section.

Functions of carcinoma-associated fibroblasts

CAFs mediate proliferation

CAFs can mediate proliferation of cancer cells in the microenvironment through direct or indirect routes. In direct stimulation, CAFs secrete growth factors or cytokines that act through specific receptors expressed on the tumor cells. Alternately, indirect stimulation is mediated by an intermediate molecule or by affecting the ECM.

The direct route certainly appears to be the case for many growth factors produced by CAFs. For example, in a model of lung cancer, co-injected fibroblasts secrete the ligand for the c-Met receptor, HGF (hepatocyte growth factor) and activate Met signaling in the adjacent carcinoma cells (Cheng et al., 2007). Similarly, EGF and PDGF produced by stromal fibroblasts stimulate the proliferation of cervical cancer cells in a co-culture model. When a chemical inhibitor to PDGF is used, this effect is abrogated (Murata et al., 2011). Another EGF family member, neuregulin (NRG) is secreted by stromal fibroblasts in pancreatic cancer model and stimulates the proliferation of epithelial cells (Liles et al., 2011). CAFs that secrete Wnt2 and keratinocyte growth factor (KGF) have pro-proliferative roles in oral squamous cell carcinomas (Fu et al., 2011; Lin et al., 2011). In prostate cancers, secreted frizzled-related protein 1 (SFRP1) is often overexpressed in the stroma during tumor progression. Treatment of prostate cancer cell lines with SFRP1 led to increased proliferation (Joesting et al., 2005). Similar roles have been attributed to stromal derived factor 1 (SDF-1/CXCL12) and syndecan-1 (a trans-membrane heparan sulfate proteoglycan) production in mammary stromal fibroblasts (Maeda et al., 2006; Orimo et al., 2005). Senescent stroma is associated with cancer progression and the secretion of osteopontin (SPP1; secreted phosphoprotein 1) by senescent fibroblasts promotes proliferation of squamous carcinoma cells (Luo et al., 2011).

Fibroblasts can also promote proliferation of cancer cells through indirect routes. Stromal fibroblast secreted TGF- β stimulates the growth of the breast epithelium. It appears to act in an autocrine fashion to induce additional growth hormones and cytokines that have pro-proliferative properties (Bhowmick et al., 2004; Kuperwasser et al., 2004). Similarly, PDGF (produced by epithelia or stromal fibroblasts) upregulates FGF7 secretion in stromal fibroblasts which acts as an epithelial mitogen (Pietras et al., 2008). MMPs secreted by stromal fibroblasts release growth factors from the ECM indirectly stimulating proliferation (Egeblad and Werb, 2002).

CAFs promote angiogenesis

Angiogenesis or neo-vascularization is the process by which blood vessels are formed at the tumor site. Observations that the presence of CAFs in the stroma was accompanied by heavy vascularization were made as early as 1979 (Seemayer et al., 1979). CAFs mediate angiogenesis by secreting pro-angiogenic molecules or indirectly through MMPs that have pro-angiogenic functions (Nyberg et al., 2008).

CAFs directly control the migration and recruitment of endothelial cells and pericytes, promote their survival and prevent apoptosis by producing growth factors and cytokines (Schmid et al., 2007; Velazquez et al., 2002). Vascular Endothelial Growth Factor A (VEGFA), produced by stromal fibroblasts induces vascular permeability and attracts endothelial cells to the site of the tumor to promote angiogenesis (Fukumura et al., 1998). Similarly, FGF2 promotes neovascularization in a mouse model of cervical carcinoma (Pietras et al., 2008). Another molecule, fibroblast specific protein (FSP1/S100A4/mts1), promotes angiogenesis by binding to annexin II on endothelial cells (Nakamura et al., 1997; Semov et al., 2005). Dr. Weinberg's group showed that SDF-1 α promotes angiogenesis by recruiting endothelial progenitor cells to the breast tumor site (Orimo et al., 2005).

Subsequently, several studies made similar observations that SDF-1 α promotes angiogenesis in oral, pancreatic and prostate cancers by recruiting endothelial cells (Begley et al., 2005; Daly et al., 2008; Matsuo et al., 2009; Menon et al., 2007).

CAF secreted molecules can mediate angiogenesis indirectly by autocrine mechanisms. For example, fibroblast secreted IL-1 β causes autocrine production of VEGF, CXCL2 and HGF that promote angiogenesis in the Lewis lung carcinoma mouse model (Saijo et al., 2002). Similarly, fibroblast secreted TGF β causes autocrine production of chemokines CXCL1, 2 and 5 that are pro-angiogenic (Ijichi et al., 2011).

CAFs also control angiogenesis indirectly by secreting matrix-metalloproteinases (MMPs). MMPs release pro-angiogenic molecules sequestered in the ECM. The glycosaminoglycans of the ECM are large reservoirs of pro-angiogenic molecules like VEGF, β FGF and TGF β (Nyberg et al., 2008). MMP13 promotes angiogenesis in mouse models of melanoma and squamous cell carcinoma (Lederle et al., 2010; Zigrino et al., 2009).

CAF-produced angiogenic molecules are not limited to soluble factors. A cell-surface bound proteoglycan Syndecan1 has proangiogenic activities in xenograft models of breast cancer cell lines. CAFs produce increased amounts of ECM components like collagens, fibronectins and laminins compared to normal resident fibroblasts. Each of these components have direct proangiogenic roles (Sottile, 2004).

CAFs remodel the ECM

The ECM is remodeled extensively throughout cancer progression. One of the main reasons to remodel the ECM is to release pro-tumor growth factors and pro-angiogenic molecules sequestered within the ECM. Another important reason is to facilitate the invasion of the tumor mass into the surrounding tissue, which will increase blood supply, nutrients and

oxygen. CAFs produce increased amounts of collagens, laminins and fibronectins (Egeblad et al., 2005).

The most common proteases that remodel the ECM are from three families: matrix-metalloproteinases (MMPs), A disintegrin and metalloproteinase family members (ADAMs) and A disintegrin and metalloproteinase with thrombospondin motif family members ADAMTS (Overall and Kleinfeld, 2006). Fibroblasts mostly mediate their roles through MMPs (Overall and Kleinfeld, 2006). CAFs express increased amounts of MMP 1, 2,3,9,11,13 and 14 (Ala-aho and Kahari, 2005; Basset et al., 1990; Bisson et al., 2003; Sternlicht et al., 1999). Fibroblasts can be stimulated by a variety of growth factors and cytokines to produce MMPs (Overall and Kleinfeld, 2006). These factors are probably produced by the tumor cells in order to stimulate the neighboring fibroblasts. Fibroblasts that lack the expression of MMP11 or MMP-14 don't support tumor progression (Masson et al., 1998; Zhang et al., 2006). When inhibitors of MMP11 such as TIMP2 are overexpressed, the growth promoting effects of fibroblasts are abrogated (Noel et al., 1998). However, not all fibroblast produced MMPs have functional roles: CAF derived MMP13 does not influence tumor progression in a mouse model of breast carcinoma although it affects fibrillar collagen in the stroma (Nielsen et al., 2008).

CAFs mediate inflammation

Although the role of inflammation in cancer has long been established (Coussens and Werb, 2002), it was thought to be mediated by immune cells such as macrophages, B and T lymphocytes and dendritic cells (Condeelis and Pollard, 2006; de Visser et al., 2005).

It was first suggested that fibroblasts mediate inflammation because they produce vast amounts of inflammatory chemokines (Smith and Hale, 1997). Chemokines recruit pro-inflammatory leukocytes to the tumor site. Recently, Erez and colleagues suggested that

when fibroblasts are activated in a model of squamous cell carcinoma they mediate inflammation by NF- κ b mediated upregulation of several proinflammatory cytokines (Erez et al., 2010). In another mouse model of breast cancer, selective ablation of TGF β receptor in fibroblasts results in inflammation mediated by CCL2 (Hembruff et al., 2010).

CAFs promote invasion, migration and metastasis

Invasion and migration are central to tumor growth and metastasis. Invasion occurs by breaching of the basement membrane and invasion of cells into the surrounding tissue. The majority of the action is brought about by MMPs produced by the fibroblasts that actively remodel the ECM and help the tumor cells invade into the surrounding stroma (Shimoda et al., 2010). Secreted molecules produced by CAFs can also help promote metastasis. For example, chemokine CCL5 produced by the fibroblast-like mesenchymal stem cells can promote metastasis of breast cancer cells to the lungs (Karnoub et al., 2007).

Epithelial to Mesenchymal transition (EMT) is a process central to metastasis (Kalluri and Weinberg, 2009). EMT was thought to be solely mediated by genetic and epigenetic changes in cancer cells but new evidence suggests that stromal cells also contribute to cancer cell EMT (Shimoda et al, 2010). Stromal secretion of TGF β induces EMT in cancer cells to facilitate invasion and metastasis (Bierie and Moses, 2009). Similarly, fibroblast-secreted Wnt2, COX-2, brain derived neurotropic factor (BDNF) and HGF are responsible for the induction of EMT in models of prostate, oral, lingual and squamous cell carcinomas (Fu et al, 2011(De Wever et al., 2004; Dudas et al., 2011; Grugan et al., 2010; Patel et al., 2012).

In addition to cancer cells, fibroblasts also promote migration of other cell types into the tumor. For example, fibroblast-secreted CXCL12 recruits endothelial progenitor cells (Orimo et al, 2005) and fibroblast-secreted CCL2 increases migration of monocytes into tumor spheroids (Ksiazkiewicz et al., 2010).

A comprehensive list of factors produced by carcinoma associated fibroblasts and their associated functions in tumor progression are listed in Table 1.2.

Table 1.2: List of factors produced by carcinoma-associated fibroblasts and their roles in tumor progression

Function	Gene	Symbol	Cancer type	Model	Reference
Proliferation	Hepatocyte growth factor	HGF	Breast	co-xenograft	Cheng et al, 2007
	Heparin binding EGF-like growth factor	HB-EGF	Cervical	co-culture	Murata et al, 2011
	Platelet derived growth factor	PDGF	Cervical	co-culture	Murata et al, 2011
			Cervical	transgenic	Pietras et al, 2008
	Fibroblast growth factor-7	FGF-7	Cervical	transgenic	Pietras et al, 2008
	Neuregulin	NRG	Pancreatic	co-xenograft co-culture	Liles et al, 2011
	Wingless-type MMTV integration site family member 2	Wnt2	Oral Squamous cell	co-culture	Fu et al, 2011
	Keratinocyte growth factor	KGF	Oral squamous cell	co-culture	Lin et al, 2011
	Secreted frizzled-related protein 1	SFRP-1	Prostate	co-culture	Joesting et al,2005
	Stromal-derived factor-1	SDF1/CXCL12	Breast	co-xenograft co-culture	Orimo et al, 2005
	Transforming growth factor-beta	TGF- β	Breast	humanized mouse	Kuperwaser et al, 2004

Table 1.2 (Continued)

Function	Gene name	Symbol	Cancer type	Model	Reference
Angiogenesis	Matrix-metalloproteinase 13	MMP13	Melanoma	co-culture	Lederle et al, 2010
			Squamous cell	co-culture	Zigrino et al, 2009
	Syndecan-1	SDC-1	Breast	co-xenograft	Maeda et al, 2006
	Vascular endothelial growth	VEGFA	various	transgenic	Fukumura et al, 1998
	Fibroblast specific protein-1	FSP-1		cell culture	Semov et al, 2005
	Interleukin -1 beta	IL-1 β	Lung	cell culture	Saijo et al, 2002
	CXC Chemokine 2	CXCL2	Lung	cell culture	
	Hepatocyte growth factor	HGF	Lung	cell culture	
	Prostate secreted protein 20	ps20	Prostate	co-xenograft	McAlhany et al, 2003
	Connective tissue growth factor	CTGF	Pancreatic	transgenic	Ijichi et al, 2011
			Prostate	co-xenograft	Yang et al, 2005
	Stromal-derived factor-1	SDF-1/CXCL12	Breast	co-xenograft	Orimo et al, 2005
				co-culture	
			Oral Squamous	co-culture	Daly et al, 2008
			Pancreatic	co-culture	Matsuo et al, 2009
		Prostate	co-culture	Begley et al, 2005	
	Fibroblast growth factor-2	FGF-2	Cervical	transgenic	Pietras et al, 2008
ECM remodeling	Matrix-metalloproteinase 1,2,3,9,11,13,14	MMP1,2,3,9,11,13,14	various	various	Ala-aho et al, 2005
					Basset et al, 1990
					Bisson et al, 2003
					Masson et al, 1998

Table 1.2 (Continued)

Function	Gene name	Symbol	Cancer type	Model	Reference
Inflammation	p65/RelA	NF-kB	Squamous cell	transgenic	Erez et al,2010
	Monocyte chemotactic factor-1	MCP-1/CCL2	Breast	transgenic	Hembruff et al,2010
	Cyclooxygenase-2	COX-2	Breast	co-xenograft	Hu et al, 2008
Invasion, migration and metastasis	RANTES	CCL5	Breast	co-xenograft	Karnoub et al, 2005
	Transforming growth factor-beta	TGF-b	various	various	Shimoda et al, 2010
	Wingless-type MMTV integration site family member 2	Wnt2	Oral Squamous cell	co-culture	Fu et al, 2011
	Cyclooxygenase-2	COX-2	Prostate	co-culture	Giannoni et al,2011
	Brain derived neurotropic factor	BDNF	Lingual	co-culture	Dudas et al, 2011
	Hepatocyte growth factor	HGF	Esophageal	co-culture	Grugan et al, 2010
			Colon	co-culture	De Wever et al, 2004
	Stromal derived factor-1	SDF-1/CXCL12	Breast	co-xenograft	Orimo et al, 2005
	Monocyte chemotactic protein-1	MCP-1/CCL2	Breast	co-culture	Ksiazkiewicz et al,
Monocyte chemotactic protein-3	MCP-3/CCL7	Oral Squamous	co-culture	Jung et al, 2010	

Breast cancer and the tumor microenvironment

Breast cancer is the second most common form of cancer in women and caused nearly half a million deaths worldwide in 2011. Despite early detection and the targeted therapies that block estrogen or Erb-B2/HER2 signaling, it remains the second most lethal form of cancer for women in the United States (American Cancer Society, 2012). Breast cancer is a heterogeneous disease with diverse pathologies and clinical outcomes and it is for this reason that it cannot be regarded as a single disease. This heterogeneity has complicated efforts to design effective therapies (Simpson et al., 2005).

The mammary gland has an ectodermal origin and is composed of several cell types that coordinate signaling to ensure normal functioning. The milk ducts are composed of two layers of cells: the outer basal myoepithelial layer that produces the extracellular matrix and the inner luminal epithelial layer that produces milk. The surrounding normal tissue is composed of fat cells, fibroblasts, blood vessels, leukocytes (Polyak and Kalluri, 2010). Figure 1.2.A shows cellular components in the normal breast.

It is generally agreed that breast cancer arises due to genetic and epigenetic changes in the normal breast epithelial cells (Polyak and Kalluri, 2010). Breast cancer has been the subject of intense studies in order to identify oncogenes, tumor suppressor genes and genomic instability genes that are causal in nature (Hicks et al., 2006).

Figure 1.2

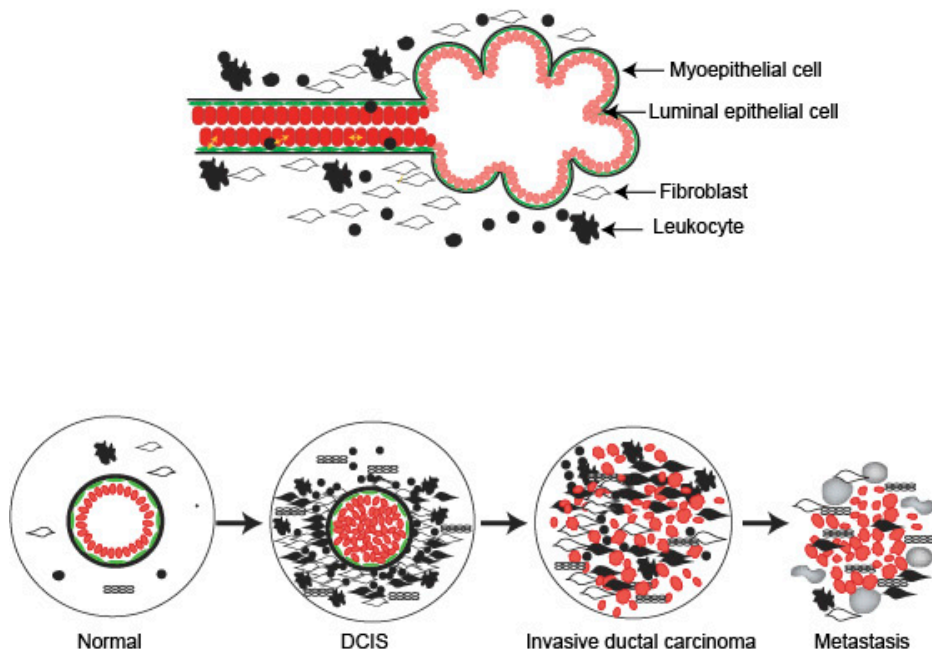


Figure 1.2.A: Cellular components of the normal breast comprising of luminal epithelial cells, myoepithelial cells, fibroblasts and leukocytes. Adapted from Polyak and Kalluri, 2010

Figure 1.2.B: Microenvironmental changes occurring breast cancer progression. Cellular composition in normal, ductal carcinoma in-situ, invasive ductal carcinoma and metastasis. Adapted from Polyak and Kalluri, 2010.

Classification of breast cancers

Clinical classification of breast cancer is based on age, lymph node status, tumor grade, estrogen response and ErbB2 oncogene status (Peppercorn et al., 2008). In addition, molecular profiling is used to classify breast cancers into four major distinct subtypes that correlate with clinical prognosis (Perou et al., 2000; Sorlie et al., 2001; Sorlie et al., 2003). The first two groups, Luminal A and B subtypes, are thought to arise from the luminal cells lining mammary ducts. Luminal A tumors are the most commonly occurring subtype and are usually positive for estrogen receptor (ER), progesterone receptor (PR) and are negative for the Her2 oncogene. Luminal A tumors are low grade and usually respond to hormone therapy but are unresponsive to chemotherapy. Luminal B tumors are often high grade tumors and are more proliferative compared to Luminal A. They are also ER and PR positive and may have amplified HER2 oncogene. The third group, HER2 tumor group, are high grade and generally ER/PR negative, and have amplified HER2 oncogene. Tumors of this subtype (~15% of total) are highly responsive to antibodies that block the HER2 receptor (Slamon et al., 1989). The fourth subtype, basal-like tumors are so called because they are thought to arise from the basal cells lining the mammary ducts. A subset of basal tumors are triple negative (ER,PR and Her2) and very proliferative and of poor grade. Basal-like tumors respond to chemotherapy but have a high rate of recurrence.

Microenvironmental regulation of breast cancer

The idea that the microenvironment could influence the development of breast cancer came from pathologists who noticed dramatic changes in the stroma accompanying tumor formation (reviewed in Hu and Polyak, 2008b). Early studies showed that normal mammary microenvironment could revert the tumor phenotype of breast cancer cells (DeCosse et al., 1975). This suggested that the microenvironment has to be modulated along with the cancer cells to achieve tumor progression. This view is supported by observations that microenvironmental composition varies drastically between different stages of cancer. Stromal cells such as leukocytes, fibroblasts and endothelial cells are dramatically increased in advanced stages whereas myoepithelial cells are decreased (Polyak and Kalluri, 2010). The tumor promoting stromal cells modulate initiation, maintenance and metastasis (Hu and Polyak, 2008b; Karnoub et al., 2007; Trimboli et al., 2009). A schema of the microenvironmental changes that occur during the various stages of breast cancer is shown in Figure 1.2.B.

Molecular mediators of tumor-stromal interactions in breast cancer

Our understanding of genes and pathways mediating interactions between stromal cells and breast epithelial cells is far from complete (Polyak and Kalluri, 2010). Early attempts to characterize the breast microenvironment relied upon analysis of stromal expression patterns of candidate genes. For example, invasion related MMPs (Bisson et al., 2003) and growth factors (Vrana et al., 1996) showed elevated expression in the stromal compartment and correlated with poor prognosis.

Subsequent roles for genes in the breast microenvironment were identified largely based on their previously known functions. It was found that cell adhesion genes played a crucial role

in the microenvironmental control of breast cancer (Weaver et al., 1997; Zutter et al., 1995). Growth factors and cytokines such as TGF β , HGF, CXCL12, CXCL14, and CCL2 modulate the breast microenvironment by controlling proliferation, migration, invasion and metastasis (Allinen et al., 2004; Bierie and Moses, 2009; Cheng et al., 2007; Condeelis and Pollard, 2006; Coussens and Werb, 2002). The role of chemokines in the microenvironment is detailed in Chapter IV.

Although numerous genes have been implicated in the breast microenvironment, their characterization has been somewhat ad hoc. It is very important to study the interactions in the breast microenvironment systematically in order to gain better understanding of the microenvironmental influence on breast cancer.

Genomic analysis of tumor stromal interactions

A genomic approach provides a broad-based, unbiased and systematic way to address questions in biological systems. One of the greatest advantages of using a genome-wide system over candidate-gene based approaches is that we can study how hundreds or thousands coordinate their functions to achieve biological endpoints.

It is clear that communication between the tumor and the non-malignant stroma dictates cancer progression. However, there have been only a small number of studies to date identifying functional interactions between different components of the microenvironment. The first comprehensive genomic study was done by Kornelia Polyak's group in 2004 (Allinen et al., 2004). Components of the breast tumor microenvironment were separated using cell-surface antigens and analyzed by comparative expression profiling using normal, DCIS and invasive breast cancer patient samples. This study was systematic in identifying overexpressed genes in

specific compartments. It identified that stromal secreted chemokines CXCL12 (by myofibroblasts) and CXCL14 (by myoepithelial cells) mediated proliferation, invasion and migration of the breast epithelial cells.

Co-culture based genome-wide studies have also provided insights into features of tumor-stromal interactions. Buess and colleagues observed that fibroblasts co-cultured with breast cancer cells overexpress interferon related genes. A signature derived from the overexpressed genes predicted poor survival and metastasis in breast cancer patients (Buess et al., 2007).

Recent studies have made use of laser capture microdissection (LCM) to perform gene expression profiling of tumor epithelial and stromal compartments separately (Casey et al., 2009; Finak et al., 2008; Ma et al., 2009). LCM is a technique in which a microscopic region of interest can be isolated from a tissue sample using a laser to guide dissection. A McGill University LCM-study identified 163-genes that were most differentially expressed in invasive breast stroma compared to normal stroma. From this, they derived a 26-gene signature that predicted poor prognosis in breast cancer patients. It was the first study in which a gene signature derived from stroma was an independent predictor of poor outcome in breast cancer patients (Finak et al., 2008). Interestingly, stromal gene signatures were also shown to predict resistance to adjuvant chemotherapy in breast cancer patients (Farmer et al., 2009).

Gene expression changes in intermediate stages of cancer can provide clues into underlying processes important in breast cancer progression. Ma and colleagues collected normal adjacent tissue, ductal carcinoma *in situ* (DCIS) tissue and invasive breast cancer tissue from the same patient and profiled the epithelial and stromal compartments from each stage separately. The authors noted widespread changes between normal and DCIS but not between DCIS and invasive stages (Ma et al., 2009) in both stromal and epithelial compartments.

Gene expression profiling of carcinoma associated fibroblasts and normal resident fibroblasts has provided insights into differentially expressed genes in the fibroblast compartment of the tumor microenvironment (Bauer et al., 2010; Santos et al., 2011) and has the potential to identify functionally important stromal genes in breast cancer progression.

Aims of this study

The three major goals of my thesis project were to (1) develop a model system of fibroblast-breast cancer cell interactions that mimics what occurs in primary breast cancers, (2) determine how many secreted factors are induced in fibroblasts by breast cancer cells, and (3) determine how many of the secreted factors play a role in promoting tumorigenicity. A majority of previous studies conducted that are highly relevant to my project fall into two categories: ones that use model systems to test individual candidate genes functionally and others that profile patient stroma using gene expression profiling but make no attempt at characterizing genes functionally. A crucial strength of my experimental design is the combination of both genomic and functional approaches to identify genes and pathways relevant to human breast cancer.

The experimental workflow corresponds to my three major goals: development of a model system; genomic analysis to identify candidates, and functional validation of the candidate genes. I used a co-culture, co-xenografting based model system composed of breast cancer cell lines and human fibroblasts. The idea was to approximate interactions of tumor epithelium and stromal fibroblasts in human breast cancer patients, which I subsequently validated by comparative genomic analysis. I identified two different classes of fibroblasts based on their ability to cooperate with breast cancer cells *in vivo*: fibroblasts that promoted growth (tumor-supportive) and those that did not (non-supportive). A comparative genomic analysis of the two

classes of fibroblasts provided a starting point to identify potential functional mediators. This was based on the rationale that functionally important mediators are likely to be selectively induced in interactions of tumor-supportive fibroblasts with breast cancer cells. Importantly, the candidates I chose for functional analysis were also upregulated in primary human breast stroma.

To fulfill the final major goal, I used RNAi to suppress the expression of candidate genes *in vivo*. I assayed tumorigenicity and characterized the tumor microenvironment using immunohistochemistry to gain insights into the possible functions of these genes.

My results indicate instead of there being a single major mediator which has been the conclusion of most previous studies, that instead there are multiple genes and processes involved in fibroblast promotion of breast cancer and based on extrapolation likely to be fifty or more such genes. In the context of this interaction being similar to tissue or organ development, our results are consistent with recent genetic analysis that the development of even simple organs requires over 200 patterning and morphogenesis genes (Ghabrial et al., 2011).

CHAPTER II

Identification of molecular mediators of breast cancer-fibroblast interactions through genome-wide transcriptional analysis

Introduction

The basis for performing gene expression profiling following *in vitro* co-culture experiments arose from the observation that fibroblasts in tissue culture can modulate the properties of breast cancer cells and vice-versa (Ronnov-Jessen et al., 1992). Early studies using co-culture based experiments noted that fibroblasts induced proliferation and invasion in breast cancer cell lines (Adam et al., 1994; Himelstein and Muschel, 1996). Subsequent studies focused on identifying candidate mediators induced by epithelial stromal interactions. Several groups found that breast cancer cells induce matrix metalloproteinases in fibroblasts upon co-culture (Himelstein and Muschel, 1996; Ito et al., 1995; Mari et al., 1998; Stuelten et al., 2005; Wang and Tetu, 2002; Wang et al., 2002). This is not surprising because fibroblasts actively remodel the ECM through the secretion of MMPs *in vivo* (Noël et al, 2008).

Recent studies have taken co-culture based genome-wide approaches to identify molecular mediators of interactions between cancer cells and fibroblasts. The first study to report a large scale induction of genes following co-culture was purely exploratory and found that induced or down-regulated genes were involved in diverse processes relevant to cancer (Fromigue et al., 2003). The second report utilized a transwell cell culture system where fibroblasts and pancreatic cancer cells were separated by a high-density membrane that allowed diffusion of soluble factors (Sato et al., 2004). This allowed for separate analysis of the

transcriptome of both cell types and led to the finding that COX2 was upregulated in the stromal fibroblast compartment. Treatment with COX2 inhibitors (either small-molecule or siRNA) was able to block the ability of fibroblasts to induce pancreatic cancer cell invasion (Sato et al., 2004). The third report found that some but not all human breast cancer cell lines could induce a gene signature of interferon signaling upon co-culture with human fibroblasts (Buess et al., 2007). Interestingly, this gene signature was associated with poor survival and was validated by immunohistochemistry analysis of primary human breast cancers (Buess et al., 2007). However, no attempt was made to determine whether this signature played a functional role or was simply a secondary consequence. In another study, the authors used genomic analysis of a co-culture based model to identify altered cellular transport systems in carcinoma-associated fibroblasts (Rozenchan et al., 2009). Recently, Tyan et al, used a transcriptome-based approach followed by functional analysis to identify fibroblast secreted HGF as a functionally important growth factor induced upon co-culture with breast cancer cells (Tyan et al., 2011). In a study using both functional and genomic approaches, Allinen et al identified overexpression of specific genes in different compartments of the breast tumor microenvironment. They noted that myoepithelial cell secreted CXCL14 and myofibroblast secreted CXCL12 had functional roles in promoting proliferation, migration and angiogenesis (Allinen et al, 2004).

Although a number of functional mediators of tumor-stromal fibroblast interactions have been identified in *in vitro* co-culture based systems, very few studies have validated their findings *in vivo* (Orimo et al., 2005). *In vivo* functional analysis is advantageous over cell-based system due to its close resemblance to events in human cancer.

The majority of studies describing gene functions involved in the interaction between carcinoma associated fibroblasts and breast epithelium have relied on either genetically

engineered mouse models (GEMM), co-xenografts of breast cancer cell lines and CAFs, or cell based co-culture models (Bierie and Moses, 2009; Ksiazkiewicz et al., 2010; Orimo et al., 2005; Pietras et al., 2008; Trimboli et al., 2009). I chose to use a co-culture and co-xenograft based model in order to simultaneously perform genomic and functional analyses on human epithelial cells and fibroblasts.

The first step in developing the model was to identify human fibroblast strains that behaved like patient-derived CAFs in terms of promoting tumorigenicity *in vivo* (tumor-supportive fibroblasts; TSF). Some fibroblast strains have been shown to accelerate tumor progression in mice (Camps et al., 1990; Noel et al., 1993) and unlike patient derived CAFs, human fibroblast strains can be passaged for longer lengths of time (Polanska et al., 2011). Other fibroblast strains behave like patient-derived normal breast fibroblasts and do not promote tumorigenicity (non-supportive fibroblasts; NSF). I took advantage of this difference in an attempt to ascertain which genes were responsible for driving tumorigenesis. In this approach, expression profiles resulting from breast cancer cells co-cultured with TSFs were compared to expression profiles resulting from breast cancer cells co-cultured with NSFs. Genes that were altered in common were discarded as functionally irrelevant while genes that were altered exclusively in expression profiles from breast cancer cells co-cultured with TSFs were considered potentially important functional mediators of tumorigenesis.

Results

Identification of tumor-supportive (TSF) and non-supportive (NSF) fibroblasts

A co-injection assay was used to test fibroblasts' ability to cooperate with admixed breast cancer cells to enhance tumor formation when injected subcutaneously in nude mice. Only ER/PR negative breast cancer cell lines were included to avoid confounding variables arising from subtype variability.

Two Her2 amplified, ER and PR negative cell lines—JIMT-1 and HCC1954 were tested for their ability to cooperate with HFFF2 (human fetal foreskin) fibroblasts and Wi38 (human fetal lung) fibroblasts to promote tumor growth in a co-xenografting assay. 1×10^6 JIMT-1 or HCC1954 cells were injected into flanks of 5-6 week old irradiated, nude female mice with or without 1.5×10^6 HFFF2 or Wi38 fibroblasts. Cell line only injections (JIMT-1 and HCC1954) were used as controls. Tumor volumes for each group were calculated and compared with the parental cell line only injections each week for six weeks post injections. Interestingly, both HFFF2 and Wi38 fibroblast strains cooperate with JIMT-1 to increase tumor growth although HFFF2 fibroblasts confer a significantly higher growth advantage (Figure 2.1.A and 2.1.B) whereas neither strain cooperates with HCC1954 to promote tumor growth (Figure 2.2 and 2.2.B).

ER, PR, HER2 negative cell lines Cal-51 and MDAMB231. 1×10^6 Cal-51 or MDAMB231 cells were then injected into either flank of 5-6 week old irradiated, nude female mice with or without 1.5×10^6 HFFF2, Wi38, HFF1 (newborn foreskin) or CCD1112Sk (adult foreskin) fibroblasts. Both cell lines cooperated with HFFF2 and HFF1 fibroblast strains but did not cooperate with Wi38 and CCD1112Sk to promote tumor growth (Figure 2.3 and 2.4). Therefore, HFFF2 and HFF1 strains were designated tumor-supportive fibroblasts (TSF)

whereas Wi38 and CCD1112Sk were designated non-supportive fibroblasts (NSF). These combinations of cells were used in co-culture assays and subsequent gene expression analysis. A complete list of the characteristics of breast cancer cell lines and human fibroblasts used in this study is presented in Table 2.1.

Table 2.1: Characteristics of breast cancer cell lines and human fibroblast strains used to identify tumor-supportive and non-supportive fibroblasts

Cell line	ER status	PR status	Her 2 amplified	Fibroblast	Origin	Tumor supportive?
JIMT-1	Negative	Negative	Yes	HFFF2	Fetal foreskin	Yes
				Wi38	Fetal lung	Yes
HCC 1954	Negative	Negative	Yes	HFFF2	Fetal foreskin	No
				Wi38	Fetal lung	No
Cal-51	Negative	Negative	No	HFFF2	Fetal foreskin	Yes
				HFF1	Newborn foreskin	Yes
				CCD1112Sk	Newborn foreskin	No
				Wi38	Fetal lung	No
MDAMB231	Negative	Negative	No	HFFF2	Fetal foreskin	Yes
				HFF1	Newborn foreskin	Yes
				CCD1112Sk	Newborn foreskin	No
				Wi38	Fetal lung	No

Figure 2.1

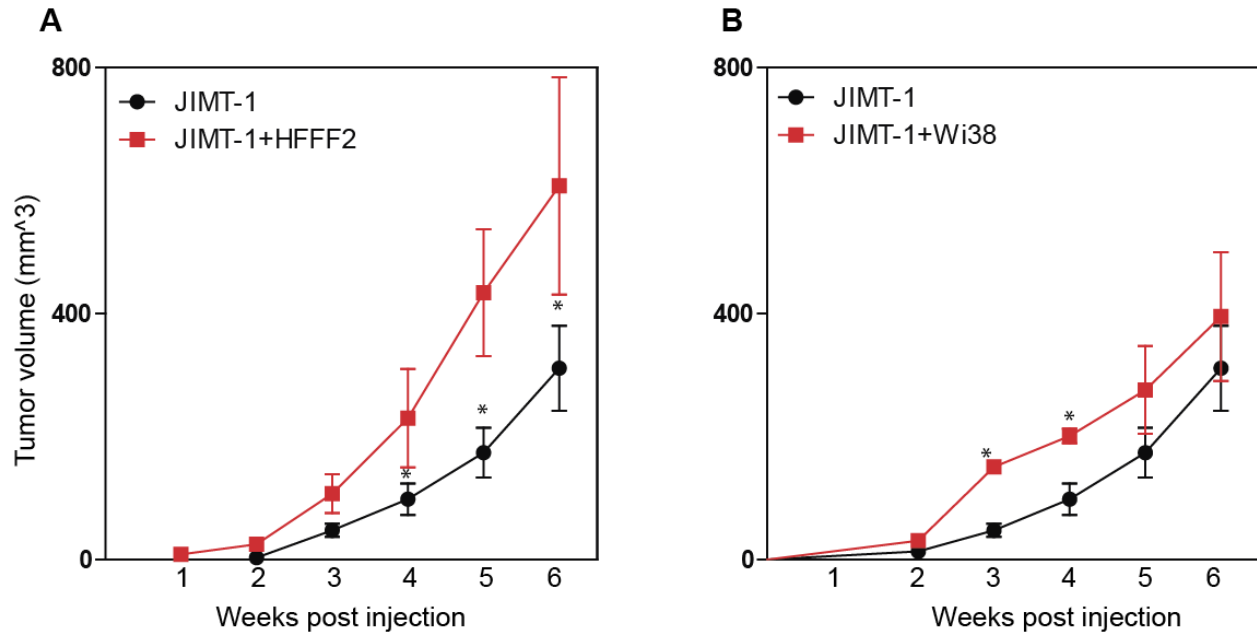


Figure 2.1: Effect of co-injected fibroblasts on JIMT-1 tumorigenicity

A: Tumor volume measurements of 1×10^6 JIMT-1 breast cancer cells injected subcutaneously into nude mice with or without 1.5×10^6 HFFF2 fibroblasts weeks 1-6 post injections. $n=6$ per group. Asterisk indicates significant differences between the two groups $*p < 0.05$. Error bars represent Mean \pm SEM.

B: Tumor volume measurements of 1×10^6 JIMT-1 breast cancer cells injected subcutaneously into nude mice with or without 1.5×10^6 Wi38 fibroblasts weeks 1-6 post injections. $n=6$ per group. Asterisk indicates significant differences between the two groups $*p < 0.05$. Error bars represent Mean \pm SEM.

Figure 2.2

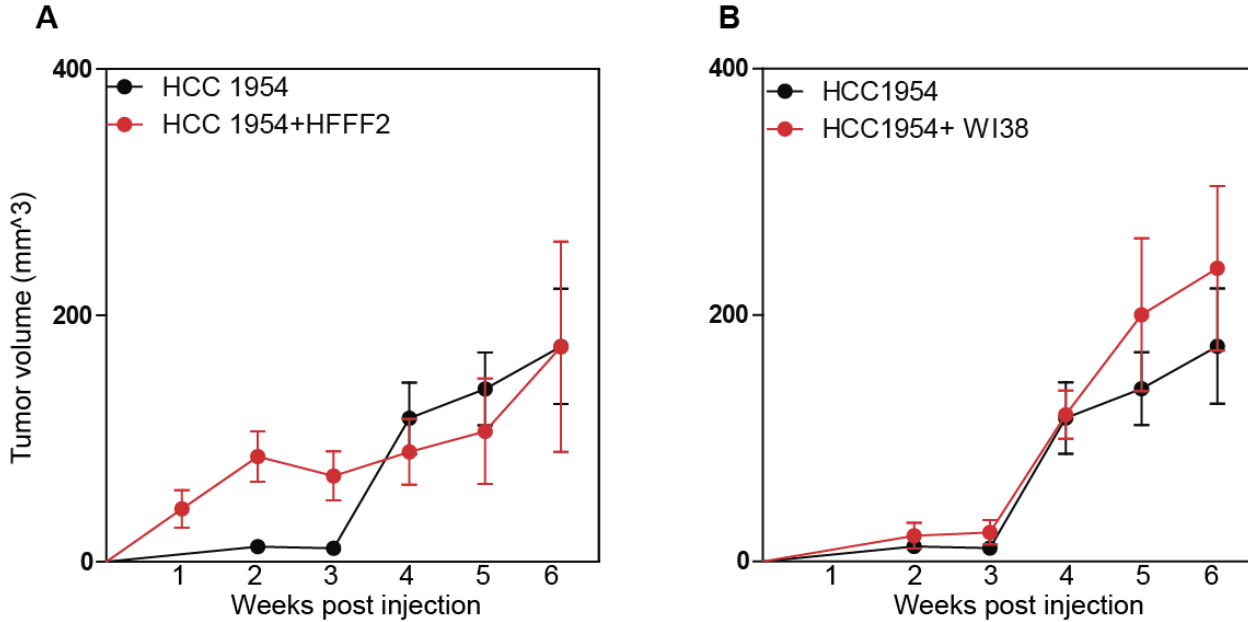


Figure 2.2: Effect of co-injected fibroblasts on HCC1954 tumorigenicity

A: Tumor volume measurements of 1×10^6 HCC 1954 breast cancer cells injected subcutaneously into nude mice with or without 1.5×10^6 HFFF2 fibroblasts, weeks 1-6 post-injection. $n=6$ per group. Error bars represent mean \pm SEM.

B: Tumor volume measurements of 1×10^6 HCC1954 breast cancer cells injected subcutaneously into nude mice with or without 1.5×10^6 Wi38 fibroblasts weeks 1-6 post-injection. $n=6$ per group. Error bars represent mean \pm SEM.

Figure 2.3

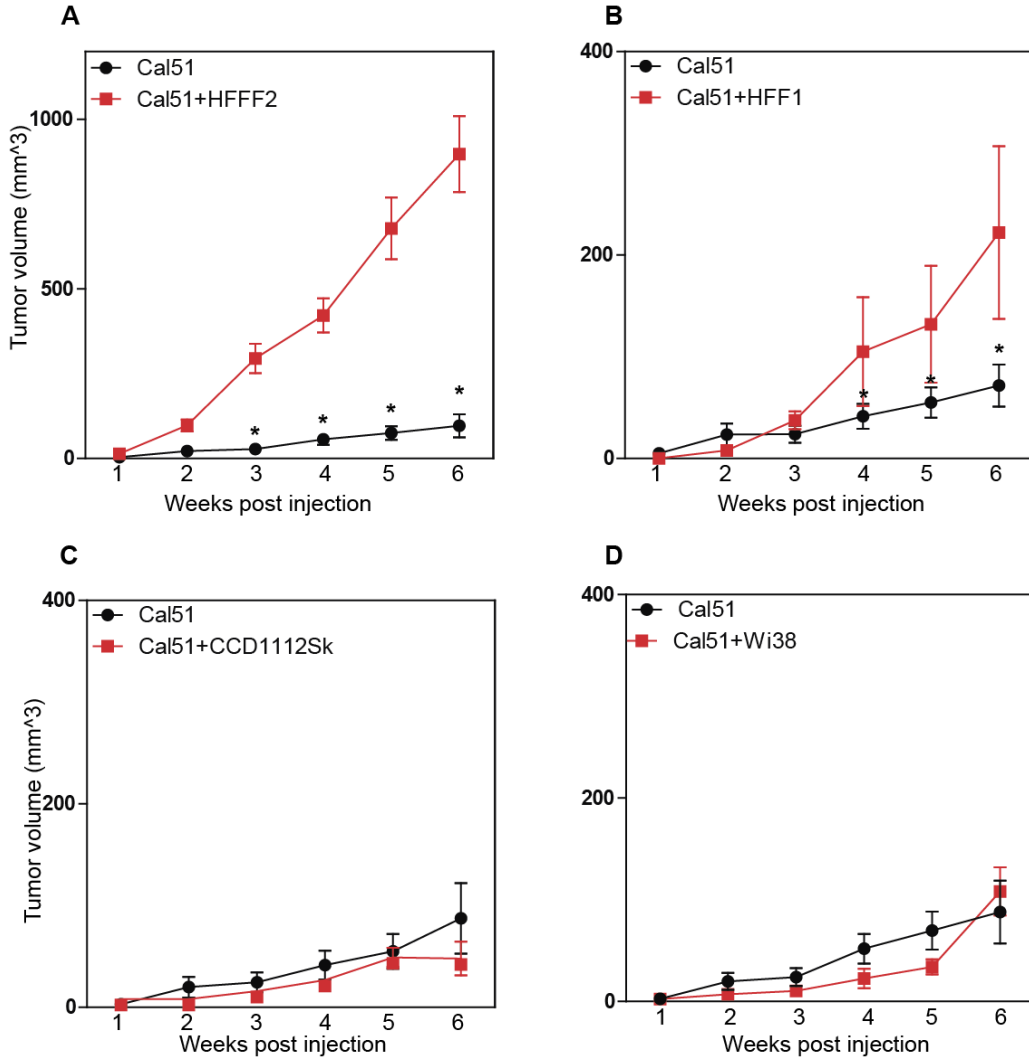


Figure 2.3: Effect of co-injected fibroblasts on Cal51 tumorigenicity

A: Tumor volume measurements of 1×10^6 Cal51 breast cancer cells injected subcutaneously into nude mice with or without 1.5×10^6 HFFF2 fibroblasts, weeks 1-6 post injection. Asterisk indicates that the indicated tumor groups are significantly different. $P < 0.05$, $n > 20$ per group. Error bars represent mean \pm SEM.

B: Tumor volume measurements of 1×10^6 Cal51 breast cancer cells injected subcutaneously into nude mice with or without 1.5×10^6 HFF1 fibroblasts weeks 1-6 post injection. Asterisk indicates that the indicated tumor groups are significantly different. $P < 0.05$, $n=10$ per group. Error bars represent mean \pm SEM.

C: Tumor volume measurements of 1×10^6 Cal51 breast cancer cells injected subcutaneously into nude mice with or without 1.5×10^6 CCD1112Sk fibroblast, weeks 1-6 post injection. $n=10$ per group. Error bars represent mean \pm SEM.

D: Tumor volume measurements of 1×10^6 Cal51 breast cancer cells injected subcutaneously into nude mice with or without 1.5×10^6 Wi38 fibroblasts, weeks 1-6 post injection. $n=10$ per group. Error bars represent mean \pm SEM.

Figure 2.4

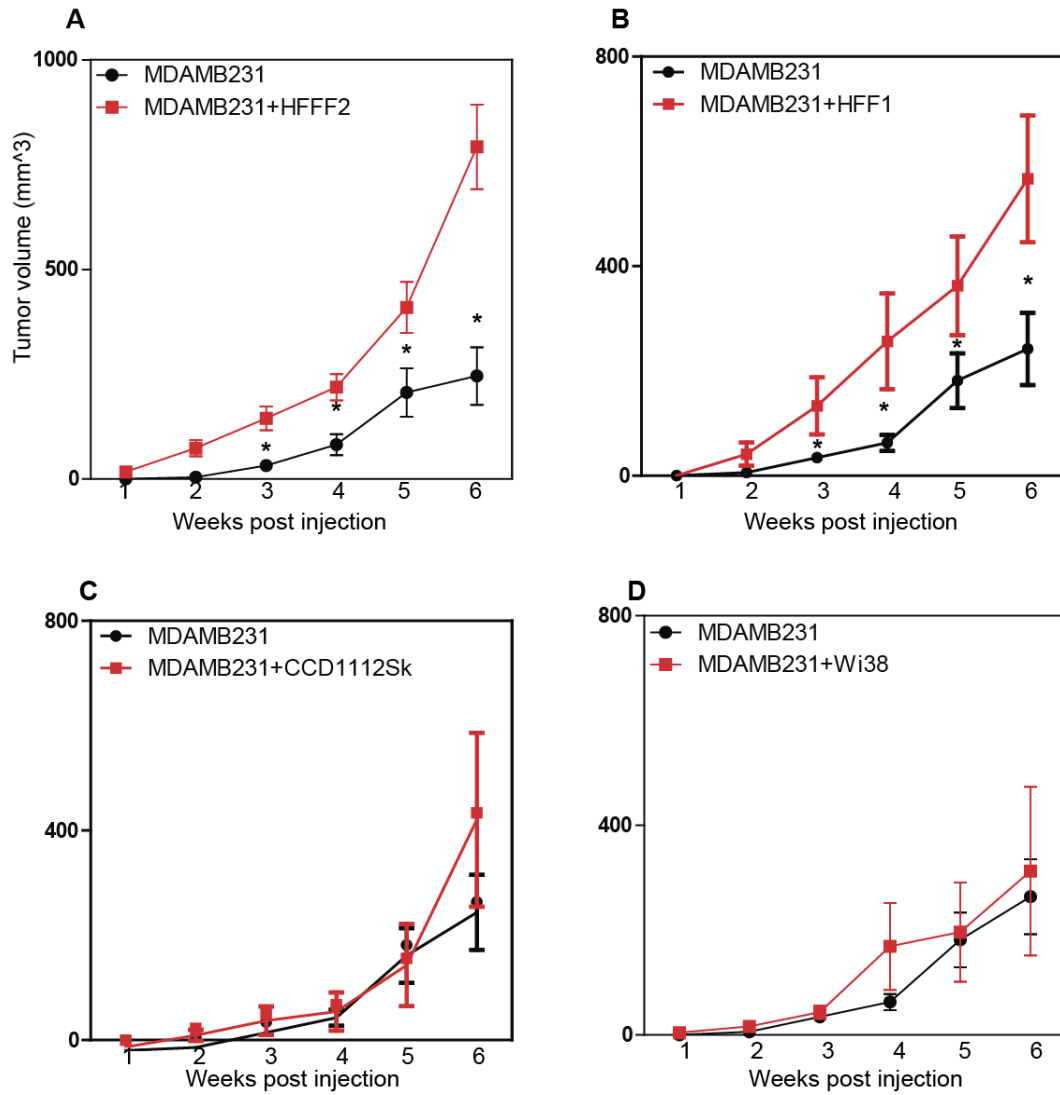


Figure 2.4: Effect of co-injected fibroblasts on MDAMB231 tumorigenicity

A: Tumor volume measurements of 1×10^6 MDAMB231 breast cancer cells injected subcutaneously into nude mice with or without 1.5×10^6 HFFF2 fibroblasts weeks 1-6 post injections. Asterisk indicates that the indicated tumor groups are significantly different. $P < 0.05$. $n=10$ per group. Error bars represent mean \pm SEM.

.B: Tumor volume measurements of 1×10^6 MDAMB231 breast cancer cells injected subcutaneously into nude mice with or without 1.5×10^6 HFF1 fibroblasts weeks 1-6 post injections. Asterisk indicates that the indicated tumor groups are significantly different. $P < 0.05$. $n=10$ per group. Error bars represent mean \pm SEM.

C: Tumor volume measurements of 1×10^6 MDAMB231 breast cancer cells injected subcutaneously into nude mice with or without 1.5×10^6 CCD1112Sk fibroblasts weeks 1-6 post injections. $n=10$ per group. Error bars represent mean \pm SEM.

D: Tumor volume measurements of 1×10^6 MDAMB231 breast cancer cells injected subcutaneously into nude mice with or without 1.5×10^6 Wi38 fibroblasts weeks 1-6 post injections. $n=10$ per group. Error bars represent mean \pm SEM.

Contributions of co- injected tumor-supportive fibroblasts to tumor progression

To use this model system to functionally assay tumor-fibroblast interactions, it is essential that injected fibroblasts recapitulate some of the functions of CAFs (Kalluri and Zeisberg, 2006). The first step was to make sure that the injected HFFF2 fibroblasts were incorporated in fully formed tumors with Cal-51 cells.

HFFF2 cells stably expressing fluorescent marker protein GFP were engineered. GFP-labeled HFFF2 fibroblasts were then co-injected with Cal51 breast cancer cells as described above. Sections from co-injected tumors were taken 3, 4, 6 and 8 weeks post injections and were immunostained using an antibody specific to GFP in order to identify HFFF2 fibroblasts. Results indicated that injected GFP positive fibroblasts are incorporated into the mature tumor (Weeks 3-6 post injections) (Figure 2.5). However, GFP positive cells were almost completely absent from the population by ~8 weeks post injection, possibly because unlike cancer cells, human fibroblasts undergo a limited number of divisions. This observation is consistent with previous reports (Hu et al., 2009).

CAFs promote tumor-supportive functions like proliferation of cancer cells, recruitment of immune cells and blood vessels (Orimo and Weinberg, 2006). To test whether co-injected HFFF2 fibroblasts promote proliferation, recruitment of immune cells and blood vessels similar to CAFs, sections from Cal51 cell line only injections and Cal51+HFFF2 co-injections were immunostained using antibodies to Ki-67, 7/4 and CD31 respectively. Co-injection of Cal51 cells and HFFF2 fibroblasts leads to an increase in the number of proliferating cells, immune cells recruited to the tumor and blood vessels compared to tumors resulting from Cal51 injections only (Figure 2.6.A-C and quantified in Chapter IV).

Co-injections of Cal51 and HFFF2 cells also have more reactive fibroblasts compared to tumors resulting from Cal51 only injections. This is evidenced by increased α -SMA staining in co-injected tumors (Figure 2.6.D and quantified in Chapter IV). Since the injected fibroblasts are no longer apparent by 6-8 weeks post injection, they cannot be attributed to the increased number of all α -SMA cells. This suggests that injected fibroblasts may affect the migration or recruitment of host cells that express α -SMA (discussed in Chapter III).

Figure 2.5

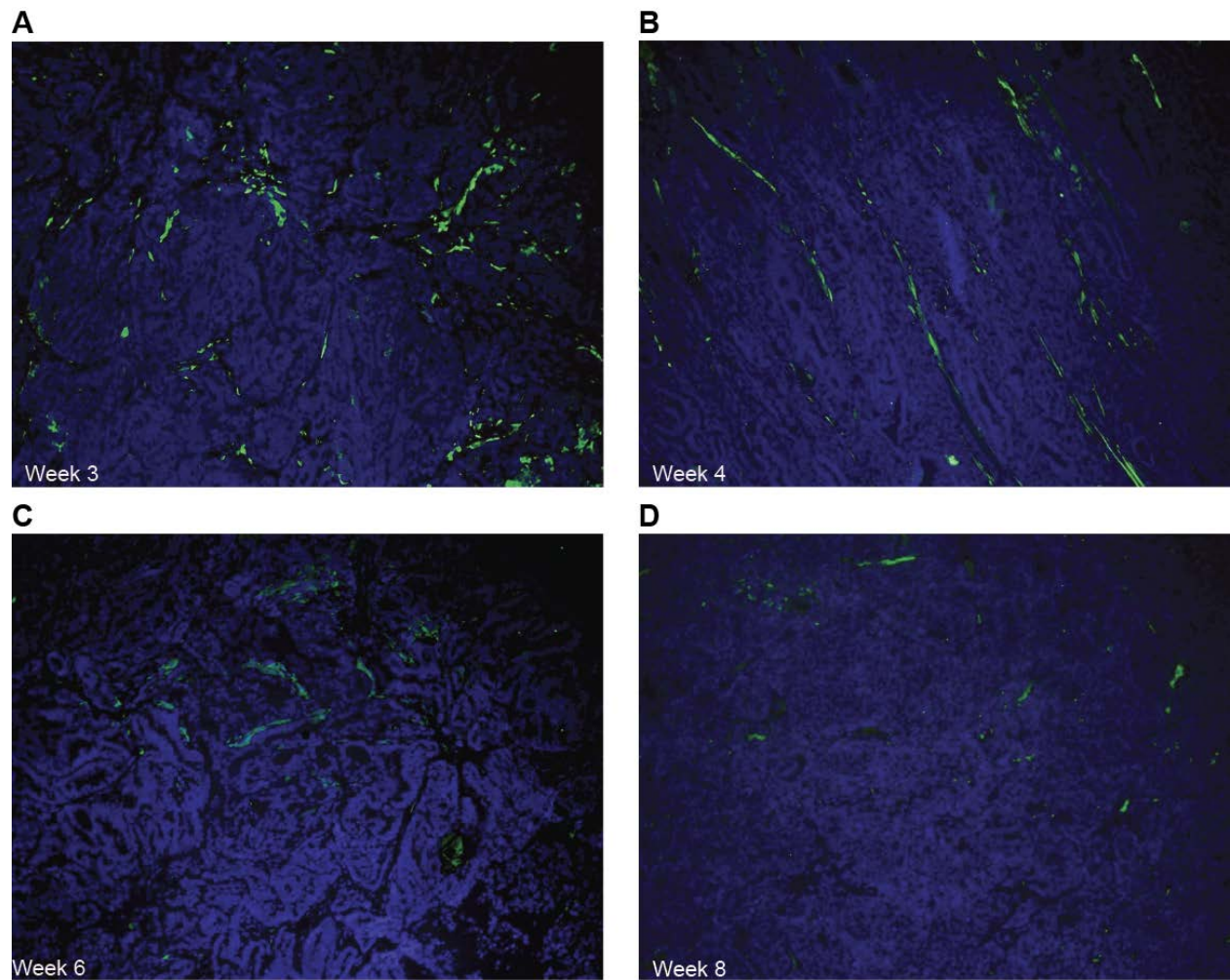


Figure 2.5: Incorporation of HFFF2 fibroblasts in Cal51 tumors.

Immunostaining of HFFF2-GFP fibroblasts in Cal51 tumors. Week 3 (A), Week 4 (B), Week 6 (C) and Week 8 (D) post injections using an antibody to GFP. Injected fibroblasts almost completely disappear 8 weeks post injections.

Figure 2.6

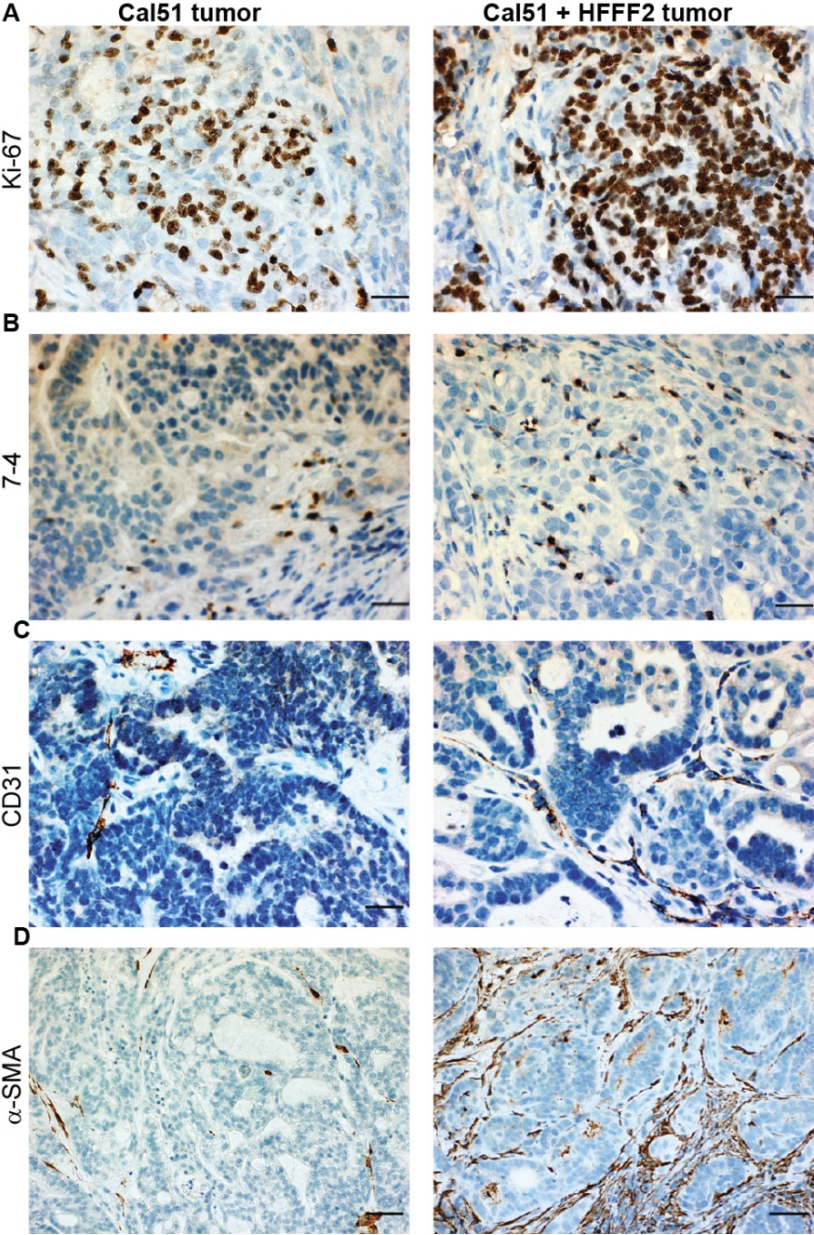


Figure 2.6: Tumor-promoting activities of co-injected fibroblasts six weeks post injections.

A: Immunostaining of proliferative cells in sections of Cal51 tumors and Cal51 co-injected with HFFF2 fibroblasts using an antibody to Ki-67. Panels are representative of multiple fields of tumor sections from three tumors per group. Scale bars represent 50 μm .

B: Immunostaining of neutrophils and monocytes in sections of Cal51 tumors (left) and Cal51 co-injected with HFFF2 fibroblasts (right) using an antibody to antigen 7-4. Panels are representative of multiple fields of tumor sections from three tumors per group. Scale bars represent 50 μm .

C: Immunostaining of blood vessels in sections of Cal51 tumors (left) co-injected with HFFF2 fibroblasts (right) using an antibody to CD31. Panels are representative of multiple fields of tumor sections from three tumors per group. Scale bars represent 50 μm .

D: Immunostaining of reactive fibroblasts and pericytes in sections of Cal51 tumors (left) and Cal5 co-injected with HFFF2 fibroblasts (right) using an antibody to α -sma. Panels are representative of multiple fields of tumor sections from three tumors per group. Scale bars represent 100 μm .

Separate transcriptional profiling of breast cancer cells and fibroblasts

Based upon observations that mediators of breast cancer-stromal fibroblast interactions are induced upon co-culture (Fromigue et al., 2003), co-culture experiments were conducted followed by gene expression profiling in order to identify candidate mediators. Breast cancer cell lines, Cal51 or MDAMB231, stably expressing red fluorescent protein (DsRed) were generated via retroviral infection. Similarly, the fibroblasts HFFF2, HFF1, Wi38 and CCD1112Sk were engineered to stably express green fluorescent protein (GFP). Independent cultures of 1.5×10^6 GFP-fibroblasts were plated in 10 cm tissue culture dishes and allowed to adhere overnight. Subsequently, 1×10^6 DsRed expressing cancer cells were plated on top of the fibroblasts and were co-cultured for six days. Following this, cells were trypsinized, washed and FACS sorted into breast epithelial cells and fibroblasts. Monocultures of corresponding cells were used as controls. RNA was prepared from 3-4 biological replicates for each experimental group and hybridized on Affymetrix® 1.0 Gene ST array. A schema of the procedure used is shown in Figure 2.7.A.

Gene Expression Analysis and identification of candidate mediators

Data from microarray experiments was background subtracted, normalized and \log_2 transformed (AROMA, R package). In the event that there were multiple probes on the microarray chip for the same gene, the mean intensity value was calculated and used for further analysis. In the resulting matrix, genes were represented as rows and samples as columns. Jinyu Li, (a bioinformatician in the Powers lab), calculated fold change induced upon co-culture of all ~20,000 genes assayed. For example, fold change of all genes from HFFF2 co-cultured with Cal51 was compared to monocultured HFFF2. Since there are two co-cultures (with Cal51 and

MDAMB231) and one monoculture for each fibroblast and there are four fibroblast groups in total, each gene has eight fold change values from different comparisons. A t-test was used to filter out genes in which the fold change was not significant ($p < 0.1$ in at least 5/8 comparisons). In the next step, a fold change ratio was calculated for each gene using comparison of tumor-supportive fibroblasts to non-supportive fibroblasts. For example, an average fold change of 1 means that the gene was neither induced nor down regulated in tumor-supportive co-cultures compared to non-supportive fibroblasts. Using a cut-off of 2 for average fold change ratio, 320 genes were identified. These genes were selectively induced in tumor-supportive fibroblasts upon co-culture (Figure 2.7.B and Table 2.2). A heatmap showing the induction of these 320 genes in co-cultures of tumor supportive fibroblasts (henceforth, known as CC-TSF) is shown in Figure 2.8. I used the 320 genes for selection of candidates and for establishing the relevance of the model system to human breast cancer.

Figure 2.7

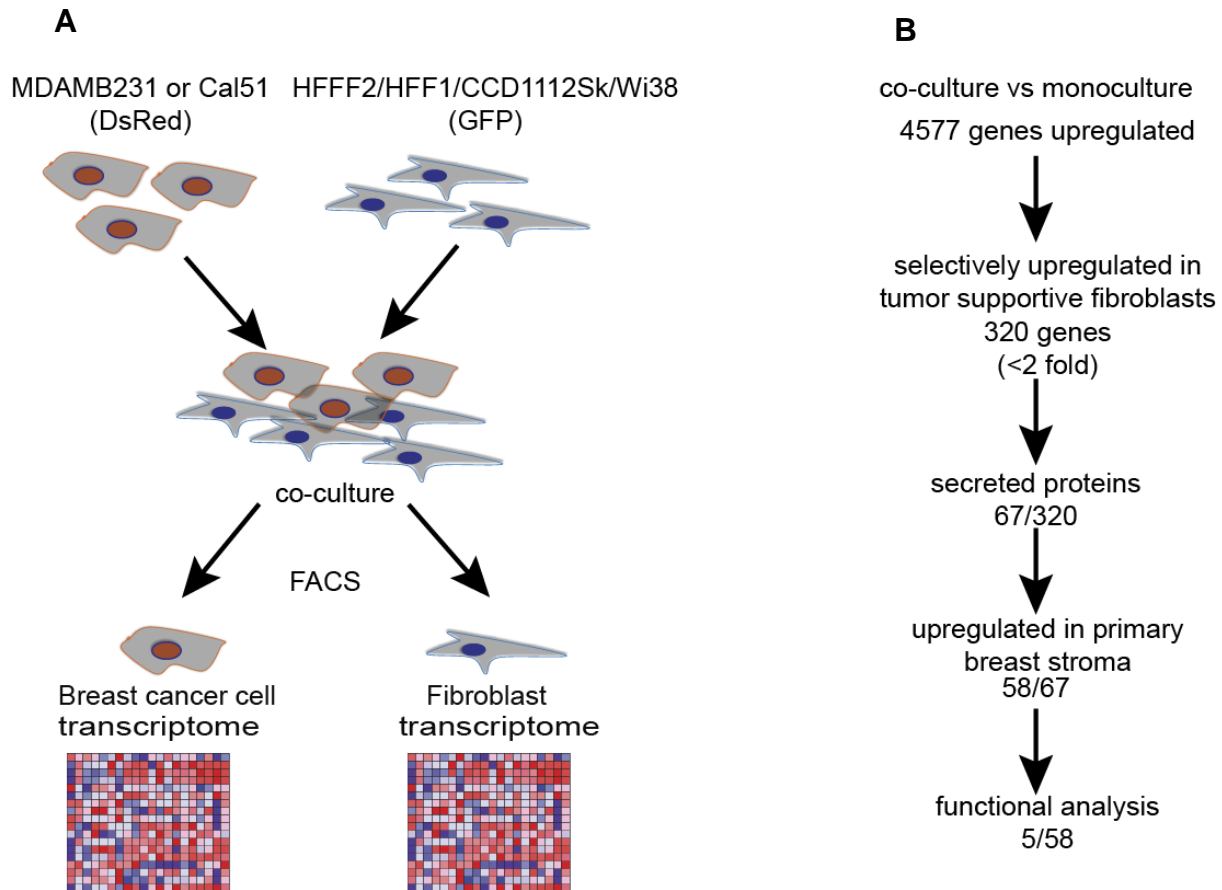


Figure 2.7: Experimental schema to identify candidate genes

A: Determination of genes induced in fibroblasts upon interaction with breast cancer cells. MDA-MB-231 or Cal51 cancer cells expressing Ds-Red marker were co-cultured for six days with human fibroblasts expressing GFP. Following flow cytometric sorting, the mRNA transcriptome of the separated cells was analyzed.

B: Identification of secreted candidate mediators of pro-tumorigenic interactions of fibroblasts with breast cancer cells. Out of approximately 20,000 mRNAs surveyed, 4,577 were significantly induced in fibroblasts in five or more of the eight combinations with breast cancer cells tested. Only 320 of these genes, however, were selectively induced more than 2-fold in the tumor-supportive fibroblasts. Of these, 67 encoded secreted proteins and 58 of these were also significantly upregulated in breast cancer stroma. Of these, 5 genes were chosen for functional analysis.

Figure 2.8

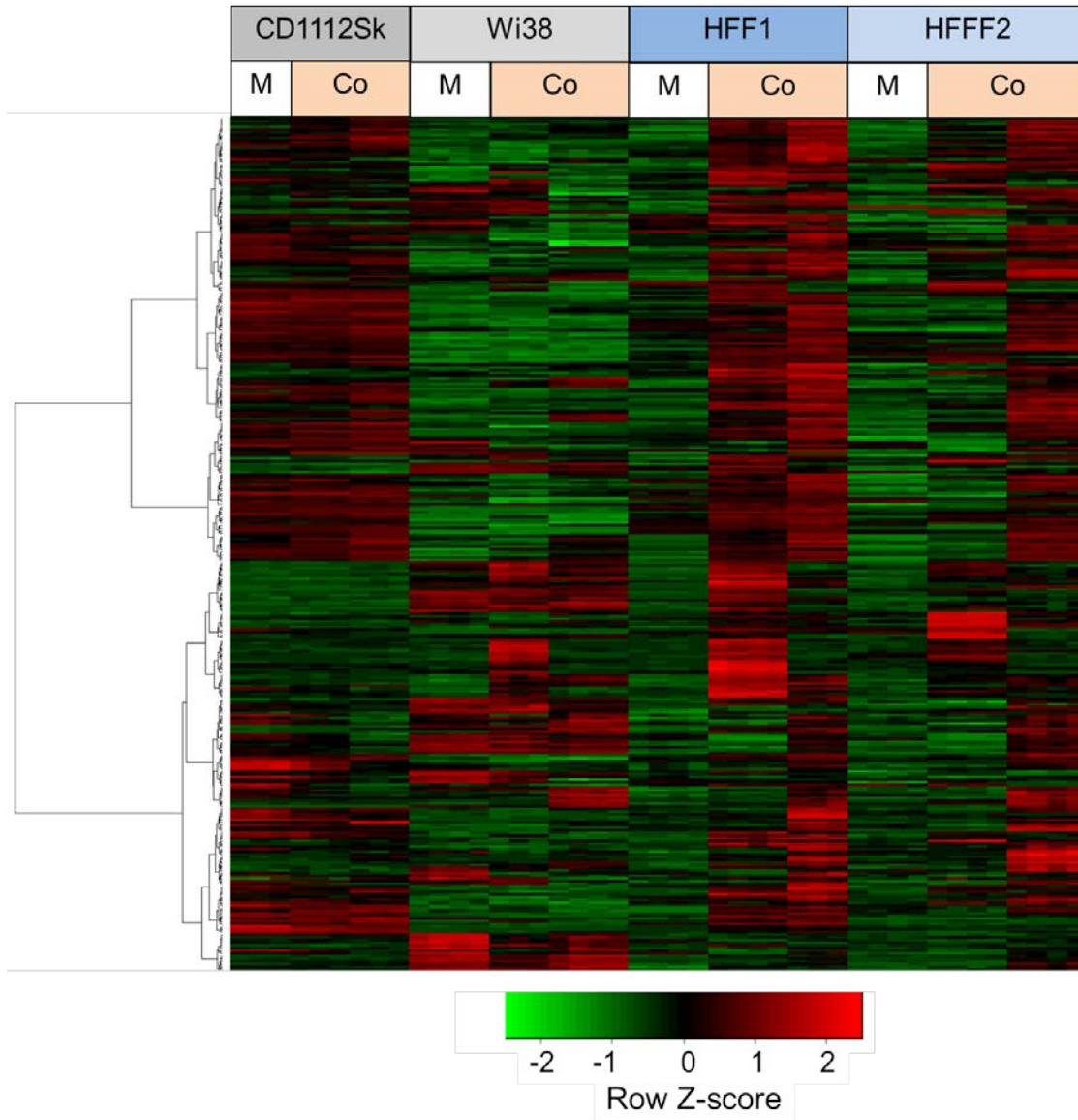


Figure 2.8: Heatmap of relative expression of the 320 genes in monocultured and co-cultured fibroblasts

Heatmap of the relative fibroblast expression of the 320 genes induced by breast cancer cells selectively in pro-tumorigenic fibroblasts (HFF1, HFFF2). Although for many of these genes the endogenous expression in mono-cultures is higher in neutral fibroblasts (Wi38, CCD1112Sk), they are not induced to higher levels upon co-culture with breast cancer cells. MC = mono-culture; Co = co-culture; for each fibroblast strain, biological replicates (either 3 or 4) of co-culture with Cal51 on shown the left and with MDA-MB-231 on the right. Red indicates relatively high expression whereas green indicates relatively low expression.

Significant enrichment of secreted molecules in primary human breast cancer stroma

67/320 genes from the CC-TSF set are well-annotated secreted molecules. I focused on secreted proteins because paracrine interactions in the breast microenvironment are thought to be mediated in large part by secreted proteins (Hu and Polyak, 2008b). Additionally, they are easy to target therapeutically making them attractive candidates for functional testing.

The analysis was restricted to only those candidate molecules that were also upregulated in human breast cancer stroma. I used three previously published studies: two that used expression profiling of breast stroma following laser capture microdissection (Finak et al., 2008; Ma et al., 2009) and one that profiled carcinoma associated fibroblasts and normal fibroblasts from patients tumor cell mRNAs (Bauer et al., 2010). I compared the expression of the 67 secreted factors in cancer stroma compared to normal stroma and found that 58/67 secreted factors were significantly upregulated in cancer stroma of at least 1 out of 3 breast stroma datasets ($p < 0.05$) (Table 2.2)

Some of these molecules have previously identified roles in the breast cancer microenvironment. ~40% these proteins (21/58) are cytokines composed mainly of chemokines and interleukins. Stromal CCL5 promotes metastasis (Karnoub et al., 2007) whereas IL-1 β mediates inflammation in the tumor microenvironment by inducing pro-inflammatory chemokines (Erez et al., 2010). Of the growth factors, stromal fibroblast produced insulin-like growth factor-2 (IGF2) and neuregulin (NRG) have direct stimulatory roles on carcinoma cells (Liles et al., 2011; Zhu et al., 2007). Stromal secretion of extracellular glycoprotein versican was recently shown to promote metastasis (Gao et al., 2012). Stromally produced MMPs-1, 3, 11 and 13 have previously identified tumor-promoting roles (Ala-aho and Kahari, 2005; Sternlicht et al., 1999).

Table 2.2: List of 58 secreted molecules upregulated in co-cultured tumor-supportive fibroblasts and in primary human breast stroma with their respective average fold change ratios.

Cytokines	avg FC ratio	Growth Factors	avg FC ratio	Others	avg FC ratio
CCL2	2.4	ANGPTL4	3.6	DPT	5.2
CCL20	2.6	AREG	11.9	EGFL6	2.0
CCL5	4.8	IGF2	2.1	FMOD	3.8
CCL7	4.4	NRG1	4.7	FST	2.0
CCL8	4.0			IGFBP5	2.3
CSF3	3.1	ECM		ISG15	2.1
CXCL1	9.8	proteins		LAMC2	7.3
CXCL10	8.7	COL7A1	2.9	POSTN	3.6
CXCL2	5.8	DCN	2.6	SERPINB2	7.5
CXCL5	4.9	VCAN	5.4	SERPINE2	2.7
CXCL6	8.4	MMP1	2.2	SPINT1	2.1
IL11	3.9	MMP11	3.6	SPON1	6.3
IL1A	5.7	MMP12	3.1	TFPI2	3.3
IL1B	4.3	MMP16	3.1	TNFAIP6	8.6
IL1RN	7.2	MMP3	50.7	UCN2	3.2
IL24	10.9			WISP1	3.1
IL6	3.8	Hormone		LAMB3	2.4
IL8	15.8	STC1	3.6	SLC39A8	2.4
SPP1	4.9			SLC43A3	2.7
TNFSF10	5.4			SLC46A3	2.1
TNFSF15	2.3			FAM20C	2.0
				FJX1	2.2

Induction of ligand-receptor pairs

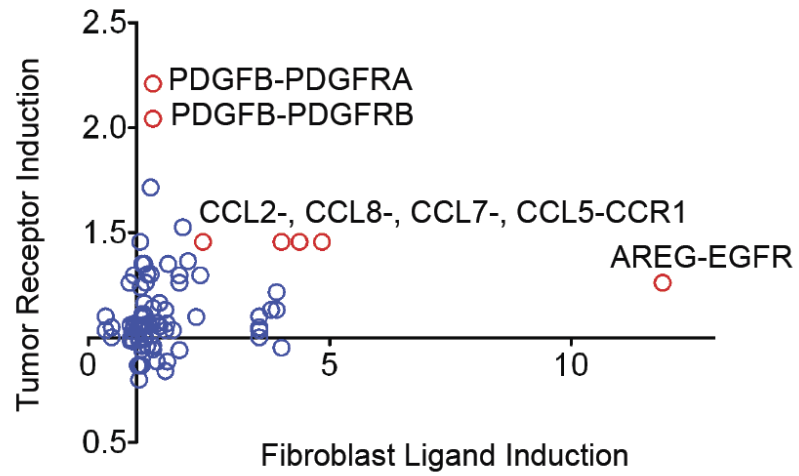
Reciprocal induction of receptors and ligands in cancer cells and fibroblasts upon co-culture is indicative of an active molecular crosstalk (Potter et al., 2012). I hypothesized that functionally important ligand-receptor pairs may be reciprocally induced upon co-culture of tumor-supportive fibroblasts and breast cancer cells.

As a starting point, I used a database of ligand-receptor pairs (Graeber and Eisenberg, 2001) to calculate reciprocal inductions of ligand-receptor pairs. Two paracrine interactions were used for comparison: 1. ligands induced in the co-cultured tumor supportive fibroblasts with induction of corresponding receptors in co-cultured epithelial cells 2. ligands induced in the co-cultured tumor epithelial cells with induction of corresponding receptors in co-cultured tumor-supportive fibroblasts (Figure 2.9, A and B).

In the first comparison, induction of chemokines CCL2, CCL5, CCL7 and CCL8 in the fibroblasts is significantly correlated with one of the receptors, CCR1, in the epithelial cells. Fibroblast produced amphiregulin (AREG) and its receptor EGFR are co-induced as well. Platelet-derived growth factor B (PDGFB) and its receptors PDGFRA and PDGFRB show coordinated induction as well. Comparing ligands induced in tumor epithelial cells with receptors in fibroblasts, FGF18-FGFR2, AREG-EGFR, BMP5-ACVR2A and IL1-A and B-IL1R1 show significantly correlated inductions.

Figure 2.9

A



B

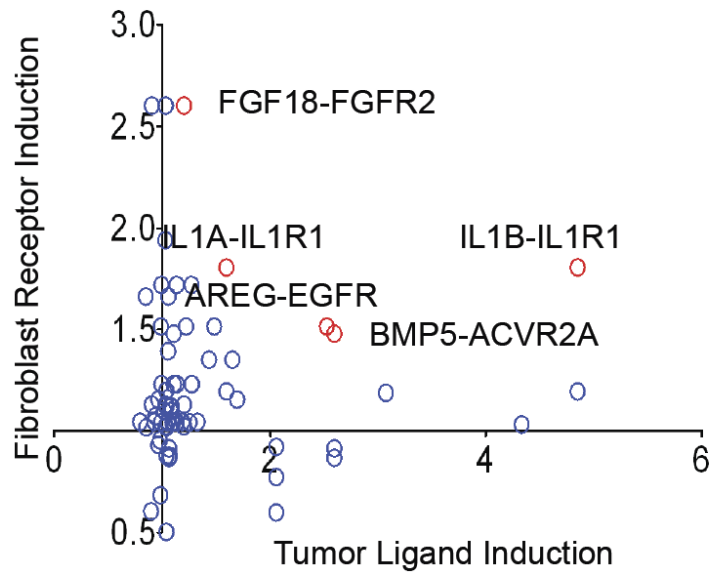


Figure 2.9: Ligand induction and receptor expression in pro-tumorigenic fibroblasts and breast cancer cells

A: Scatter plot of the coordinated paracrine induction of ligand expression in pro-tumorigenic fibroblasts and corresponding receptor expression in co-cultured breast cancer cells, expressed as the ratio to the values observed in co-culture with neutral fibroblasts (ratio of 1 = identical induction in both classes). Of the total 456 ligand-receptor pairs in the database of ligand-receptor partners (DLRP, <http://dip.doe-mbi.ucla.edu/dip/DLRP.cgi>) only those that showed a statistically significant correlation (Pearson; two-tailed $P < 0.05$) in paracrine expression (ligands in pro-tumorigenic fibroblasts, receptors in breast cancer cells) are shown. The indicated pairs correspond to the nearby red circles.

B: As in A, but here the scatter plot is of the coordinated paracrine induction of ligand expression in breast cancer cells and corresponding receptor expression in co-cultured pro-tumorigenic fibroblasts.

Selection of candidates for functional analysis

Candidates for functional analysis were secreted molecules, selectively upregulated in co-cultured tumor supportive fibroblasts and in primary human breast cancer stroma. Amphiregulin (AREG) and its receptor EGFR are significantly co-induced in both breast cancer cells and fibroblasts. AREG has been implicated in mammary gland development and breast cancer although a functional role for stromal AREG in breast cancer has not been identified (Busser et al., 2011). Functional analysis detailing the role of AREG in the breast microenvironment is described in Chapter III.

Chemokines CCL2, CCL7 and CCL8 (Monocyte chemotactic proteins) are members of the same subfamily of C-C chemokines. One of the C-C receptors, CCR1, is reciprocally induced in co-cultured breast epithelial cells. CCL2 plays roles in tumor growth, angiogenesis, migration and metastasis (Balkwill, 2012) but the roles for CCL7 and CCL8 in the tumor microenvironment are not clear. Functional analysis of the roles of these chemokines and their receptor is described in Chapter IV.

Stanniocalcin1 (STC1) is a calcium hormone that is overexpressed in several cancers (Liu et al., 2010; Tamura et al., 2011). A functional role for stromal STC1 is not fully elucidated making it a potentially novel mediator in breast cancer-stromal fibroblast interactions. Functional analysis of STC1 is described in the Appendix. Expression of CCL2, CCL7, CCL8, AREG and STC1 in stromal compartments of breast cancer is shown in Figure 2.10 A and B.

Figure 2.10: 320 gene signature distinguishes cancer stroma from normal stroma; expression of candidate genes in primary human cancer stroma.

A: Ability of the 320-gene signature to classify primary breast stroma. Samples microdissected from primary breast stroma (Finak et al, 2008) were clustered based on the 320-gene signature. The colored bar above the sample dendrogram indicates normal breast stroma (green) and invasive carcinoma (red). All but one normal sample is correctly classified. The variability of expression of the 5 candidate mediators is shown in the heatmap underneath.

B: Same as A but results obtained with independent dataset of primary breast stroma (Ma et al, 2009). The colored bar above the sample dendrogram indicates normal breast stroma (green), in situ carcinoma (blue), and invasive carcinoma (red). All but one normal sample is correctly classified. The variability of expression of the 5 candidate mediators is shown in the heatmap underneath.

Relevance of model system to human breast cancer

This system is composed of breast cancer cell lines and human fibroblast strains. Therefore, it is essential to prove that genes used for functional testing are relevant to human breast cancer. Genes whose expression is inversely correlated with parameters such as time to death (survival), time to relapse or metastasis are more likely to be clinically relevant targets (van 't Veer et al., 2002). Similarly, gene signatures with higher expression in cancer epithelium or stroma compared to normal counterparts are more likely have a functional role in cancer progression (Allinen et al., 2004)

CC-TSF genes can classify primary human breast stroma

Gene expression profiles of laser-capture microdissected primary breast stroma were clustered based on the CC-TSF genes in two previously published studies (Finak et al, 2008; Ma et al, 2009). The CC-TSF genes are able to distinguish cancer stroma from normal stroma nearly perfectly in both studies. This indicates that the candidates chosen from functional validation are highly relevant to breast cancer stroma (Figure 2.10.A and B).

High expression of 320 genes is inversely correlated with survival

To establish the relevance of the model system to human breast cancer, I tested if the CC-TSF genes could predict poor survival in breast cancer patients. The NKI dataset contains gene expression profiling data for 295 breast cancer patients analyzed on 25000 spot oligonucleotide arrays. These patients were treated at the Netherlands Cancer Institute (NKI) for early stage breast cancer between 1984 and 1995. This dataset contains patient specific clinical information such as time to relapse, metastasis and survival (van de Vijver et al., 2002). The CC-TSF genes

were mapped on the NKI dataset and the resulting data matrix had 219 unique identifiers. This matrix was used for unsupervised hierarchical clustering using Ward linkage. A heatmap of the unsupervised clustering with the dead/live status of the patients is shown in red/green labels. I assigned CC-TSF-high or CC-TSF-low to clusters expressing relatively high and low levels of 320-genes (Figure 2.11.A). When I plotted Kaplan-Meier survival curves for each group based on the clinical information available, the patient group expressing the CC-TSF-high signature had significantly worse overall survival (Figure 2.11.B). This indicates that the genes induced selectively in co-cultures of tumor-supportive fibroblasts are highly relevant to breast cancer progression.

Figure 2.11

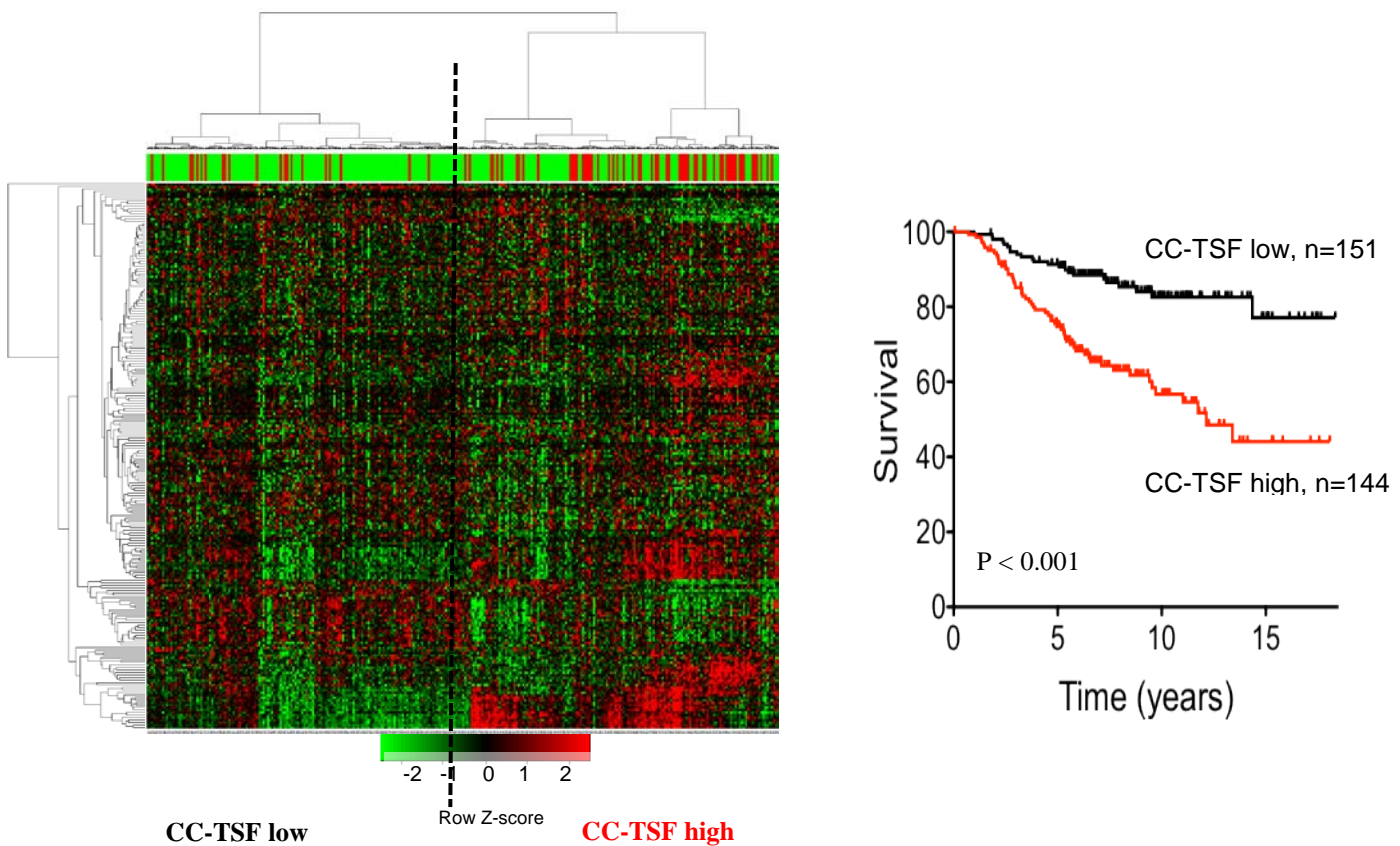


Figure 2.11: Co-culture tumor supporting fibroblast gene expression in human breast cancer

A: Heatmap showing expression of the CC-TSF genes in 295 cases of breast cancer (van de Vijver et al., 2002). Red is high expression and green is low. Death is marked by red label on the top panel. Groups of patients showing relatively high and low expression levels of CC-TSF genes are indicated by the CC-TSF high and CC-TSF low labels. The dashed line indicates the samples belonging to CC-TSF high and CC-TSF low respectively.

B: Effect of expression of the CC-TSF-gene signature (genes induced selectively in pro-tumorigenic fibroblasts by breast cancer cells) in the tumors of breast cancer patients on their long-term survival (NKI dataset). Patients with high expression (red curve; n=144) of the signature in their tumors show poorer survival than do patients with lower expression (black curve; n=151). $P < 0.001$.

Discussion

For selecting functional candidates of breast cancer-fibroblast interactions, I've developed a novel model system composed of breast cancer cells and stromal fibroblasts. TSFs cooperate with breast cancer cells in xenograft assays and behave like CAFs with respect to increasing proliferation of cancer cells and the number of blood vessels and immune cells. Using transcriptional profiling, I've presented a method to select and functionally test candidates that are upregulated in both co-cultured tumor-supportive fibroblasts and primary human breast stroma.

Pros and cons of the model system

The cell-based model system has two components: tumor cells and fibroblasts. The fibroblasts are functionally either tumor-supportive or non-supportive. This classification is based on previous studies that have identified carcinoma-associated fibroblasts as being more “supportive” compared to normal-adjacent fibroblasts (Erez et al., 2010; Olumi et al., 1999; Orimo et al., 2005). The rationale behind comparing genomic interactions of two different functional classes of fibroblasts was that interactions specific to the “supportive” group would be more functionally relevant.

Subcutaneous injections of breast cancer cells and fibroblasts in nude mice were used to identify “supportive” and “non-supportive” pairs. Previous studies have used *in vitro* assays to identify such pairs (Wadlow et al., 2009) but have focused on fibroblasts' effect on proliferation as the only parameter. Fibroblasts mediate proliferation, angiogenesis, inflammation, ECM remodeling, migration, invasion and metastasis (Chapter I) involving many other components of the microenvironment. Therefore an *in vivo* experimental approach using tumor volume as a

surrogate of tumor growth is more effective in accurately identifying tumor-supportive fibroblasts.

Existing mouse models of tumor-stromal interactions provide excellent tools to study the microenvironment but are clearly difficult to manipulate. Testing the role of one gene in a specific compartment of the microenvironment (e.g. CXCL12 in stromal fibroblasts) requires transgenic animals with tissue specific promoters. Using this model either or both cellular compartments can be manipulated genetically with relative ease.

One limitation of this model is the use of immunocompromised (nude) mice. Though nude mice have almost intact components of the innate immune system, they lack crucial components of the adaptive system such as reactive B- and T-lymphocytes. Therefore, any study conducted using this model largely ignores the contributions of the adaptive immune system. One way this could be overcome is by using mouse carcinoma cells and associated fibroblasts from already established mouse models (Erez et al., 2010). Alternately, the immune system of mice can be replaced completely by a humanized immune system prior to transplantation of xenografts to ensure graft tolerance (Ishikawa et al., 2005a).

Another disadvantage of this system is that injected human fibroblasts fully disappear 6-8 weeks post injections. This limitation prevents the model to be used for fibroblast factors that have roles in sustained tumor maintenance functions. This drawback can be overcome by immortalizing the fibroblasts without altering their gene expression profile drastically (Kojima et al., 2010).

Expression profiling of epithelial and stromal compartments

In vitro co-cultures of breast cancer cells and fibroblasts have been shown to induce physiologically relevant molecules previously (Himmelstein and Muschel, 1996). Fluorescently tagged markers were used to achieve complete separation of the two compartments post co-culture. Often, co-cultures of cancer and stromal cells are not separated resulting in ambiguity about the source of the induced gene (Buess et al., 2007). In this model, epithelial and fibroblast compartments are profiled separately leaving no room for such ambiguity.

However, this experimental set-up ignores the interactions of fibroblasts with other cells in the microenvironment (e.g. endothelial cells). Transcriptional profiling of cells from *in vivo* co-cultures (i.e. subcutaneous injections) may provide a more biologically accurate snapshot of interactions between fibroblasts and other components of the microenvironment.

Relevance to human breast cancer

A system composed of breast cancer cell lines and human fibroblasts from distant anatomic sites seems rather irrelevant to the study of human breast cancer at first. Therefore, it is important to establish its relevance to human breast cancer. Selectively upregulated genes in co-cultured tumor supportive fibroblasts (CC-TSF) can distinguish between cancer and normal stroma. This indicates that the genes chosen for functional validation are highly relevant to breast cancer stroma. Previous studies have derived gene signatures from co-cultures of fibroblasts and breast cancer cells that can accurately predict survival, time to relapse and metastasis in breast cancer patients (Chang et al., 2004). I found that the CC-TSF gene signature can accurately predict poor survival of breast cancer patients implying the relevance of this model system.

Candidate genes and functional analysis

I focused on secreted factors for functional analysis using RNAi. A majority of targeted therapies are based on secreted molecules and their receptors (Sawyers, 2005). Of the secreted factors upregulated in co-cultured tumor-supportive fibroblasts, ~80% are also upregulated in primary human breast stroma- and/or cancer-associated fibroblasts. This enrichment provides confidence that candidates selected for functional testing may have significant relevant roles in human breast cancer.

In summary, I have developed a model using a combination of *in vitro* and *in vivo* approaches and genomic analysis to establish its relevance to human breast cancer. Furthermore, the candidates used for functional analysis are upregulated in human breast stroma and relevant to breast tumor progression (Chapter III and IV).

CHAPTER III

Role of fibroblast secreted amphiregulin in breast cancer-stromal fibroblast interactions

Introduction

Amphiregulin is a member of the epidermal growth factor (EGF) family of ligands. EGF family members and their corresponding receptors play a central role in human development and cancer (Navolanic et al., 2003). EGF family of ligands consist of EGF, amphiregulin (AREG), transforming growth factor- α (TGF- α), epigen, heparin-binding epidermal-like growth factor (HB-EGF), betacellulin, epiregulin and neuregulin (NRG1-4). The ligands bind EGF receptors EGFR or ErBB1, HER2 or ErBB2, ErBB3 and ErBB4 resulting in activation of downstream signaling pathways that affect proliferation, migration, survival and inhibition of apoptosis of cells (Willmarth and Ethier, 2008). The discovery of Amphiregulin (AREG) was based on its similarity to EGF. Unlike EGF, it has both inhibitory and stimulatory effects on the proliferation, invasion and migration of cancer cells (Shoyab et al., 1988; Shoyab et al., 1989).

The AREG gene is about 10 Kb long, consists of six exons and is located on Chromosome 4 at 4q13-q21 (Busser et al., 2011). The resulting 252-amino acid pro-AREG protein is produced as a transmembrane glycoprotein (Figure 3.1). Proteolytic cleavage of pro-AREG by tumor necrosis factor- α converting enzyme (TACE/ADAM17) releases the mature protein, approximately ~19 Kd in size (Busser et al., 2011).

Amphiregulin expression is detectable in ovary, placenta, spleen, skin, breast and the gastrointestinal tract under normal conditions (Plowman et al., 1990). During embryonic development AREG is required for blastocyst implantation (Das et al., 1995) and bone growth (Qin et al., 2005). It plays an essential role in mammary gland development during puberty and gestation by inducing ductal outgrowths of terminal end buds. Not surprisingly, AREG knockout mice have severely impaired mammary glands that lack ductal outgrowth (McBryan et al., 2008).

AREG expression is elevated in human cancers compared to normal tissues suggesting a possible functional role in cancer progression (McBryan et al., 2008). In breast cancer, higher expression of AREG is correlated with lymph-node metastasis (LeJeune et al., 1993). Similarly, higher levels of AREG concentration in the serum correlate inversely with survival in lung cancer patients (Ishikawa et al., 2005b). It was subsequently demonstrated that AREG mediates resistance to EGFR inhibitors in lung cancers (Busser et al., 2010). *In vitro*, AREG stimulates the growth of hepatocellular carcinoma cell lines. Treatment of these cell lines with AREG neutralizing antibody attenuates their growth (Castillo et al., 2006).

AREG regulates invasion and remodeling of the ECM during cancer progression by inducing a number of cytokines and proteases. For example, AREG treatment results in upregulation of proinflammatory cytokines like IL-8, IL-1A, IL-1B, COX-2 and GM-CSF. These cytokines that mediate invasion, recruitment of immune cells and migration (Blanchet et al., 2004; Chokki et al., 2006; Coffey et al., 1997; Mahtouk et al., 2005; Streicher et al., 2007; Tsai et al., 2006). AREG also induces regulates the urokinase plasmin system thereby playing a role in invasion and remodeling the ECM during development and cancer (Giusti et al., 2003; Silvy et al., 2001).

Figure 3.1

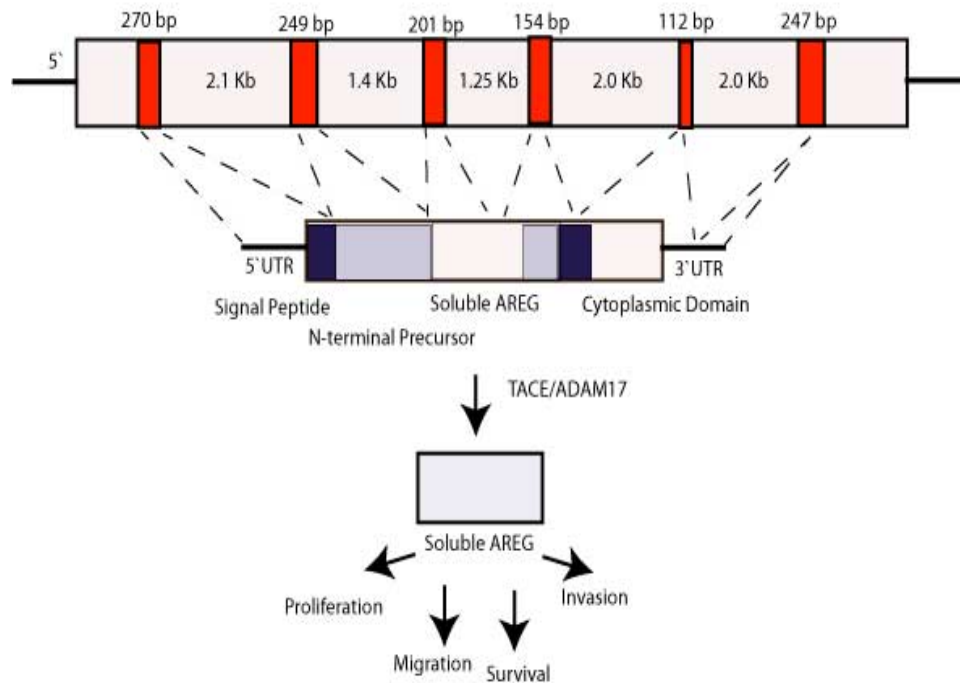


Figure 3.1: Representation of gene and protein domains of human amphiregulin (AREG)

Exon and intron domains are indicated by red and white boxes, respectively. Corresponding mRNA and protein domains are shown in grey. Pro-amphiregulin protein is cleaved by ADAM17/TACE to produce mature and soluble AREG. AREG elicits cellular functions such as proliferation, invasion, migration and survival by binding its receptor EGFR. UTR: untranslated region. Adapted from Busser et al, 2011.

AREG expression is elevated in cancer associated stroma compared to normal adjacent stroma. The first report analyzed sections co-stained for AREG and EGFR and found ~60% invasive stroma was positive for AREG compared to 31% positive for EGFR. This suggests that AREG produced by the invasive stroma acts on the tumor epithelium in a paracrine manner (Ma et al., 2001). The second study noted stromal staining of AREG in breast cancer patients is significantly correlated with survival (Visscher et al., 1997).

In the present study, AREG is induced in both co-cultured, tumor-supportive fibroblasts (TSPs) as well as co-cultured breast cancer cells. Moreover, AREG and its receptor EGFR are induced reciprocally in both breast cancer cells and fibroblasts. In addition, its expression is upregulated in primary cancer stroma from breast cancer patients (Finak et al., 2008). Therefore, I decided to test whether fibroblast produced AREG promoted tumorigenicity and the mechanisms by which it mediates its effects in the tumor microenvironment..

I demonstrate that RNAi mediated silencing of amphiregulin in the fibroblasts causes a significant reduction in the tumor growth when co-injected with human breast cancer cells. This effect is mediated in part by a reduction on EGFR phosphorylation and fibroblast migration.

Results

Amphiregulin is induced in membrane-separated co-cultures of tumor-supportive fibroblasts

I performed qRT-PCR analysis of AREG expression in membrane-separated co-cultures of Cal51 or MDAMB231 cells with either tumor-supportive fibroblasts (HFF1 and HFFF2) or non-supportive fibroblasts (Wi38 and CCD1112Sk). Following six days of co-culture, AREG was strongly induced in both HFF1 (9.9 and 11.6 fold) and HFFF2 (8.7 and 10.6 fold) co-cultured with Cal51 and MDAMB231 and weakly in Wi38 (0.19 and 0.39 fold) and CCD1112Sk (2.7 and 1.2 fold) fibroblasts (Figure 3.2).

RNAi suppression of amphiregulin restricts ability of tumor-supportive fibroblasts to promote tumorigenicity

To determine the effects of AREG silencing on the tumor-promoting ability of the HFFF2 fibroblasts, I generated HFFF2 cells stably expressing shRNAs targeting AREG by lentiviral infection. HFFF2 cells stably expressing a non-targeting shRNA (shN.T.) sequence was used as control. I tested four different shRNA constructs for their ability to silence AREG expression in HFFF2 fibroblasts. To determine knockdown efficiency, I performed qRT-PCR and western blot analysis. Three of four short hairpin constructs (shAREG-1, 2 and 3) effectively silence AREG expression below 20% of control (Figure 3.3, A & C). To ensure that AREG silencing did not result in effects on cell viability and proliferation, I performed MTT assays in fibroblasts and selected the two most growth neutral shRNA constructs for functional testing (Figure 3.3 B). To rule out non-specific effects of viral infections and shRNA targeting, HFFF2

cells expressing shRNAs targeting AREG were generated three times and knockdown efficiency was verified by qRT-PCR each time.

Figure 3.2

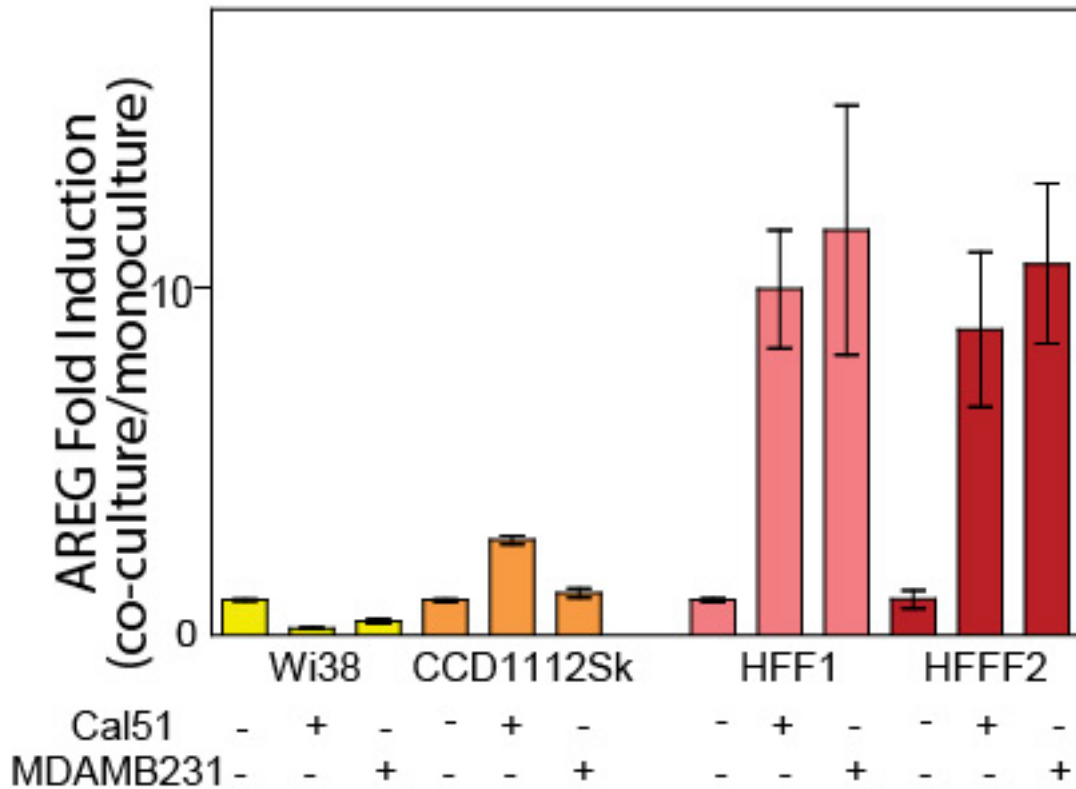


Figure 3.2: Amphiregulin is induced in co-cultured tumor-supportive fibroblasts

qRT-PCR analysis of Amphiregulin expression in non-supportive fibroblasts (NSFs)- Wi38 (yellow bars) or 1112Sk (orange bars) and tumor supportive fibroblasts (TSFs)- HFF1 (pink bars) or HFFF2 (red bars) using membrane separated co-cultures (CC) with breast cancer cells or monocultures. “+” CC Cal51 and “+” CC 231 indicate co-culture over six days with Cal51 and MDAMB231 cell lines respectively. Fold induction is represented as fold change of co-culture over monoculture in the same fibroblast line. Experiments were conducted from 3-4 independent co-cultures in triplicate wells. Error bars denote mean +/- SD.

Figure 3.3

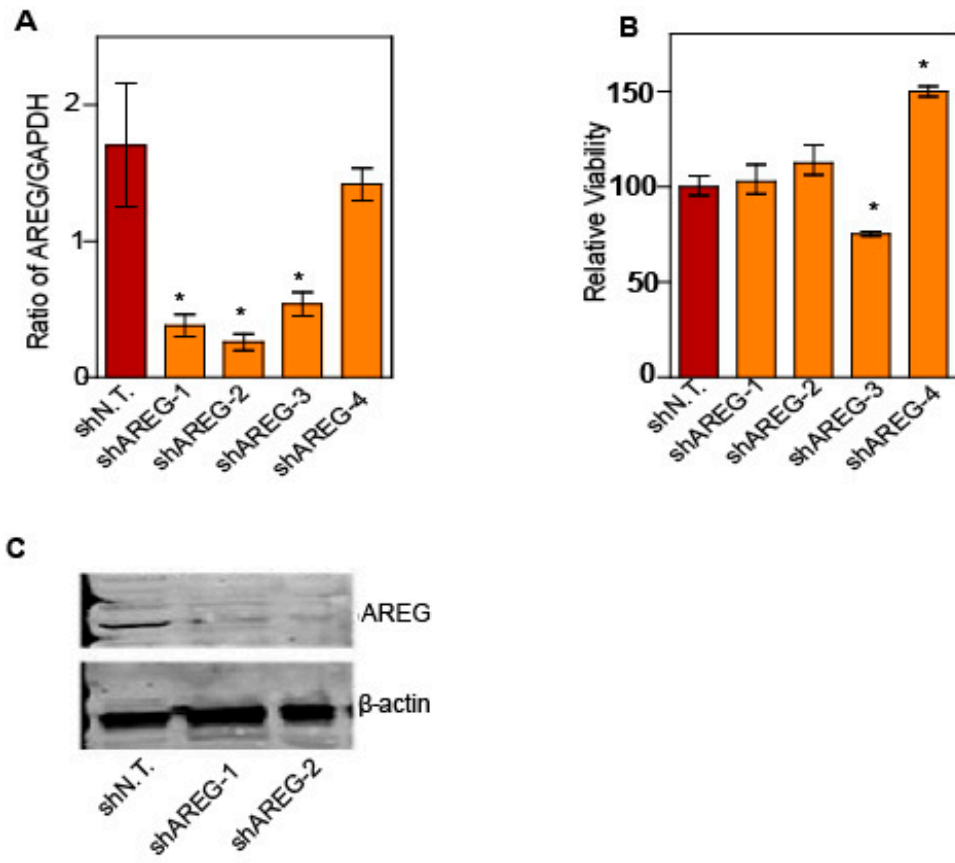


Figure 3.3: shRNA mediated silencing of amphiregulin expression in HFFF2 fibroblasts

A: qRT-PCR analysis of amphiregulin knockdown in HFFF2 fibroblasts. Ratio of Amphiregulin to GAPDH was used to quantify knockdown in HFFF2 fibroblasts expressing shRNA towards amphiregulin (shAREG-1, 2, 3 or 4) compared to HFFF2 cells expressing non-target shRNA (shN.T.). n= 4; bars represent the mean +/- SD. Asterisks indicate that the expression of amphiregulin is significantly different between the control (shN.T.) and the indicated group (shAREG-1, shAREG-2 or shAREG-3). * P < 0.01.

B: Relative viability of HFFF2 fibroblasts expressing shRNA towards amphiregulin (shAREG-1, 2, 3 or 4) compared to HFFF2 cells expressing non-target shRNA (shN.T.) was quantified using a 72-hour MTT assay. n=6; bars represent the mean +/- SD. Asterisks indicate that the expression of Amphiregulin is significantly different between the control (shN.T.) and the indicated group (shAREG-3 or shAREG-4). * P < 0.01.

C: Western blot analysis of amphiregulin knockdown in HFFF2 fibroblasts expressing shRNA towards amphiregulin (shAREG-1 and 2) compared to HFFF2 cells expressing non-target shRNA (shN.T.) using an antibody towards amphiregulin. β -actin was used as a loading control.

HFFF2 cells (1.5×10^6) expressing either non-target shRNA (shN.T.) or shRNA targeting amphiregulin (shAREG-1 and shAREG-2) were co-injected along with 1×10^6 Cal51 or MDAMB231 cells subcutaneously into 5-6 week old irradiated female nude mice. Tumor volumes are significantly smaller 3, 4, 5 and 6 weeks post injection with Cal51 cells and 5 and 6 weeks post injection with MDAMB231 cells compared to respective control groups. Growth kinetics of the subcutaneous injections are shown in Figure 3.4.A and 3.4.B.

Effects of amphiregulin silencing in vitro and in vivo

Since AREG is an EGF ligand and induces proliferation in some cancer cells, (Shoyab et al., 1988), I tested if addition of recombinant AREG could increase the proliferation of Cal51 and MDAMB231 cell lines *in vitro*. Doses from 10 to 100 ng/ml did not affect cell viability or proliferation 72 hours after treatment (Figure 3.5.A). In addition, recombinant amphiregulin caused a very small increase in proliferation of HFFF2 fibroblasts (Figure 3.5.B). To check if AREG played a role in proliferation of cancer cells *in vivo*, I analyzed tumors resulting from injection of Cal51 cells with HFFF2 cells expressing either non-targeting shRNA (shN.T.) or shRNA targeting AREG (shAREG-2) for the expression of Ki-67, a marker of proliferating cells (Figure 3.5 C). Silencing AREG in fibroblasts had a small effect on the proliferation of Cal51 cells *in vivo*, but this effect was not statistically significant ($P = 0.057$; Figure 3.5 D).

Figure 3.4

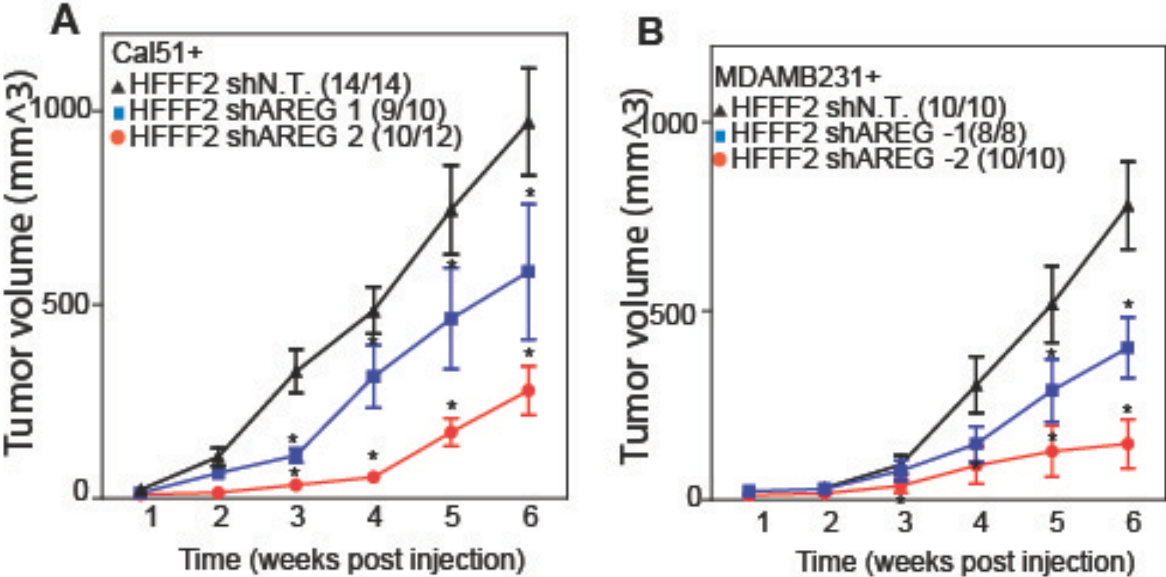


Figure 3.4: RNAi suppression of amphiregulin restricts pro-tumorigenic effect of tumor-supportive fibroblasts

A: Subcutaneous growth of Cal51 breast cancer cells co-injected with HFFF2 cells stably expressing either control shRNA (shN.T.; black triangles), shRNA targeting amphiregulin (shAREG-1; blue squares or shAREG-2; red circles). Tumor volumes were determined 1-6 weeks after injection. Tumor take rate/total injections for each group are indicated in parenthesis. Asterisks denote that the mean tumor group volume (shAREG-1 or shAREG-2) is significantly different than the control (shN.T). * $P < 0.05$. Error bars denote the mean \pm SEM.

B: Subcutaneous growth of MDAMB231 breast cancer cells co-injected with HFFF2 cells stably expressing either control shRNA (shN.T.; black triangles), shRNA targeting amphiregulin (shAREG-1; blue squares or shAREG-2; red circles). Tumor volumes were determined 1-6 weeks after injection. Tumor take rate/total injections for each group are indicated in parenthesis. Asterisks denote that the mean tumor group volume (shAREG-1 or shAREG-2) is significantly different than the control (shN.T). * $P < 0.05$. Error bars denote the mean \pm SEM.

Figure 3.5

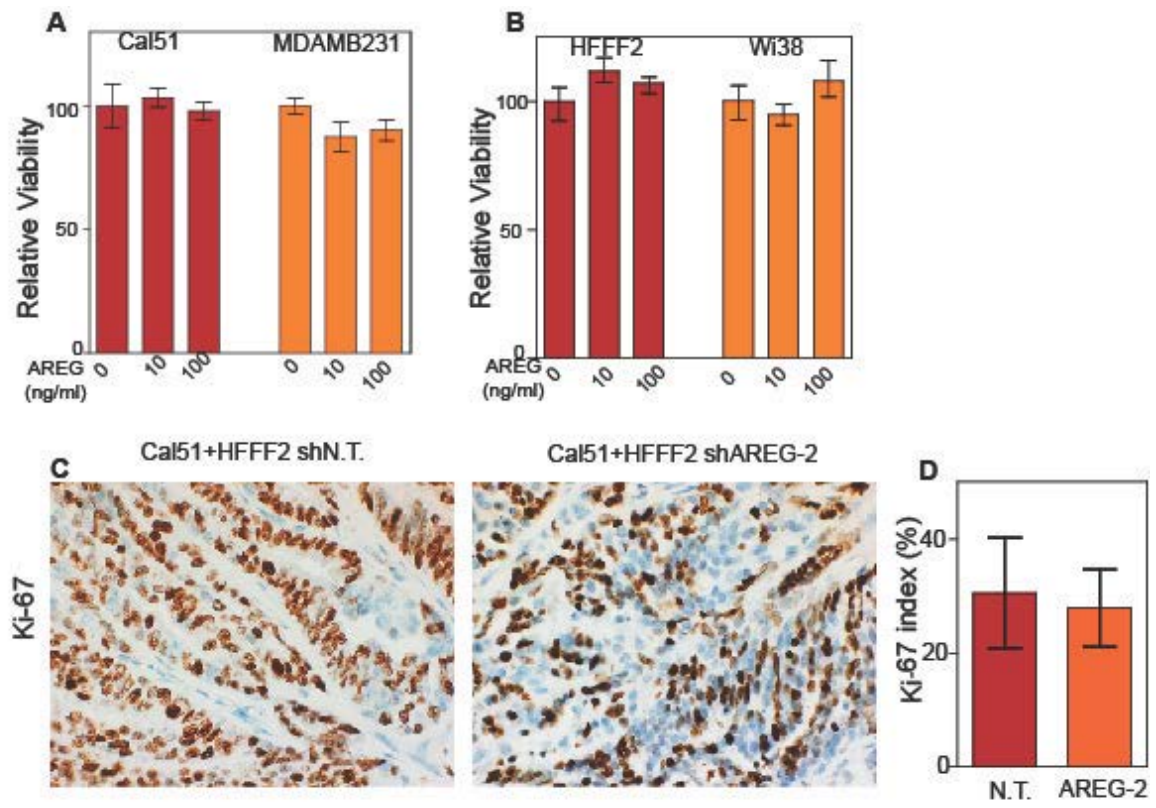


Figure 3.5: Amphiregulin does not cause proliferation *in vitro* or *in vivo*

A: Relative viability of Cal51 and MDAMB231 breast cancer cells treated with indicated dose of recombinant Amphiregulin (AREG-0, 10 or 100 ng/ml) was calculated using MTT assay 72-hour post treatment. Relative viability is expressed as a percentage of the untreated group (0 ng/ml) for each breast cancer cell line. n=6; Error bars denote the mean +/- SD.

B: Relative viability of HFFF2 and Wi38 fibroblasts treated with indicated dose of recombinant amphiregulin (AREG- 0, 10, 50 or 100 ng/ml) was calculated using MTT assay 72-hour post treatment. Relative viability is expressed as a percentage of the untreated group (0 ng/ml) for each fibroblast cell line. n=6; Error bars denote the mean +/- SD.

C: Immunostaining of proliferative cells in Cal51+HFFF2 tumors with control shRNA (shN.T.) or with shRNA targeting amphiregulin (shAREG-2) using an antibody to Ki-67. Panels are representative of multiple fields of tumor sections from five tumors per group.

D: Quantification of Ki-67 positive cells in Cal51+HFFF2 tumors with control shRNA (shN.T.) or with shRNA targeting Amphiregulin (shAREG-2). The number of Ki-67 positive cells were calculated as a percentage of total number of cells from five different fields of five different tumors per group. Error bars denote the mean +/- SD

However, tumors in which fibroblast secreted had been silenced (Cal51+ HFFF2shAREG-2) showed a drastic increase in necrosis when compared to the control group (Cal51+shN.T.) (Figure 3.6, A and B). Necrosis is dead tissue. AREG has been shown to have a role in both cell survival and death (Busser et al, 2011) indicating that silencing it in the fibroblast might affect survival signaling as well as vascularization (discussed below).

Since AREG binds and activates the EGF receptor, I hypothesized that silencing AREG might reduce the levels of phosphorylation of EGF on the epithelial cells. Indeed, when I compared phospho-EGFR levels (Tyr 1068) in tumor sections of Cal51 cells co-injected with HFFF2 fibroblasts expressing either non-targeting shRNA (shN.T.; control) or shRNA targeting AREG (shAREG-2), by immunostaining, phospho-EGFR was significantly lower in the AREG silenced tumors compared to the control (Figure 3.7, A and B).

Figure 3.6

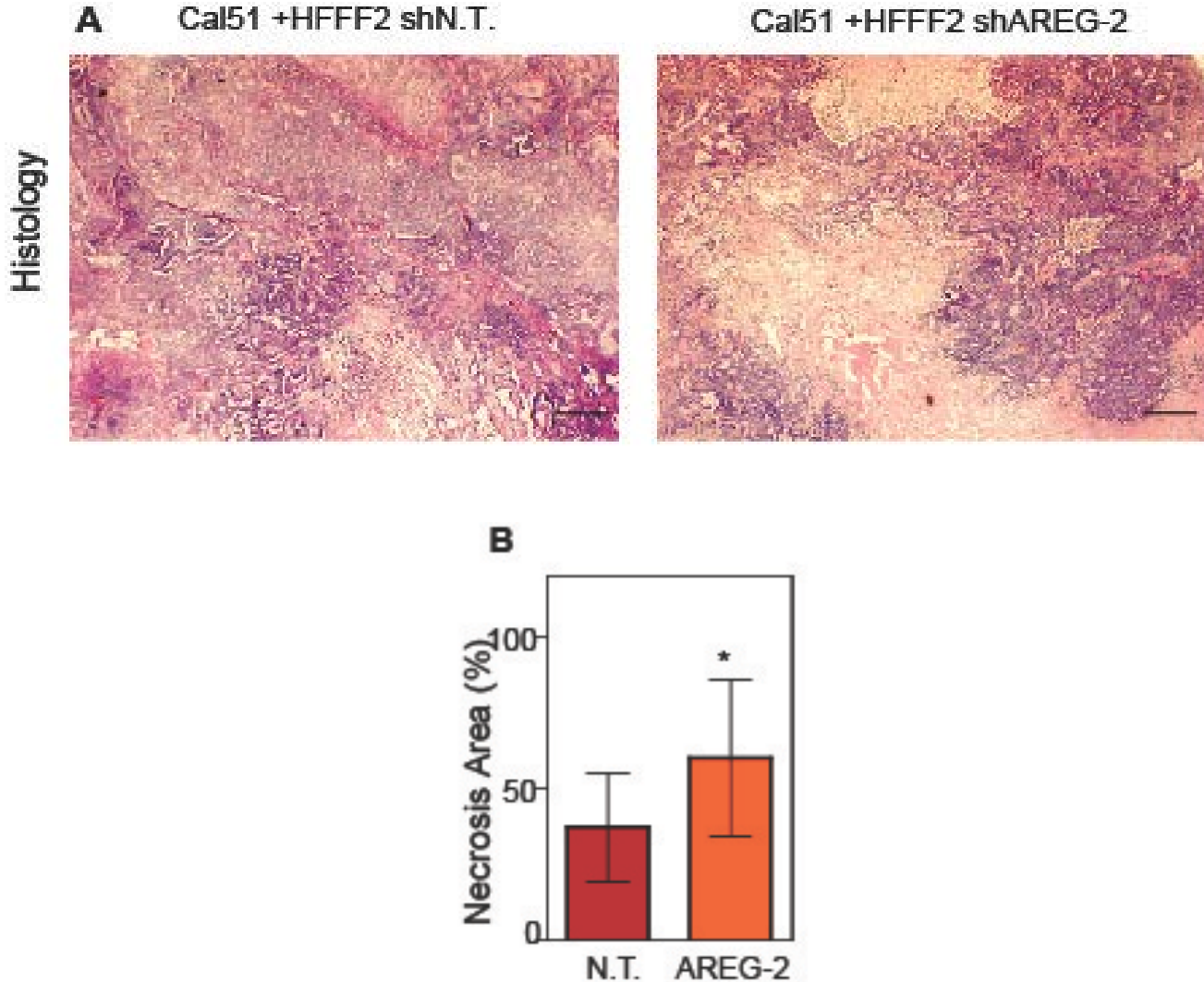


Figure 3.6: Amphiregulin silencing causes necrosis

A: Necrosis in Cal51+HFFF2 tumors with control shRNA (Cal51+HFFF2 shN.T.; left) or with shRNA targeting amphiregulin (shAREG-2; right) as visualized by H & E staining. Panels are representative of multiple fields of tumor sections from five tumors per group.

B: Quantification of necrosis in Cal51+HFFF2 tumors with control shRNA (shN.T.) or with shRNA targeting Amphiregulin (shAREG-2). Necrotic area was calculated from five different tumors per group. Asterisk indicates that the tumor group (shAREG-2) is significantly different than the control (shN.T.). * P < 0.05. Bars denote mean +/- SD.

Figure 3.7

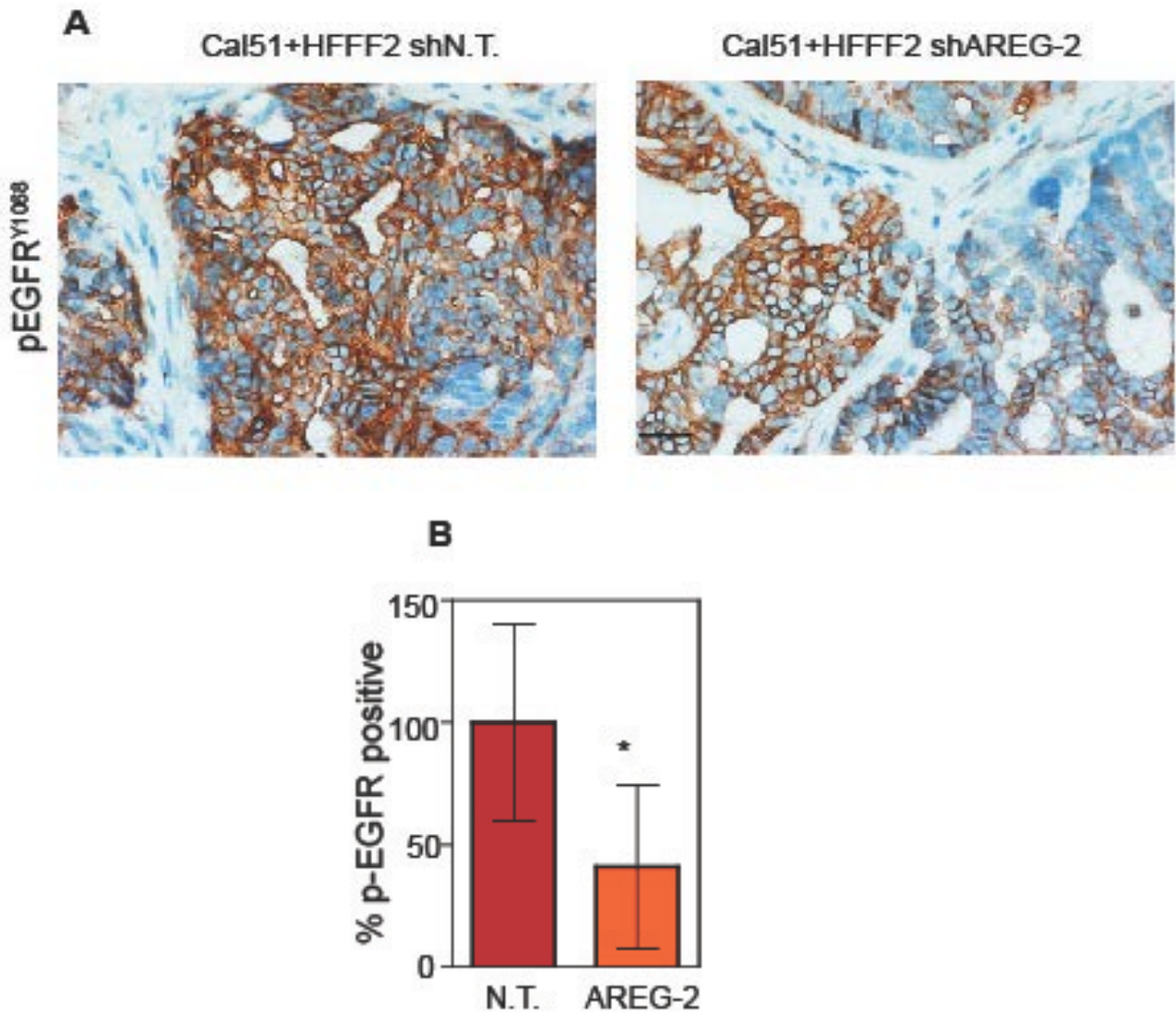


Figure 3.7: Amphiregulin silencing in fibroblasts affects phosphorylation of EGFR

A: Immunostaining of EGFR phosphorylation in Cal51+HFFF2 tumors with control shRNA (shN.T.) or with shRNA targeting amphiregulin (shAREG-2) using an antibody to phospho-EGFR (pEGFR; Tyr1068). Panels are representative of multiple fields of tumor sections from five tumors per group.

B: Quantification of phospho-EGFR positive cells in Cal51+HFFF2 tumors with control shRNA (shN.T.) or with shRNA targeting amphiregulin (shAREG-2). Area positive for pEGFR was calculated from five different fields of five different tumors per group. Asterisk indicates that the tumor group (shAREG-2) is significantly different than the control (shN.T.). *P < 0.05. Bars denote mean +/- SD.

Fibroblasts within tumors are often involved in recruitment of tumor-promoting immune cells as a mechanism to promote tumorigenicity (Mishra et al., 2011). AREG has previously been shown to attract immune cells (Hirota et al., 2012), so I wanted to determine if silencing AREG affects recruitment of monocytes and neutrophils by using an antibody to the marker 7-4 (Rosas et al., 2010). There was no difference in the recruitment of 7-4 positive cells to the tumors between the shAREG-2 and shN.T. groups (Figure 3.8, A and B).

In this system, injected HFFF2 fibroblasts increased the recruitment of α -SMA positive cells to the tumor (Chapter 2). Therefore, I tested if silencing AREG had an effect on number of α -SMA within the tumors. Indeed, α -SMA positive staining in the shAREG-2 tumor group was dramatically reduced compared to the control group (Figure 3.9, A and B). α -SMA is also marker of pericytes of blood vessels, but there was no difference in the pericyte coverage of blood vessels (data not shown). Additionally, there was no statistically significant difference in blood vessels between the two tumor groups (counting CD31 positive blood vessels in non-necrotic areas only) (Figure 3.9, C and D) indicating that the reduction was indeed in the reactive fibroblasts themselves.

To explain the effect of AREG silencing on the reduction in α -SMA positive cells in AREG silenced tumors, I explored two different mechanisms. In the first hypothesis, I tested if α -SMA expression was induced upon treatment with recombinant AREG. If this was true, then the reduction in α -SMA positive cells in AREG silenced tumors could be partially explained. Indeed, when HFFF2 cells were treated with different doses of AREG, α -SMA was significantly upregulated in HFFF2 fibroblasts. This induction was less striking in Wi38 fibroblasts (Figure 3.10)

Figure 3.8

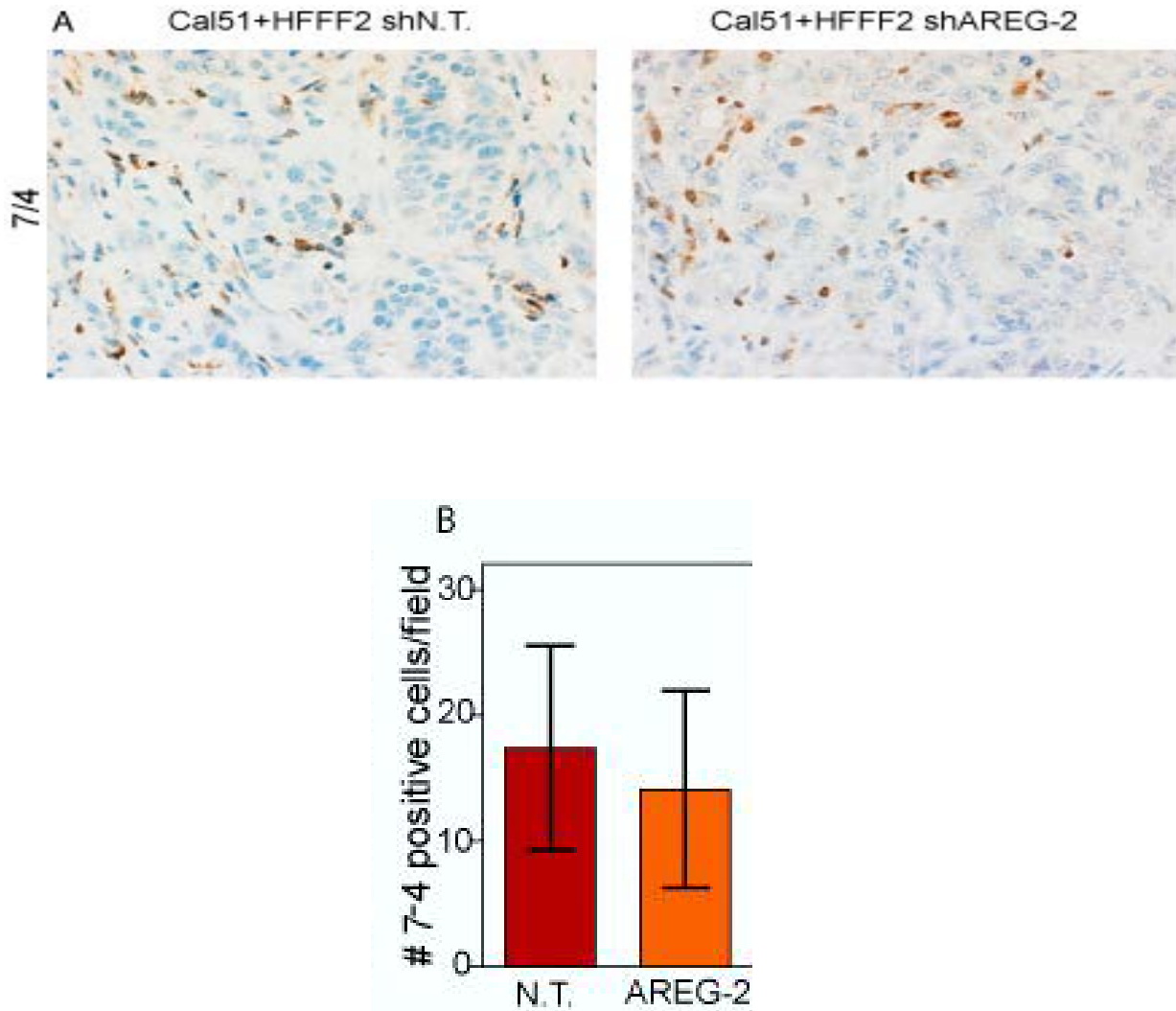


Figure 3.8: Amphiregulin silencing in fibroblasts does not affect immune cell recruitment

A: Immunostaining of neutrophils and monocytes in Cal51+HFFF2 tumors with control shRNA (shN.T.) or with shRNA targeting amphiregulin (shAREG-2) using an antibody to antigen 7-4 . Panels are representative of multiple fields of tumor sections from five tumors per group.

B: Quantification of 7/4 positive cells in Cal51+HFFF2 tumors with control shRNA (shN.T.) or with shRNA targeting amphiregulin (shAREG-2). 7/4 positive cells calculated from five different fields of five different tumors per group. Asterisk indicates that the tumor group (shAREG-2) is significantly different than the control (shN.T.). * P < 0.05. Bars represent mean +/- SD.

Figure 3.9

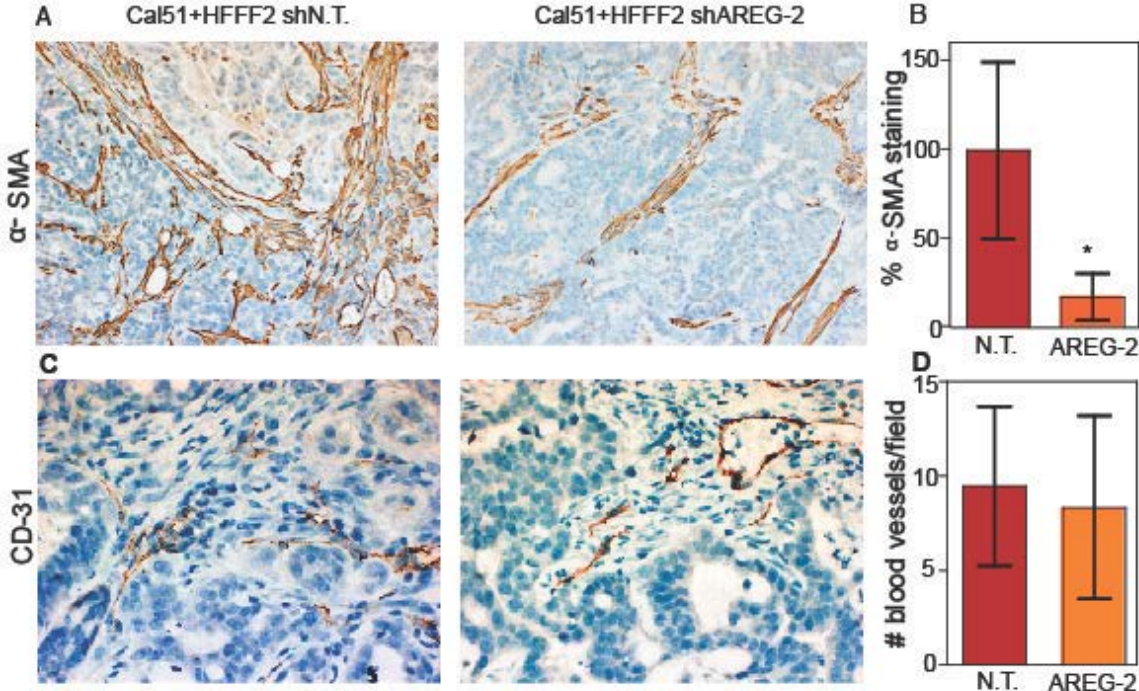


Figure 3.9: Amphiregulin silencing in fibroblasts affects recruitment of host fibroblasts

A: α -SMA immunostaining in Cal51+HFFF2 tumors with control shRNA (Cal51+HFFF2 shN.T.) or with shRNA targeting Amphiregulin (shAREG-2) using an antibody to α -SMA. Panels are representative of multiple fields of tumor sections from five tumors per group.

B: Quantification of α -SMA staining in Cal51+HFFF2 tumors with control shRNA (shN.T.) or with shRNA targeting amphiregulin (shAREG-2). α -SMA positive area was calculated from five different fields of five different tumors per group. Asterisk indicates that the tumor group (shAREG-2) is significantly different than the control (shN.T.). * $P < 0.05$. Bars represent mean \pm SD.

C: Immunostaining of blood vessels in Cal51+HFFF2 tumors with tumors with control shRNA (shN.T.) or with shRNA targeting Amphiregulin (shAREG-2) using an antibody to antigen CD31. Panels are representative of multiple fields of tumor sections from five tumors per group.

D: Quantification of blood vessels in Cal51+HFFF2 with control shRNA (shN.T.) or with shRNA targeting amphiregulin (shAREG-2) using an antibody to CD31. Number of blood vessels was calculated from five different fields of five different tumors per group. Bars represent mean \pm SD.

Figure 3.10

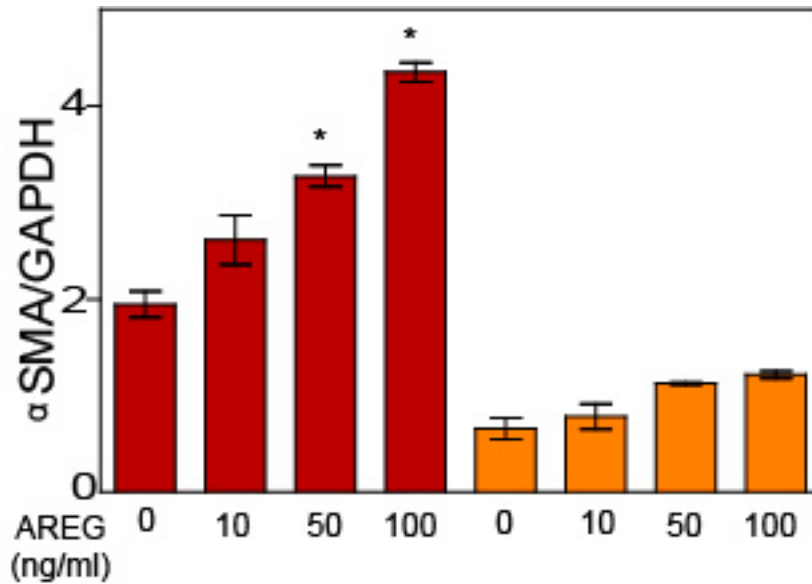


Figure 3.10: Amphiregulin upregulates α -SMA expression in tumor-supportive fibroblasts

A: qRT-PCR analysis of α -SMA expression in HFFF2 (red bars) and Wi38 (orange bars) fibroblasts treated with 10, 50 or 100 ng/ml of recombinant amphiregulin. α -SMA expression is represented as a ratio of α -SMA to GAPDH. Three independent treatments were used to quantify α -SMA and GAPDH expression. Asterisks indicate a significant difference in expression between untreated HFFF2 fibroblasts and recombinant AREG treated fibroblasts at 50 and 100ng/ml. * P < 0.05. Bars denote the mean \pm SD.

In the second hypothesis, I wanted to test a role for AREG in fibroblast migration. If AREG affected the migration (thereby recruitment) of host fibroblasts to the tumor site, it could explain, in part, the reduction of α -SMA positive fibroblasts in AREG silenced tumors. I assayed the role of AREG in fibroblast migration using wild-type mouse embryonic fibroblasts (WT-MEFs) in two independent *in vitro* migration assays. In the first assay, I tested the ability of WT-MEFs to migrate in a wound-healing assay using conditioned medium from HFFF2shN.T. (control) or HFFF2-shAREG-2 fibroblasts. Wound healing migration of WT-MEFS in conditioned medium from HFFF2-shAREG-2 fibroblasts was severely compromised (Figure 3.11, A and B). In the second assay, I used a Boyden chamber to assess if the migration of WT-MEFs towards HFFF2 AREG silenced fibroblasts was affected. Indeed, WT-MEF migration towards HFFF2-shN.T. (control) was significantly higher than towards HFFF2-shAREG-2 silenced fibroblasts (Figure 3.12, A and B).

Figure 3.11

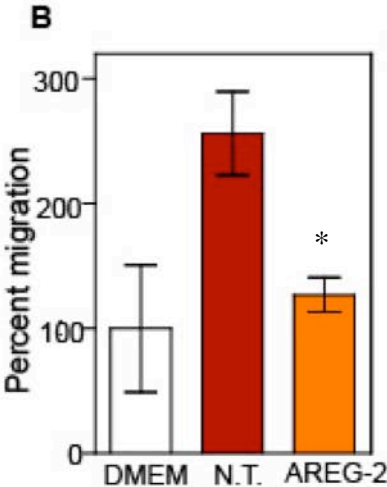
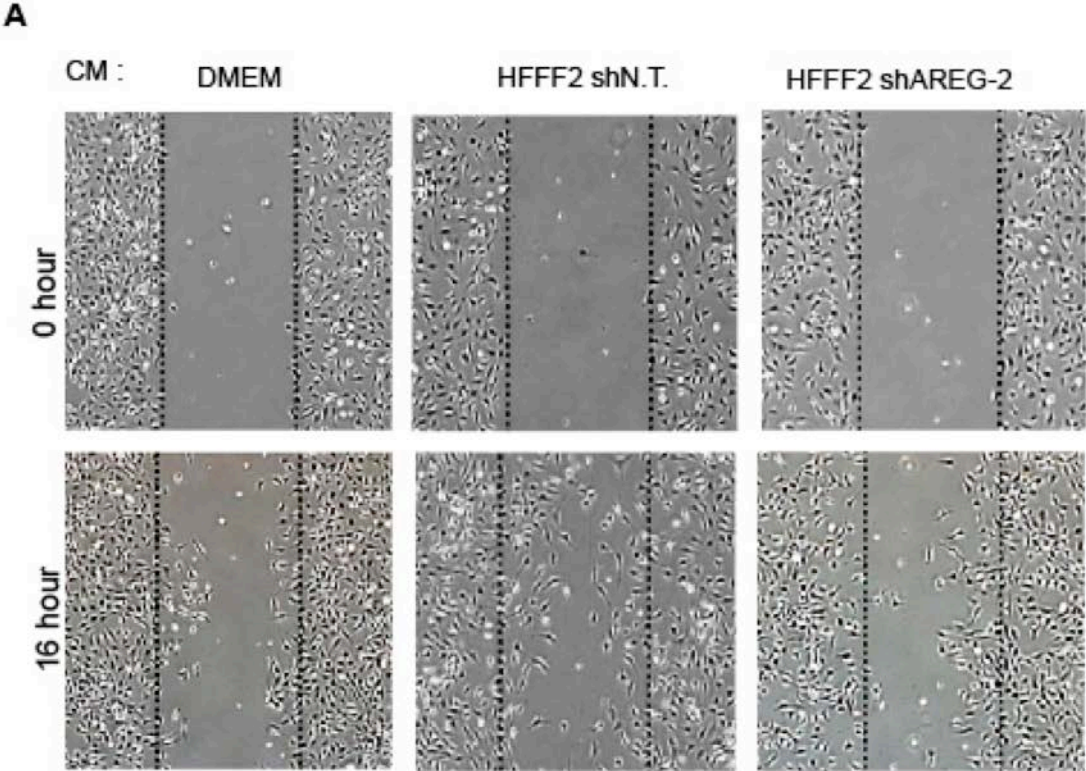


Figure 3.11: Amphiregulin affects migration of fibroblasts (SWHA)

A: Migration of wild-type Mouse Embryonic Fibroblasts in a scratch wound healing assay (SWHA) using DMEM (left), 24 hour-conditioned medium (CM) from HFFF2 fibroblasts expressing non-target shRNA (HFFF2shN.T.; center) or shRNA towards amphiregulin HFFF2shAREG-2; right). Migration was assessed at 0 and 16 hours post-scratch. Panels are representative of multiple fields from three independent experiments.

B: Quantification of migration (wound healing) in a scratch wound healing assay using DMEM (white bar), 24 hour-conditioned medium (CM) from HFFF2 fibroblasts expressing non-target shRNA (HFFF2shN.T.; red bar) or shRNA towards amphiregulin HFFF2shAREG-2; orange bar). Relative migration was quantified using migration in DMEM as 100%. n=9; Bars denote the mean +/- SD. Asterisk indicates a significant difference in mean migration between HFFF2shN.T. or HFFF2shAREG-2. * P <0.05.

Figure 3.12

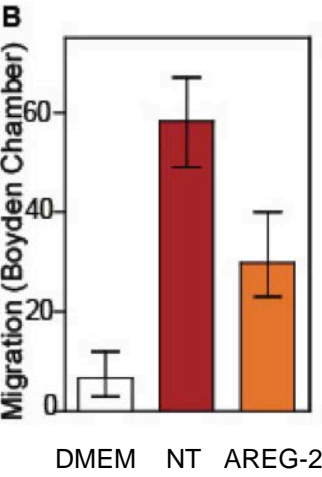
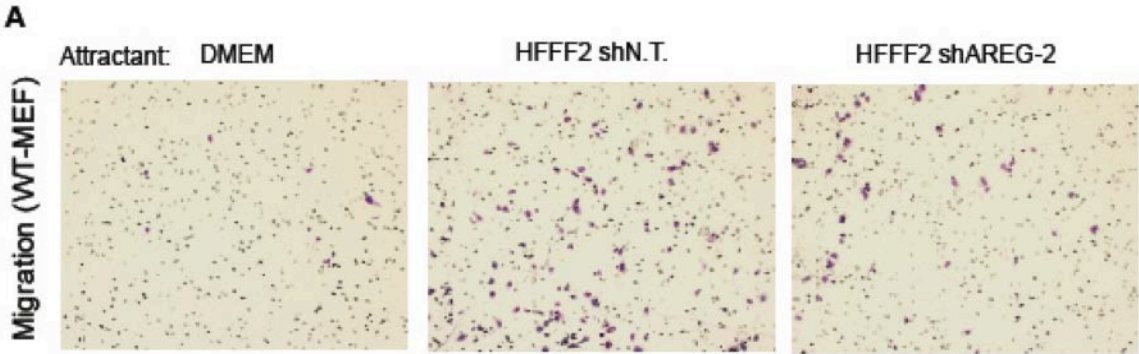


Figure 3.12: Amphiregulin affects migration of fibroblasts (BMA)

A: Migration of wild-type MEFs in a Boyden migration assay (BMA). DMEM, HFFF2 fibroblasts expressing control shRNA (HFFF2shN.T) or shRNA towards amphiregulin (HFFF2shAREG-2) were used as attractants in the lower chamber of the Boyden apparatus. Migration was calculated 5 hours post-plating. Panels are representative of multiple fields of view in three independent experiments.

B: Quantification of chemotaxis of wild-type MEFs in a boyden migration assay. DMEM (white bar), HFFF2 fibroblast non-target shRNA (HFFF2shN.T.; red bar) or shRNA towards Amphiregulin HFFF2shAREG-2; orange bar) were used as attractants in the lower chamber of the Boyden apparatus. Migration was calculated 5 hours post plating from five fields of triplicate experiments. Bars denote the mean +/- SD.

Discussion

The role of epithelial AREG in mammary development and cancer suggests that stromal AREG may play a functional role in breast cancer progression (Busser et al., 2011; McBryan et al., 2008; Willmarth and Ethier, 2008). Moreover, stromal AREG expression correlates with poor prognosis in breast cancer patients (Ma et al., 2001). Despite these indications, the functional role of stromally secreted AREG not been well characterized.

I demonstrate that RNAi mediated knockdown of fibroblast secreted AREG can significantly decrease tumor growth in xenograft tumors. This is distinct from the identification of an autocrine, functional role for AREG in breast cancer cells wherein silencing AREG in the breast epithelial cells affects tumor growth (Ma et al., 1999). This is consistent with previous studies identifying paracrine mechanisms of AREG action (Yasumoto et al., 2011). Despite affecting tumor growth, recombinant AREG does not induce proliferation of Cal51 and MDAMB231 cells *in vitro cells*. In addition, silencing AREG in fibroblasts does not affect proliferation of Cal51 *in vivo*. Basal breast cancer cell lines like Cal51 and MDAMB231 are known to be unresponsive to EGF (Lu et al., 2009). Hence, the lack of a proliferative response in relation to AREG is not surprising. Phosphorylation of the EGF-receptor can activate several other signaling cascades that regulate migration, invasion, survival and regulation of apoptosis (McBryan et al., 2008). I demonstrate that fibroblast produced AREG phosphorylates the EGF receptor on Cal51 *in vivo*, While this could partly explain why silencing fibroblast produced AREG restricts tumor growth, cellular mechanisms downstream of EGFR activation that are mediated by AREG are not fully clear. Further investigation would provide insight into the specific pathways stromal AREG regulates in breast cancer cells.

Areas of necrosis are composed of dead or dying cells and usually indicate poor vasculature (Paris et al., 1982). Tumors resulting from co-injections of Cal51 cells and shAREG-2 fibroblasts are highly necrotic. While there is no difference in the number of blood vessels in regions of live cells, I cannot preclude the possibility that silencing AREG causes a reduction in vasculature. This may be an additional mechanism through which fibroblast produced AREG affects tumor growth.

AREG upregulates the production of several cytokines that attract immune cells (Busser et al., 2011). However, in this system, silencing AREG does not affect the recruitment of antigen 7-4 expressing immune cells to the tumor site. Antigen 7-4 is expressed on neutrophils and a subset of monocytes. AREG may not recruit these cells, but could possibly have a role in recruitment of many other types of immune cells (Hirota et al., 2012). Immunostaining of tumor sections with markers of other types of immune cells will provide provide clues into the role of possible roles of AREG in immune cell recruitment.

Co-injected HFFF2 fibroblasts usually disappear within six-eight weeks post-injections (Chapter 2). However, the number of α -SMA positive cells in co-injected tumors remain significantly higher compared to the cell only injections even six weeks post injections (Chapter 2). Since Cal51+HFFF2-shAREG-2 tumors have significantly lower levels of α -SMA positive cells, I hypothesized that AREG may be involved in migration of fibroblasts to the tumor site. My results indicate that AREG plays a role in the migration of fibroblasts. This is quite likely because AREG has been shown to recruit granulocytes (Nakagome and Nagata, 2011) and epithelial cells (Fernandes et al., 1999). Moreover, other EGF family members like HB-EGF have roles in fibroblast migration (Yasumoto et al., 2011).

Induction of α -SMA is indicative of a reactive-fibroblast phenotype (Kojima et al., 2010). Recombinant AREG induces the expression of α -SMA in TSFs and NSFs. Further investigation could reveal if AREG is involved in generation of a reactive fibroblast phenotype during breast cancer progression.

In conclusion, I have identified three potentially different mechanisms through which stromal fibroblast secreted AREG may exert its actions. AREG regulates phosphorylation of EGFR on epithelial cells, migration of fibroblasts and α -sma expression in fibroblasts. A proposed model of amphiregulin action is shown in Figure 3.13.

Figure 3.13

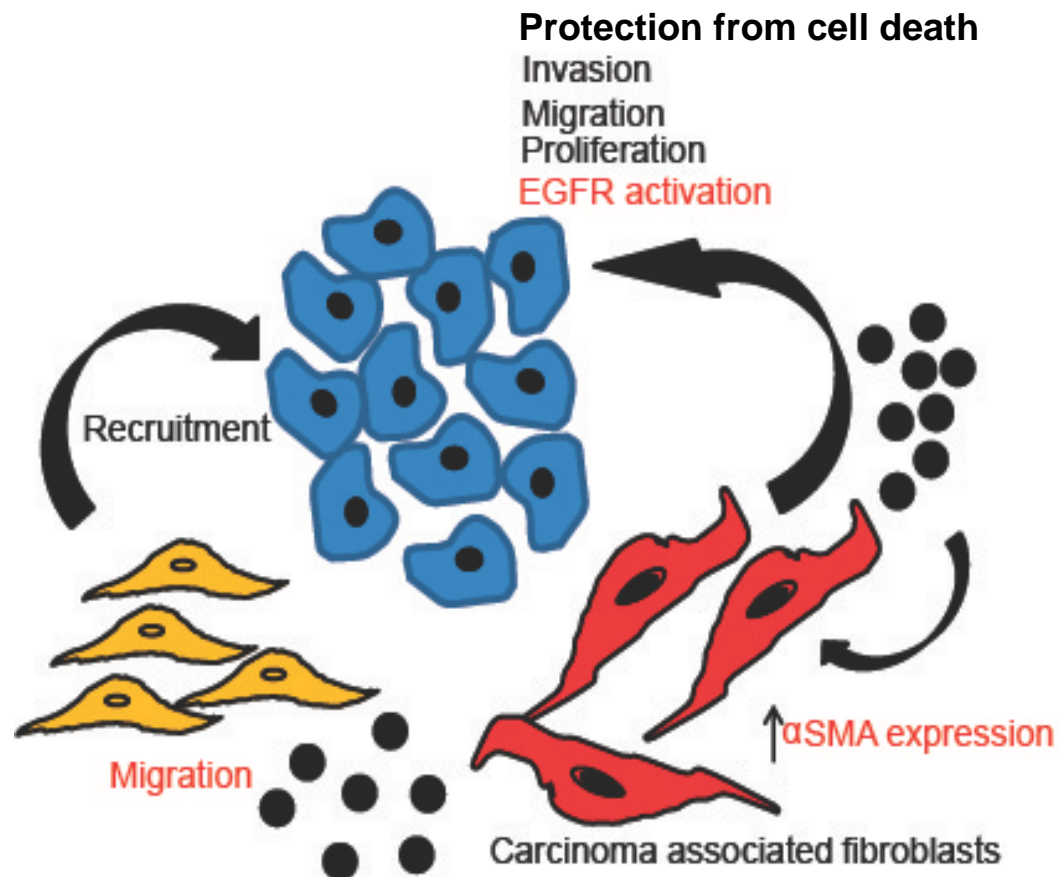


Figure 3.13: Modes of Amphiregulin action

Proposed modes of amphiregulin action. Autocrine or paracrine action of carcinoma-associated fibroblast (CAF; red shaded cells) induction of amphiregulin (black dots) causes proliferation, invasion and migration of breast cancer cells (blue shaded cells), migration of host fibroblasts (yellow shaded cells) and upregulation of α -SMA. Modes of action observed in this study are indicated in red text.

CHAPTER IV

Functional roles of fibroblast secreted CCL2, CCL7 and CCL8 in breast tumor-fibroblast interactions

Introduction

Chemokines (chemotactic cytokines) are a family of about 40 small, secreted proteins, ~8-14 Kd in size (Barbieri et al., 2010). They were first discovered for their ability to induce chemotaxis during tissue injury and wound healing (Fernandez and Lolis, 2002). Chemokines and their receptors play crucial roles in development, immune responses to infections and cancer (Balkwill, 2004).

A common structural feature of chemokines is the presence of four conserved cysteine residues that form disulphide bonds (Laing and Secombes, 2004). Depending on how many amino acids intervene the cysteine bonds, chemokines belong to one of four different classes: α chemokines (CXC- one amino acid); β chemokines (CC- no amino acid); γ chemokines (CX3C- three amino acids) and δ chemokines (only one cysteine).

Functionally, chemokines are either homeostatic or inflammatory based on their roles in normal tissues. Homeostatic chemokines modulate processes during embryonic development and under physiological conditions. For example, CXCL12 and its receptor CXCR4 are involved in blastocyst implantation (Ashley et al., 2011) and migration of neural crest cells (Rezzoug et al., 2011). Similarly, CCL19, CCL21 and their receptor CCR7 induce dendritic cell migration and lymph node development (Zlotnik et al., 2011). Inflammatory chemokines, on the other hand, are

induced upon tissue injury. CCLs 1- 21 and CXCLs 1-11 mediate wound healing by attracting innate immune cells, B and T lymphocytes, dendritic cells, natural killer cells and fibroblasts to sites of damaged tissue (Laing and Secombes, 2004; Thelen, 2001).

Chemokine signaling associated with wound healing is often coopted by tumors. One of their major functions is mediating inflammation (Balkwill, 2004). Proinflammatory, tumor-associated chemokines recruit endothelial cells and tumor promoting leukocytes. For example, CCL2 and CCL5 (Balkwill, 2004; Barbieri et al., 2010) recruit monocytes that undergo differentiation to become tumor-associated macrophages (TAMs). TAMs mediate a variety of functions in the microenvironment including ECM remodeling, angiogenesis and proliferation (Lin and Pollard, 2004). CCL17 recruits tumor-promoting T-lymphocytes (Faget et al., 2011) whereas CXCL12 and CXCL8 stimulate angiogenesis by recruiting endothelial cells to the tumor site (Mishra et al., 2011; Orimo et al., 2005). Chemokines can directly act on the cancer cells themselves: by inducing proliferation (Goede et al., 1999; Mishra et al., 2011), invasion (Jung et al., 2010) or migration (Lin et al., 2012).

Chemokines bind to G-protein coupled receptors resulting in their activation (Murdoch and Finn, 2000). Each class of chemokines binds to class-specific receptors. Though cross-reactivity between chemokines and receptors is common, inter-class cross-reactions are rare (Rossi and Zlotnik, 2000). The number of chemokines exceeds the number of receptors. Yet, chemokines bind multiple receptors. One of the main reasons for this crisscross pattern of ligand-receptor binding is to counteract the effects of viral proteins that inhibit host responses (Balkwill, 2012).

Chemokines CCL 2, 7 and 8 (Monocyte Chemotactic Proteins 1,2 and 3)

C-C Chemokines 2, 7 and 8 (Monocyte chemotactic proteins- MCP 1, 3 and 2) are closely related chemokines belonging to the β chemokine class. Their corresponding genes are located in a cluster on chromosome 17q11.2-12 suggesting that individual genes arose as a result of gene duplication events (Noso et al., 1994). The resulting proteins have a ~60% identity in amino acid sequences (Proost et al., 1996).

Of the three, CCL2 is best characterized in terms of its structure and functions (Rollins et al., 1988). CCL7 and 8 were identified as CCL2-related molecules (Alam et al., 1994; Decock et al., 1990; Van Damme et al., 1992). CCL2 is induced by the cytokines IL-1, TNF- α and IFN- γ (Larsen et al., 1989; Sica et al., 1990; Strieter et al., 1989) in endothelial cells, fibroblasts and monocytes (Vandamme et al., 1994). It mediates chemotaxis of monocytes, basophils, T-cells and NK cells (Noso et al., 1994; Taub et al., 1995), increases cellular calcium concentration, releases leukotrienes (Dahinden et al., 1994), arachidonic acid (Locati et al., 1994), histamines (Alam et al., 1992) and hydrogen peroxide (Rollins et al., 1991) from basophils and monocytes. CCL2 primarily binds to CCR2 (Neote et al., 1993) and may bind CCR1 at higher concentrations although this has been disputed by many groups.

CCL7 and CCL8 can also enhance chemotactic activities monocytes, NK cells, T-cells and basophils though they are less effective than CCL2 (Noso et al., 1994). In addition, they regulate the migration of eosinophils and dendritic cells (Alam et al., 1994; Noso et al., 1994). Both CCL7 and CCL8 induce histamine release from basophils (Uguccioni et al., 1995) whereas only CCL7 increases cellular calcium levels causing the release of leukotrienes (Sozzani et al., 1995). CCL7 and CCL8 bind CCR1, CCR2 and CCR5 (Proost et al., 1996).

CCL2, CCL7 and CCL8 in tumor progression

CCL2 immunostaining in invasive breast carcinoma samples is correlated with poorly differentiated tumor grade (Valkovic et al., 1998), increased neovascularization (Saji et al., 2001) and macrophage infiltration (Ueno et al., 2000). However, serum CCL2 levels are not prognostic (Lebrecht et al., 2004). Functionally, CCL2 regulates migration of leukocytes and mesenchymal stem cells to the tumor site and increases angiogenesis (Dwyer et al., 2007; Mishra et al., 2011). It also induces proliferation of cancer cells (Soria et al., 2011). CCL2 is a pro-metastatic molecule promoting breast cancer metastasis to the lungs (Nam et al., 2006) (Lu and Kang, 2009) by recruiting inflammatory monocytes (Qian et al., 2011).

Though CCL7 has been associated with recruitment of monocytes and inflammatory macrophages to the tumor site, functional roles for CCL7 in the tumor microenvironment have not been fully characterized (Okada et al., 2009). It was recently demonstrated that CAF secreted CCL7 promotes migration and invasion of oral squamous carcinoma cells in a co-culture model (Jung et al., 2010). Similarly, stromal CCL8 has been associated with inflammation but a functional role has not been well studied (Bianchi-Frias et al., 2010).

CCR1 is one of the receptors for CCL7 and CCL8 and may be a receptor for CCL2 at higher concentrations although this claim has been disputed (Noete et al, 1993). It is expressed on hepatoma, colon, oral squamous, non-small cell lung and breast carcinoma cells (Dagouassat et al., 2010; Jung et al., 2010; Kitamura et al., 2010; Robinson et al., 2003; Wang et al., 2009) and shown to have a role in migration of immature myeloid cells, proliferation and metastasis (Jung et al., 2010; Kitamura et al., 2010; Robinson et al., 2003).

In this experimental system, CCL2, 7 and 8 are selectively induced in co-cultures of tumor-supportive fibroblasts with breast cancer cells. They are also upregulated in primary

human breast stroma compared to normal stroma (Bauer et al., 2010; Finak et al., 2008; Ma et al., 2009). Interestingly, CCR1 is reciprocally upregulated in co-cultured breast epithelial cells. This reciprocal induction is an attractive model for testing direct and indirect effects of fibroblast produced chemokines in the tumor microenvironment.

I used shRNAs targeting either CCL2, 7 or 8 to silence their expression in tumor-supportive HFFF2 fibroblasts. In parallel, I silenced the expression of CCR1 in Cal51 and MDAMB231 breast cancer cells. I used co-injection assays to investigate the effect of silencing these genes on tumor growth and their ability to modulate the microenvironment. I demonstrate that silencing CCL2, 7 and 8 affect tumor growth significantly. These chemokines play diverse, non-redundant roles in tumor progression. CCL2 affects recruitment of neutrophils, inflammatory monocytes and blood vessels with no effects on tumor cell proliferation. CCL7 affects proliferation of tumor cells with no effect on recruitment of neutrophils and inflammatory monocytes and blood vessels. Silencing CCL8 does not affect tumor proliferation, yet has a minor but significant impact on recruitment of neutrophils and inflammatory monocytes.

Silencing CCR1 in breast cancer cells leads to a significant reduction in tumor growth in the presence of co-injected tumor-supportive fibroblasts. It affects cancer cell proliferation and recruitment of neutrophils and inflammatory monocytes.

Results

CCL2, CCL7 and CCL8 are induced in membrane-separated co-cultures of tumor-supportive fibroblasts

I measured transcript levels of fibroblast CCL2, CCL7 and CCL8 in membrane-separated co-cultures of Cal51 or MDAMB231 cells with tumor-supportive and non-supportive fibroblasts following six days of co-culture. All three chemokines were strongly induced in TSFs- HFF1 and HFFF2 co-cultured with Cal51 and MDAMB231 cells compared to NSFs- Wi38 and CCD1112Sk. Interestingly, CCL8 is not expressed in Wi38 fibroblasts (Figure 4.1).

RNAi suppression of CCL2, CCL7 and CCL8 restricts ability of tumor-supportive fibroblasts to promote tumorigenicity

To determine the effects of silencing CCL2, CCL7 and CCL8 on the tumor-promoting ability of the HFFF2 fibroblasts, I generated HFFF2 cells stably expressing shRNAs to target either CCL2, CCL7 or CCL8 by lentiviral transduction. HFFF2 cells stably expressing a non-targeting shRNA sequence was used as control. The ability of the shRNA to silence gene expression was evaluated by qRT-PCR or western blot by comparing HFFF2 cells expressing either control shRNA (shN.T.) or shRNAs targeting CCL2, CCL7 or CCL8. For each gene, two independent shRNA sequences effectively silenced expression (Figure 4.2, A-C). To make sure that shRNA targeting did not affect the growth of the fibroblasts negatively, I performed MTT assays to determine the relative viability of the shRNA transfectants and compared them to the control (shN.T.) (Figure 4.2, D-F).

Figure 4.1

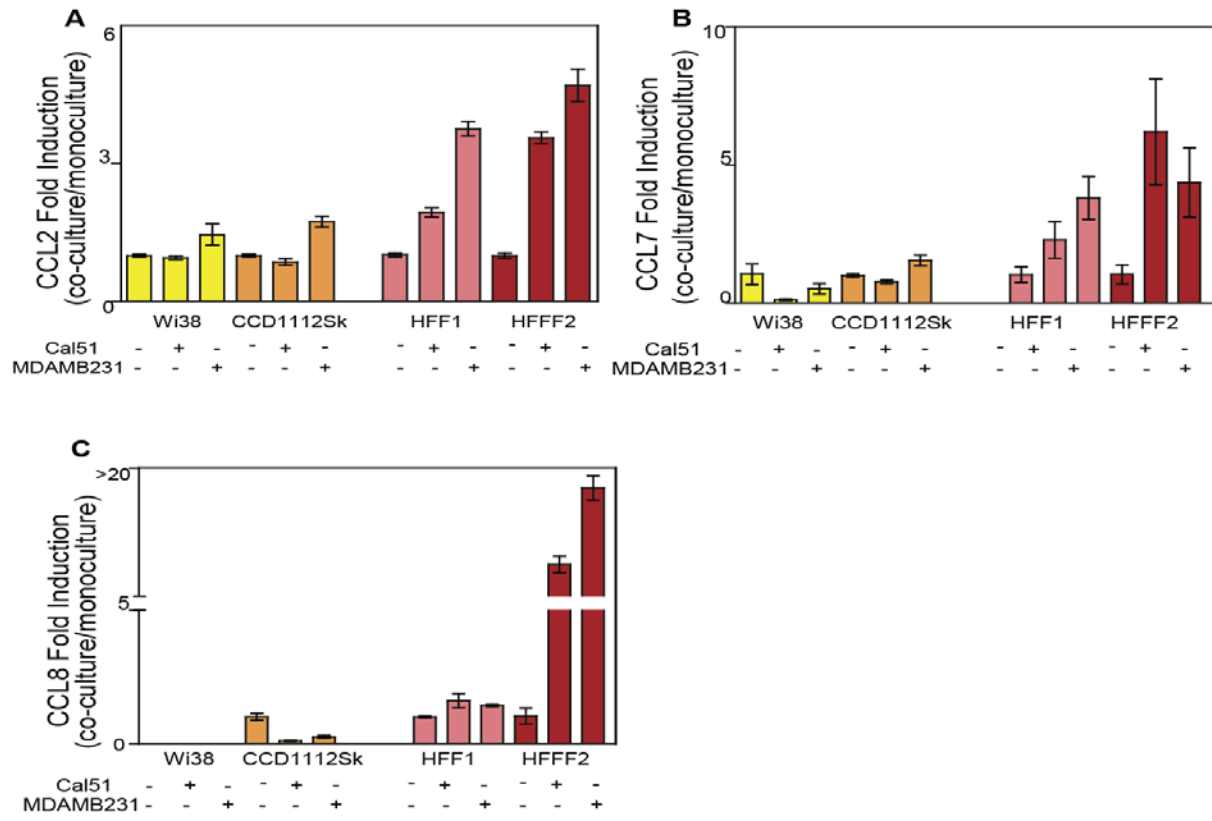


Figure 4.1: CCL2, CCL7 and CCL8 are induced in membrane-separated co-cultures of tumor-supportive fibroblasts and breast cancer cell lines

A: qRT-PCR analysis of CCL2 expression in non-supportive fibroblasts (NSFs)- Wi38 (yellow bars) or CCD1112Sk (orange bars) and tumor supportive fibroblasts (TSFs)- HFF1 (pink bars) or HFFF2 (red bars) using membrane separated co-cultures with breast cancer cells or monocultures. “+” Cal51 and “+” MDAMB231 indicate co-culture over six days with Cal51 and MDAMB231 cell lines respectively. Fold induction is represented as fold change of co-culture over monoculture in the same fibroblast line. n=6; Error bars represent mean +/- SD.

B: qRT-PCR analysis of CCL7 expression in non-supportive fibroblasts (NSFs)- Wi38 (yellow bars) or CCD1112Sk (orange bars) and tumor supportive fibroblasts (TSFs)- HFF1 (pink bars) or HFFF2 (red bars) using membrane separated co-cultures with breast cancer cells or monocultures. “+” Cal51 and “+” MDAMB231 indicate co-culture over six days with Cal51 and MDAMB231 cell lines respectively. Fold induction is represented as fold change of co-culture over monoculture in the same fibroblast line. n=6; Error bars represent mean +/- SD.

C: qRT-PCR analysis of CCL8 expression in non-supportive fibroblasts (NSFs)- CCD1112Sk (orange bars) and tumor supportive fibroblasts (TSFs)- HFF1 (pink bars) or HFFF2 (red bars) using membrane separated co-cultures with breast cancer cells or monocultures. “+” Cal51 and “+” MDAMB231 indicate co-culture over six days with Cal51 and MDAMB231 cell lines respectively. Wi38 fibroblasts do not express CCL8. Fold induction is represented as fold change of co-culture over monoculture in the same fibroblast line. n=6; Error bars represent mean +/- SD.

Figure 4.2

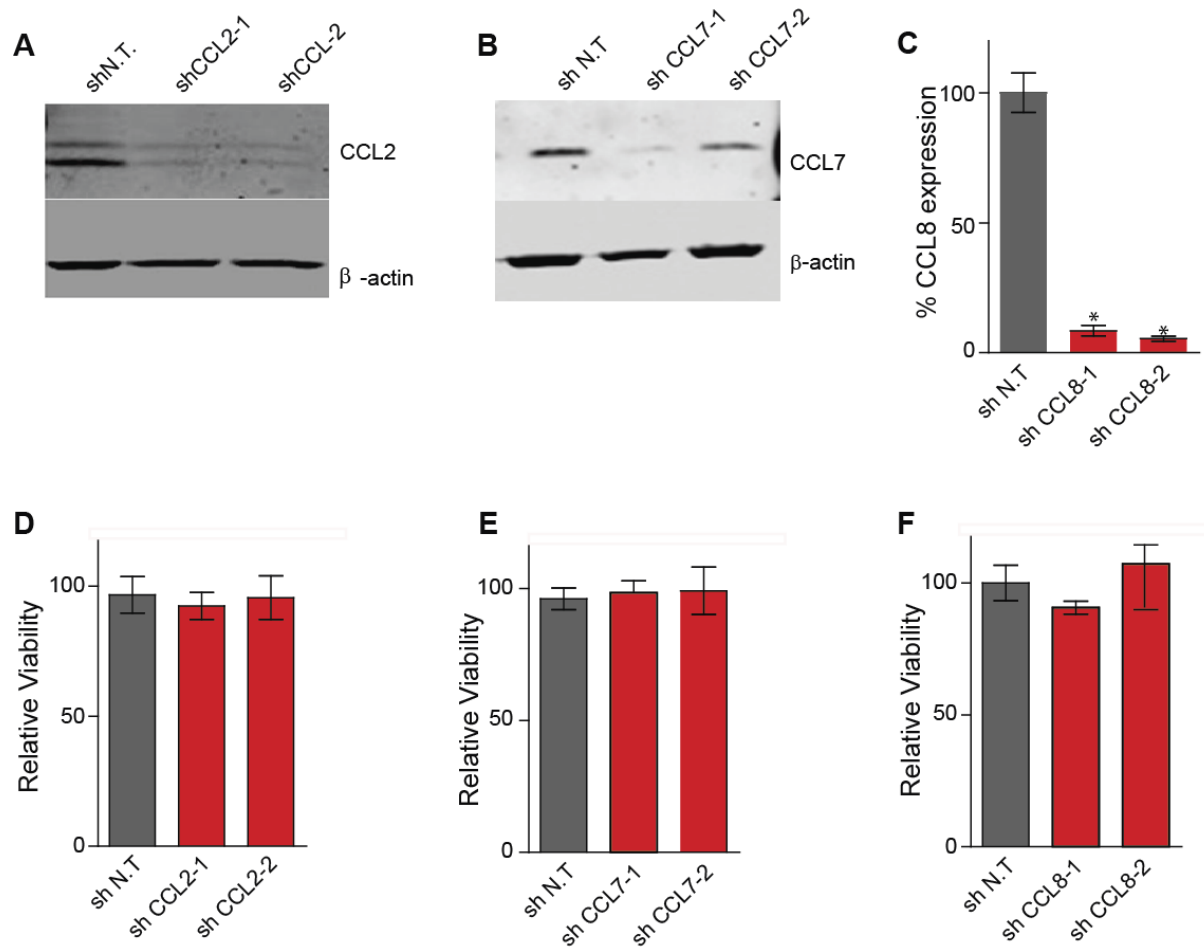


Figure 4.2: shRNAs targeting CCL2, CCL7 and CCL8 efficiently silence expression and are growth neutral

A: Western blot analysis of CCL2 knockdown in HFFF2 fibroblasts expressing shRNA towards CCL2 (shCCL2-1 and 2) compared to HFFF2 cells expressing non-target shRNA using an antibody towards CCL2. β -actin was used as a loading control.

B: Western blot analysis of CCL7 knockdown in HFFF2 fibroblasts expressing shRNA towards CCL7 (shCCL7-1 and 2) compared to HFFF2 cells expressing non-target shRNA using an antibody towards CCL2. β -actin was used as a loading control.

C: qRT-PCR analysis of CCL8 knockdown in HFFF2 fibroblasts. CCL8 expression in HFFF2 cells expressing either non-target shRNA (shN.T.) or CCL8 (shCCL8-1 or shCCL8-2) was calculated as a ratio of CCL8/GAPDH and expressed as a percentage of shN.T. n= 6, Error bars= +/- SD. Asterisks indicate that the expression of CCL8 is significantly different between the control (shN.T.) and the indicated group (shCCL8-1 and shCCL8-2). *P < 0.01.

D: Relative viability of HFFF2 fibroblasts expressing shRNA towards CCL2 (shCCL2-1 and shCCL2-2) compared to HFFF2 cells expressing non-target shRNA (shN.T) was quantified using a 72-hour MTT assay. n=6; Bars represent mean +/- SD.

E: As in D, but with HFFF2 fibroblasts expressing shRNA towards CCL7 (shCCL7-1 and shCCL7-2)

F: As in D, but with HFFF2 fibroblasts expressing shRNA towards CCL8 (shCCL8-1 and shCCL8-2)

HFFF2 cells (1.5×10^6) expressing either non-target shRNA (shN.T.) or shRNA targeting chemokines CCL2, CCL7 and CCL8 (shCCL2-1, 2; shCCL7-1, 2 and shCCL8-1, 2, respectively) were admixed with 1×10^6 Cal51 or MDAMB231 cells and injected subcutaneously into 5-6 week old irradiated female nude mice. Growth kinetics of these injections are shown in Figure 4.3 (CCL2), Figure 4.4 (CCL7) and Figure 4.5 (CCL8) respectively. Silencing CCL2 and CCL7 have significant reductions in tumor volume whereas the effect is less pronounced with silencing CCL8.

In vitro effects of CCL2, CCL7 and CCL8

Since shRNA mediated silencing of CCL2, CCL7 and CCL8 affected the protumorigenic ability of co-injected fibroblasts, I wanted to test if they had a direct effect on the proliferation of the breast cancer cell lines. Addition of recombinant CCL2, CCL7 or CCL8 to either Cal51 or MDAMB231 cells failed to cause a significant increase in proliferation (Figure 4.6). This indicates that some or all of their roles in tumor progression are mediated by interactions with other components of the tumor microenvironment.

Effects of silencing fibroblast-secreted CCL2, CCL7 and CCL8 on the tumor microenvironment

Chemokines modulate the tumor microenvironment by stimulating cancer cells to proliferate, promote angiogenesis and recruit pro-tumorigenic immune cells (Mishra et al., 2011). CCL2 has previously described roles in immune cell recruitment (Qian et al., 2011) and angiogenesis (Soria et al., 2011) so I wanted to test if silencing CCL2 in the HFFF2 fibroblasts had an effect on these processes. When sections resulting from co-injections of Cal51 tumor cells with HFFF2 fibroblasts expressing non-targeting shRNA (shN.T.) were compared with those

expressing shRNA targeting CCL2 (shCCL2-1), there was a significant decrease in the number of neutrophils and inflammatory monocytes (as evidenced by immunostaining using an antibody to 7-4) and the number of blood vessels (as evidenced by immunostaining using an antibody to CD31 (Figure 4.7 A, B and E-F). However, tumor cell proliferation and the number of reactive fibroblasts between the two tumor groups remained unchanged (Figure 4.7 C-D and G-H).

Functional roles of chemokines CCL7 and CCL8 in modulating the tumor microenvironment have not been well defined. As a starting point, I decided to test if silencing CCL7 or CCL8 expression had effects on tumor cell proliferation, neutrophil recruitment, number of blood vessels and reactive fibroblasts. Silencing CCL7 in the fibroblasts resulted in a significant reduction in tumor cell proliferation (Figure 4.8 A, E) compared to the control group, whereas it had no effect on recruitment of neutrophils and inflammatory monocytes, blood vessels and reactive fibroblasts (Figure 4.8 B-D, F-G). Silencing CCL8, on the other hand, caused a reduction in the recruitment of neutrophils and monocytes (Figure 4.8 B, F) and reactive fibroblasts (Figure 4.8 D, H), but did not affect tumor cell proliferation and number of blood vessels (Figure 4.8 A, C, E and G).

Figure 4.3

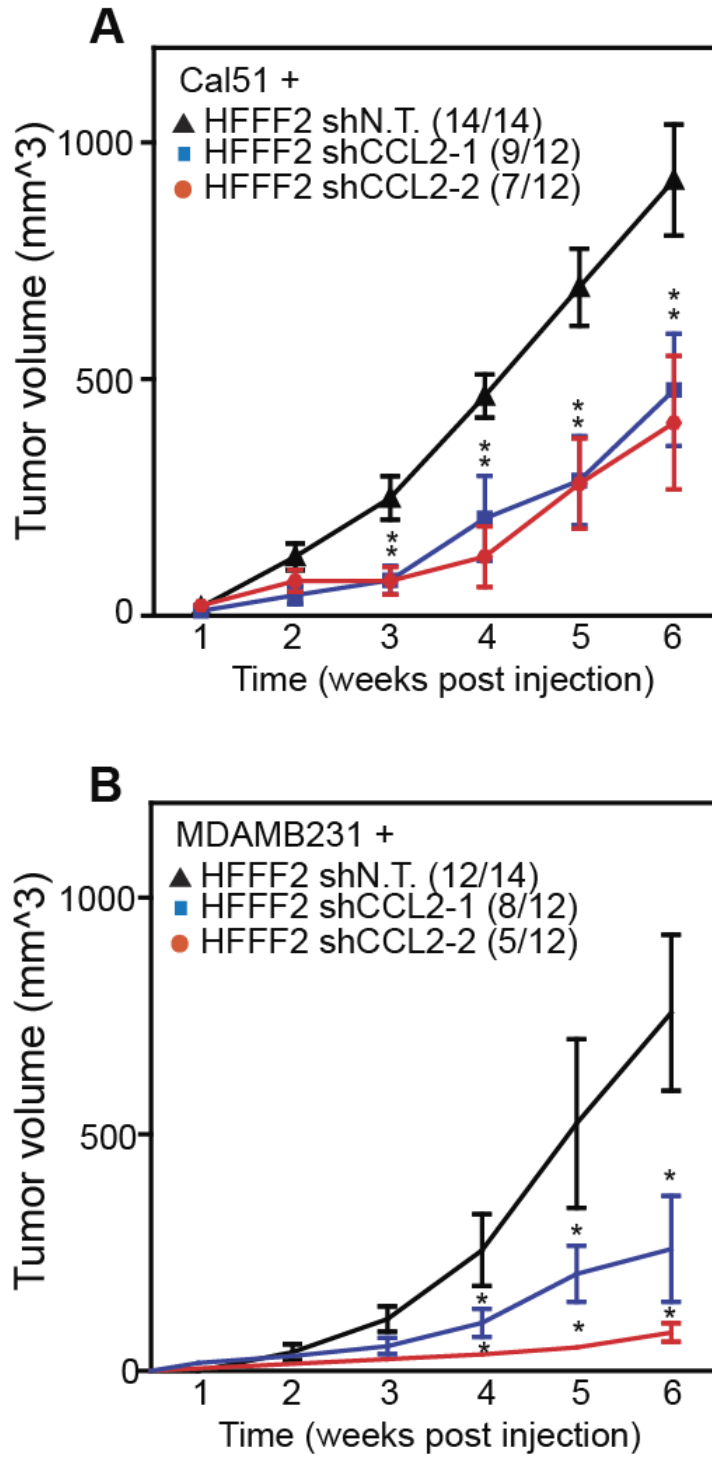


Figure 4.3: RNAi suppression of CCL2 restricts protumorigenic ability of tumor-supportive fibroblasts

A: Subcutaneous growth of Cal51 breast cancer cells co-injected with HFFF2 cells stably expressing either control shRNA (shN.T; black triangles), shRNA targeting CCL2 (shCCL2-1; blue squares or shCCL2-2; red circles). Tumor volumes were determined 1-6 weeks after injection. Tumor-take rate/total injections for each group are indicated in parenthesis. Asterisks denote that the tumor group (shCCL2-1 or shCCL2-2) is significantly different than the control (shN.T). * P < 0.05. Error bars represent the mean \pm SEM.

B: Subcutaneous growth of MDAMB231 breast cancer cells co-injected with HFFF2 cells stably expressing either control shRNA (shN.T; black triangles), shRNA targeting CCL2 (shCCL2-1; blue squares or shCCL2-2; red circles). Tumor volumes were determined 1-6 weeks after injection. Tumor take rate/total injections for each group are indicated. Asterisks denote that the tumor group (shCCL2-1 or shCCL2-2) is significantly different than the control (shN.T.). * P < 0.05. Error bars represent the mean \pm SEM.

Figure 4.4

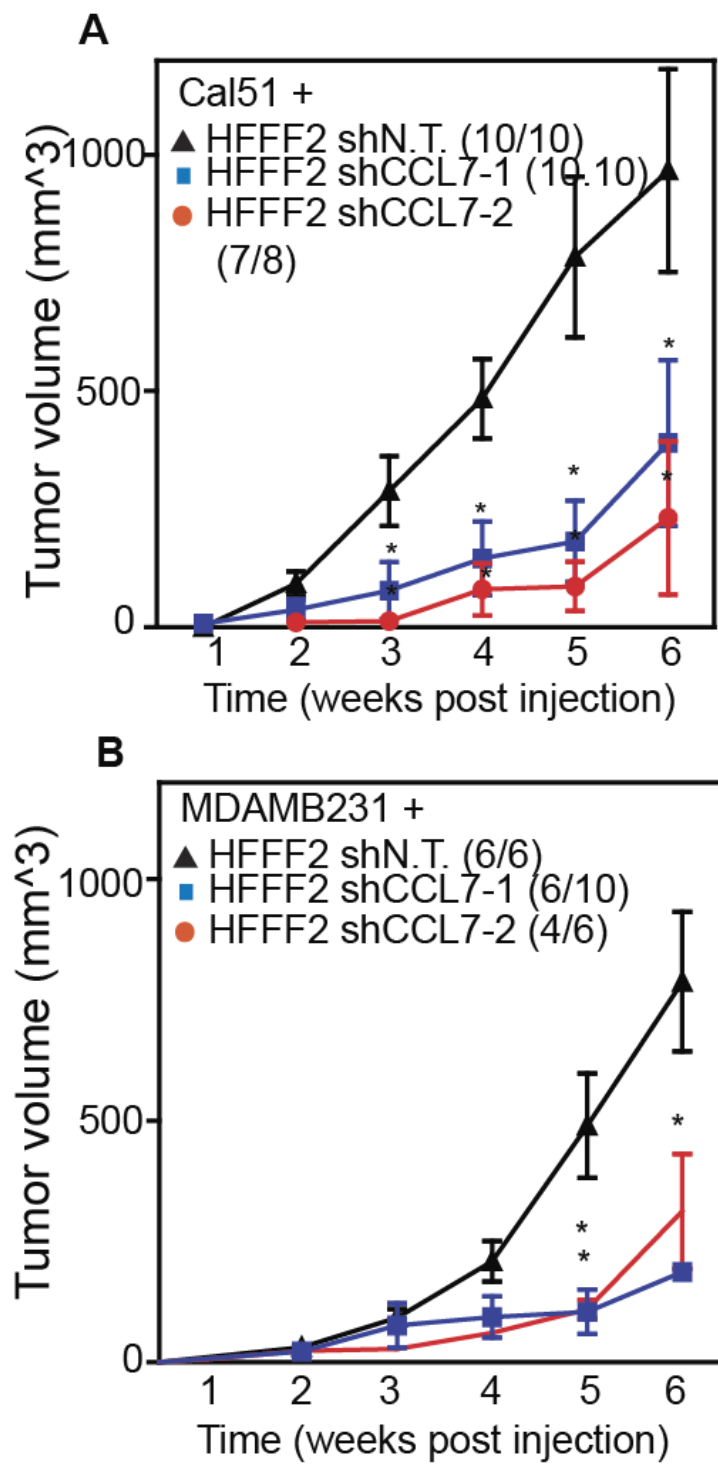


Figure 4.4: RNAi suppression of CCL7 restricts protumorigenic ability of tumor-supportive fibroblasts

A: Subcutaneous growth of Cal51 breast cancer cells co-injected with HFFF2 cells stably expressing either control shRNA (shN.T; black triangles), shRNA targeting CCL7 (shCCL7-1; blue squares or shCCL7-2; red circles). Tumor volumes were determined 1-6 weeks after injection. Tumor take rate/total injections for each group are indicated. Asterisks denote that the tumor group (shCCL7-1 or shCCL7-2) is significantly different than the control (shN.T). * $P < 0.05$. Error bars represent the mean \pm SEM.

B: Subcutaneous growth of MDAMB231 breast cancer cells co-injected with HFFF2 cells stably expressing either with control shRNA (shN.T; black triangles), shRNA targeting CCL7 (shCCL7-1; blue squares or shCCL7-2; red circles). Tumor volumes were determined 1-6 weeks after injection. Tumor take rate/total injections for each group are indicated. Asterisks denote that the tumor group (shCCL7-1 or shCCL7-2) is significantly different than the control (shN.T). * $P < 0.05$. Error bars represent the mean \pm SEM.

Figure 4.5

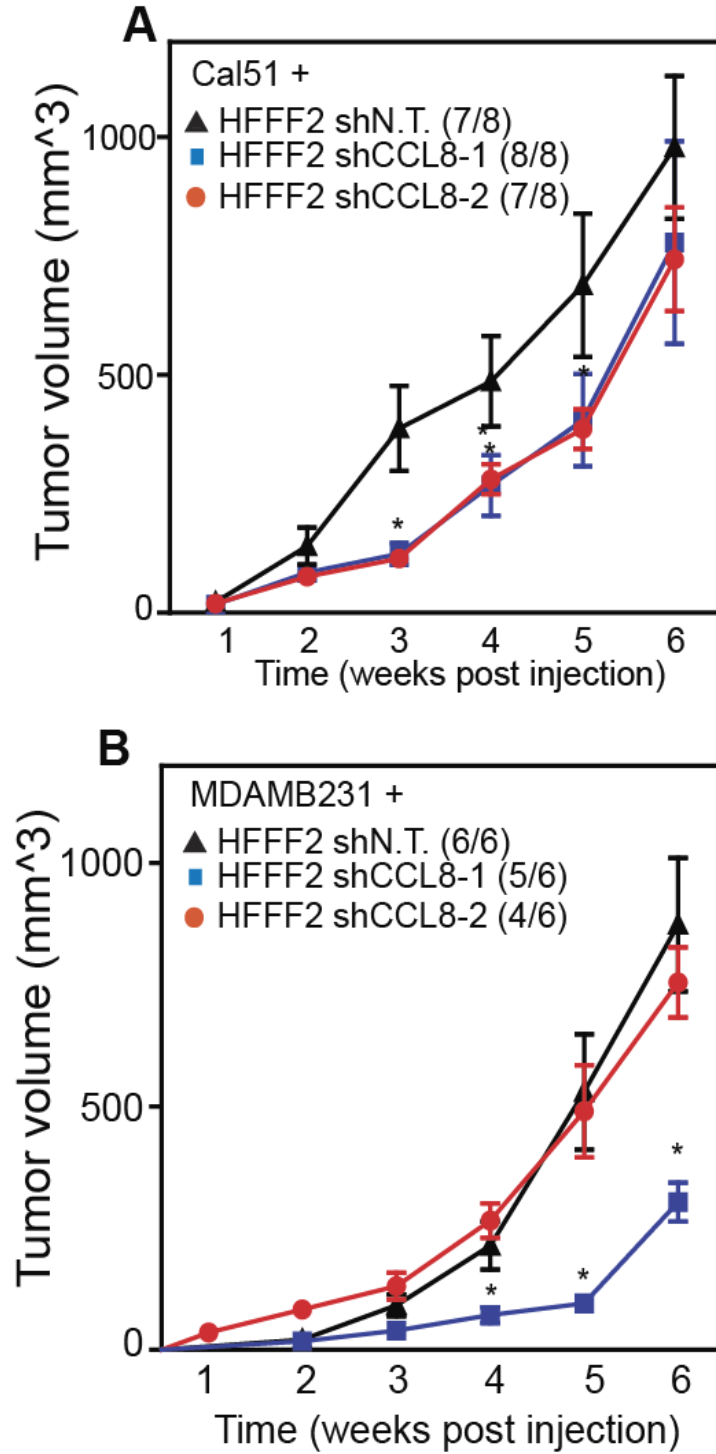


Figure 4.5: RNAi suppression of CCL8 has a minor effect on the protumorigenic ability of tumor-supportive fibroblasts

A: Subcutaneous growth of Cal51 breast cancer cells co-injected with HFFF2 cells stably expressing either control shRNA (shN.T.; black triangles), shRNA targeting CCL8 (shCCL8-1; blue squares or shCCL8-2; red circles). Tumor volumes were determined 1-6 weeks after injection. Tumor take rate/total injections for each group are indicated. Asterisks denote that the tumor group (shCCL8-1 or shCCL8-2) is significantly different than the control (shN.T). * $P < 0.05$. Error bars represent the mean \pm SEM.

B: Subcutaneous growth of MDAMB231 breast cancer cells co-injected with HFFF2 cells stably expressing either control shRNA (shN.T.; black triangles), shRNA targeting CCL8 (shCCL8-1; blue squares or shCCL8-2; red circles). Tumor volumes were determined 1-6 weeks after injection. Tumor take rate/total injections for each group are indicated. Asterisks denote that the tumor group (shCCL8-1) is significantly different than the control (shN.T). * $P < 0.05$. Error bars represent the mean \pm SEM.

Figure 4.6

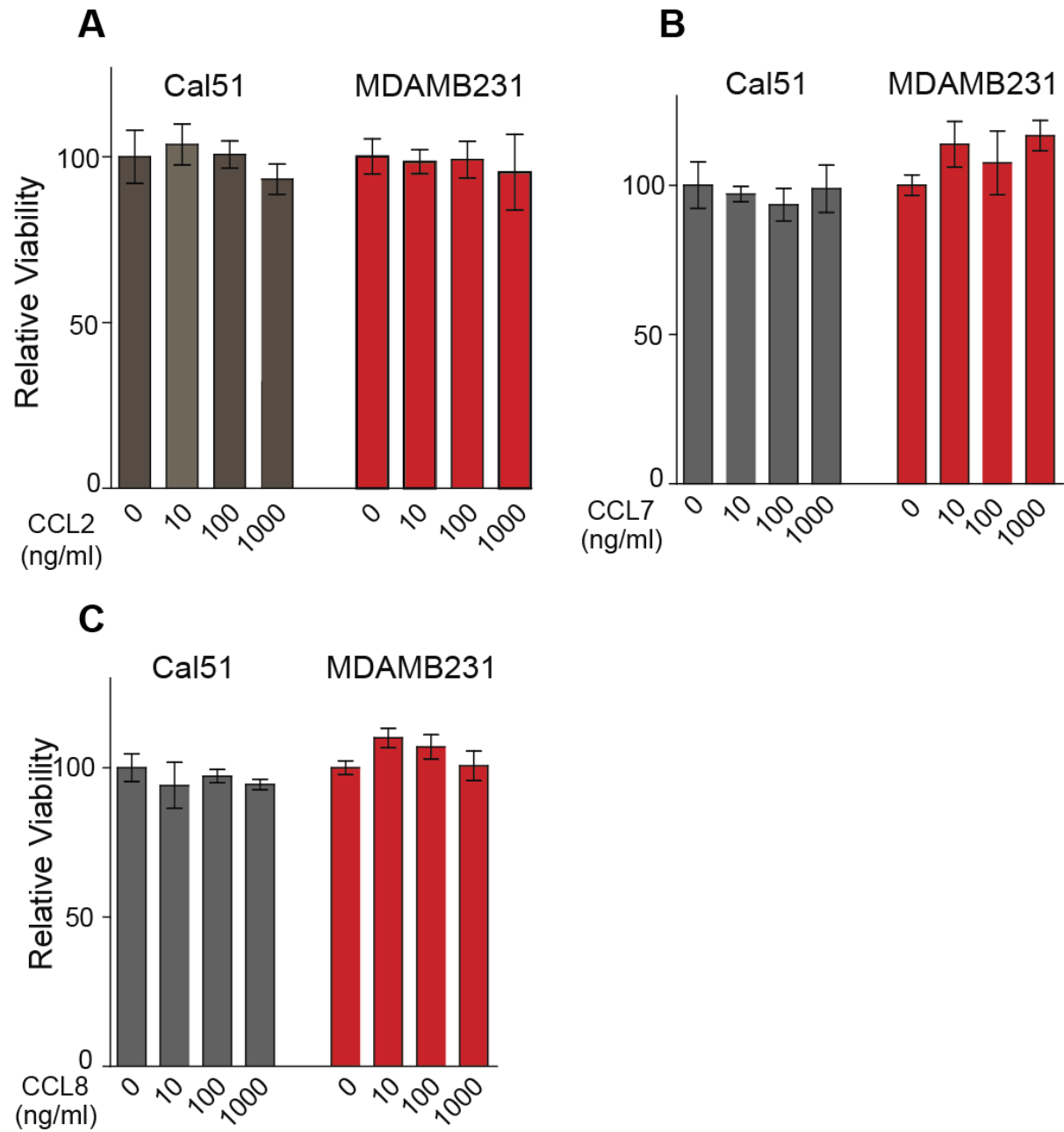


Figure 4.6: CCL2, CCL7 and CCL8 do not affect proliferation of breast cancer cells *in vitro*

A: Relative viability of Cal51 and MDAMB231 breast cancer cells treated with indicated dose of recombinant CCL2 (CCL2-0, 10, 100 or 1000 ng/ml) was calculated using MTT assay 72-hour post treatment. Relative viability is expressed as a percentage of the untreated group (0 ng/ml) for each cell line. n=6; Error bars represent the mean +/- SD.

B: Relative viability of Cal51 and MDAMB231 breast cancer cells treated with indicated dose of recombinant CCL7 (CCL7-0, 10, 100 or 1000 ng/ml) was calculated using MTT assay 72-hour post treatment. Relative viability is expressed as a percentage of the untreated group (0 ng/ml) for each cell line. n=6; Error bars represent the mean +/- SD.

C: Relative viability of Cal51 and MDAMB231 breast cancer cells treated with indicated dose of recombinant CCL8 (CCL8-0, 10, 100 or 1000 ng/ml) was calculated using MTT assay 72-hour post treatment. Relative viability is expressed as a percentage of the untreated group (0 ng/ml) for each cell line. n=6; Error bars represent the mean +/- SD.

Figure 4.7

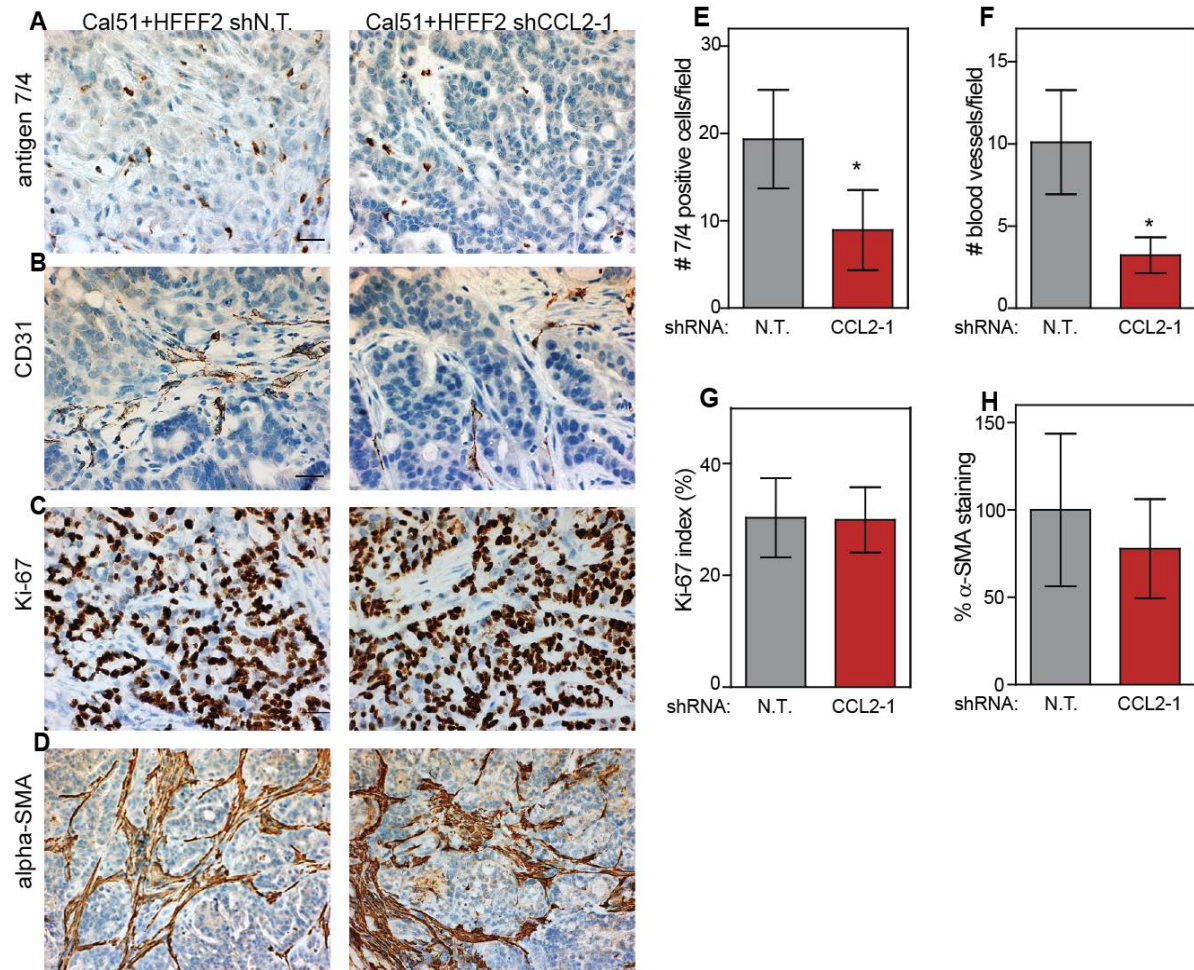


Figure 4.7: In vivo effects of silencing fibroblast secreted CCL2

A: Immunostaining of neutrophils and a monocytes in Cal51+HFFF2 tumors with control shRNA (shN.T.) or with shRNA targeting CCL2 (shCCL2-1) using an antibody to antigen 7-4. Panels are representative of multiple fields of tumor sections from five tumors per group.

B: Immunostaining blood vessels in Cal51+HFFF2 tumors with control shRNA (shN.T.) or with shRNA targeting CCL2 (shCCL2-1) using an antibody to CD31. Panels are representative of multiple fields of tumor sections from five tumors per group.

C: Immunostaining of proliferative cells in Cal51+HFFF2 tumors with control shRNA (shN.T.) or with shRNA targeting CCL2 (shCCL2-1) using an antibody to Ki-67. Panels are representative of multiple fields of tumor sections from five tumors per group.

D: Immunostaining of reactive fibroblasts in Cal51+HFFF2 tumors with control shRNA (shN.T.) or with shRNA targeting CCL2 (shCCL2-1) using an antibody to α -SMA. Panels are representative of multiple fields of tumor sections from five tumors per group.

E: Quantification of neutrophils and monocytes in Cal51+HFFF2 tumors with control shRNA (shN.T.) or with shRNA targeting CCL2 (CCL2-1) using an antibody to antigen 7/4. Number of 7/4 positive cells were calculated from five different fields of five different tumors per group. Error bars represent mean \pm SD. Asterisk indicates a significant difference between HFFF2shN.T and HFFF2shCCL2-1. *P < 0.05.

F: As in E, but quantification of blood vessels using an antibody to CD31.

G: As in E, but quantification of proliferative cells using an antibody to Ki-67.

H: As in E, but quantification of reactive fibroblasts using an antibody to α -SMA

Figure 4.8

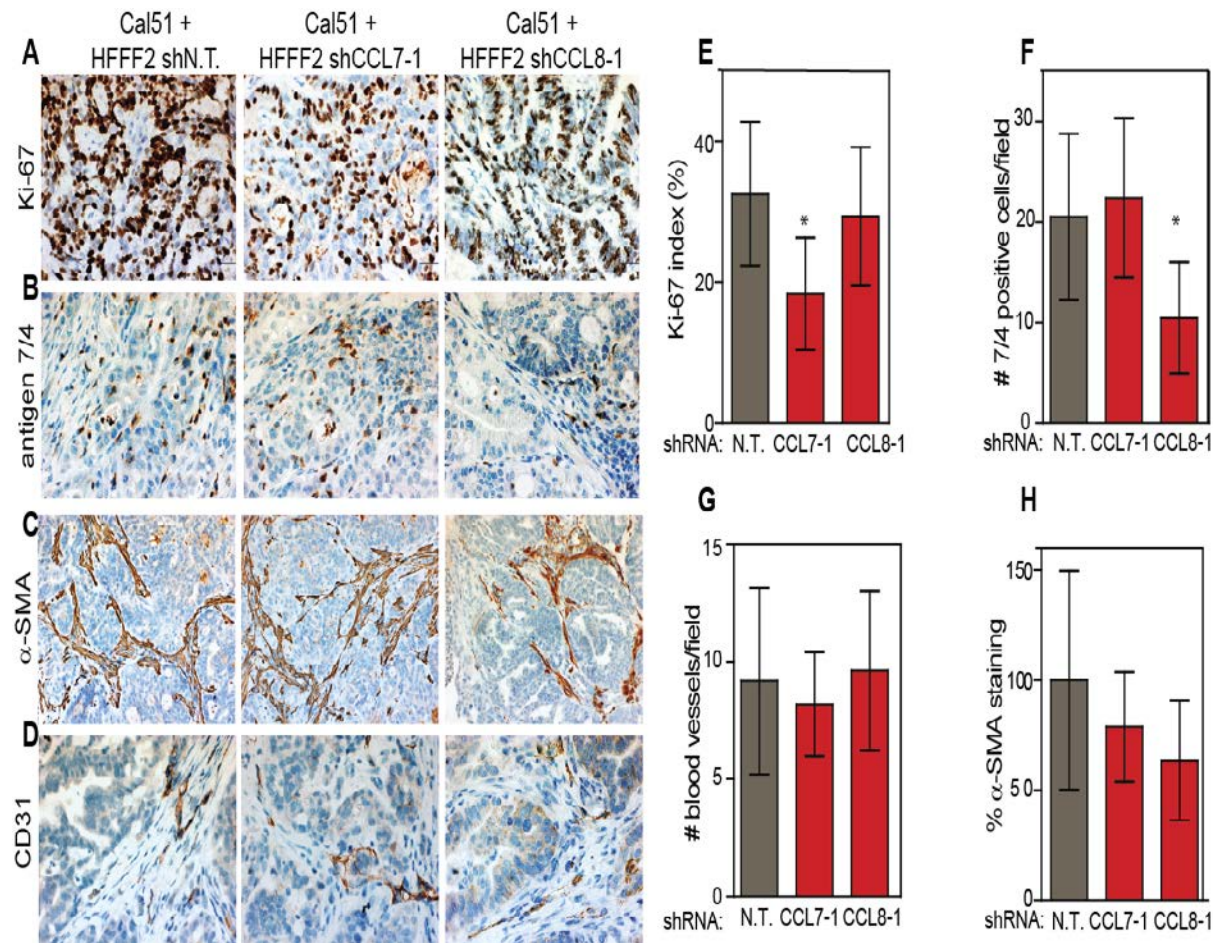


Figure 4.8: In vivo effects of silencing fibroblast produced CCL7 and CCL8

A: Immunostaining of proliferative cells in Cal51+HFFF2 tumors with control shRNA (shN.T.; left) or with shRNA targeting CCL7 (shCCL7-1; center) or CCL8 (shCCL8-1; right) using an antibody to Ki-67. Panels are representative of multiple fields of tumor sections from three tumors per group.

B: Immunostaining of neutrophils and monocytes in Cal51+HFFF2 tumors with control shRNA (shN.T.; left) or with shRNA targeting CCL7 (shCCL7-1; center) or CCL8 (shCCL8-1; right) using an antibody 7/4. Panels are representative of multiple fields of tumor sections from three tumors per group.

C: As in A, but immunostaining of reactive fibroblasts using an antibody to α -sma.

D: As in A, but immunostaining of blood vessels using an antibody to CD31.

E: Quantification of Ki-67 positive cells in Cal51+HFFF2 tumors with control shRNA (shN.T.) or with shRNA targeting CCL7-1 (shCCL7-1) or CCL8 (shCCL8-1). The number of Ki-67 positive cells was calculated as a percentage of total number of cells from five different fields of three different tumors per group. Bars represent the mean \pm SD. Asterisk indicates a significant difference between control (shN.T) and experimental groups (shCCL7-1) *P < 0.05.

F: Quantification of neutrophils and monocytes in Cal51+HFFF2 tumors with control shRNA (shN.T.) or with shRNA targeting CCL7 (CCL7-1) or CCL8 (shCCL8-1) using an antibody to antigen 7/4. Number of 7/4 positive cells were calculated from five different fields of three different tumors per group. Bars represent the mean \pm SD. Asterisk indicates a significant difference between control (shN.T) and experimental groups (shCCL8-1) *P < 0.05.

G: As in E, but quantification of blood vessels.

H: As in E, but quantification of reactive fibroblast.

RNAi suppression of CCR1 on tumor cells restricts tumor promotion in the presence of stromal fibroblasts

CCR1 is a receptor for CCL2, CCL7 and CCL8 and is concomitantly upregulated in co-cultures of breast cancer with TSFs. To test if silencing CCR1 on the tumor-cells restricts the ability of fibroblast secreted chemokines to promote tumor growth, I generated Cal51 and MDAMB231 cells stably expressing shRNAs targeting CCR1 by lentiviral infection. Parental cells stably expressing a non-targeting shRNA (shN.T.) sequence were used as control. Knockdown efficiency was quantified by comparing CCR1 expression in shRNA transfectants compared to control using qRT-PCR and western blot (Cal51: Figure 4.9 A, B and MDAMB231: Figure 4.9 D, E). I performed MTT assays to determine the relative viability of the transfectants compared to the control (shN.T.) (Figure 4.9 C and F, respectively).

For co-injection assays, I injected 1×10^6 Cal51 or MDAMB231 cells expressing either non-target shRNA (shN.T.) or shRNA targeting CCR1 (shCCR1-1 and shCCR1-2) with 1.5×10^6 HFFF2 fibroblasts subcutaneously into 5-6 week old irradiated female nude mice. Growth kinetics of these injections are shown in Figure 4.10 A and C. In parallel, I injected Cal51 and MDAMB231 cells expressing non-targeting shRNA or shRNA targeting CCR1 (shCCR1-1 and shCCR1-2) and monitored tumor growth (Figure 4.10 B, D). Interestingly, silencing CCR1 in the breast cancer cells did not significantly affect tumor volume when the cells were injected alone. However, when these cells were co-injected with HFFF2 fibroblasts, there was a significant reduction in tumor growth (Figure 4.10). It is instructive to note that silencing CCR1 in tumor cells reduces the tumor-take rates significantly in both cell line only and co-injected experimental groups.

I tested if silencing CCR1 on breast cancer cells had affected tumor cell proliferation, recruitment of neutrophils and inflammatory monocytes, blood vessels and reactive fibroblasts. Comparing tumors in which CCR1 was silenced (Cal51shCCR1-1+HFFF2) to the control group (Cal51shN.T.+ HFFF2 tumors), I found that silencing CCR1 significantly reduces the proliferation of Cal51 breast cancer cells as evidenced by Ki-67 immunostaining (Figure 4.11 A, E). It further restricts the recruitment of neutrophils and inflammatory monocytes to the tumor (Figure 4.11 B, F) with no effect on the number of blood vessels and reactive fibroblasts (Figure 4.11, D, H and C, G, respectively). In the absence of co-injected fibroblasts, there is no difference in tumor cell proliferation, recruitment of neutrophils and monocytes, number of blood vessels and reactive fibroblasts between the control and experimental groups (Cal51shN.T and Cal51shCCR1-1; Figure 4.11 A-H).

Figure 4.9

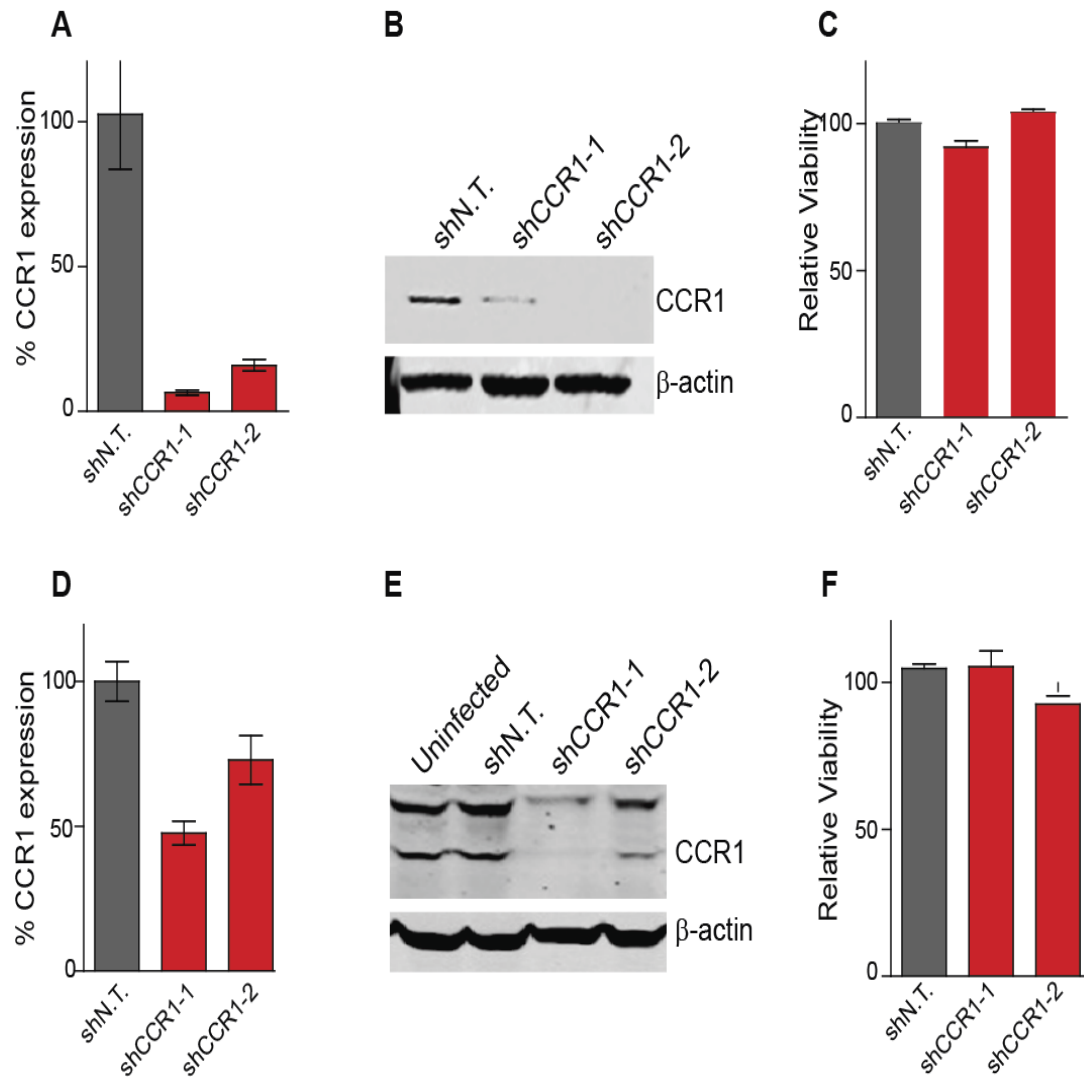


Figure 4.9: shRNAs targeting CCR1 efficiently silence expression in breast cancer cells

A: qRT-PCR analysis of CCR1 knockdown in Cal51 breast cancer cells. CCR1 expression in Cal51 cells expressing either non-target shRNA (shN.T.) or CCR1 (shCCR1-1 or shCCR1-2) was calculated as a ratio of CCR1/GAPDH and expressed as a percentage of shN.T. n= 3, Bars represent the mean +/- SD.

B: Western blot analysis of CCR1 knockdown in Cal51 breast cancer expressing shRNA towards CCR1 (shCCR-1 and 2) compared to Cal51 cells expressing non-target shRNA (shN.T.) using an antibody towards CCR1. β -actin was used as a loading control

C: Relative viability of Cal51 cells expressing shRNA towards CCR1 (shCCR1-1 and shCCR1-2) compared to Cal51 cells expressing non-target shRNA (shN.T) was quantified using a 72-hour MTT assay. n=6; Bars represent the mean +/- SD.

D: As in A but using MDAMB231 cells.

E: As in B, but using MDAMB231 cells.

F: As in C, but using MDAMB231 cells.

Figure 4.10

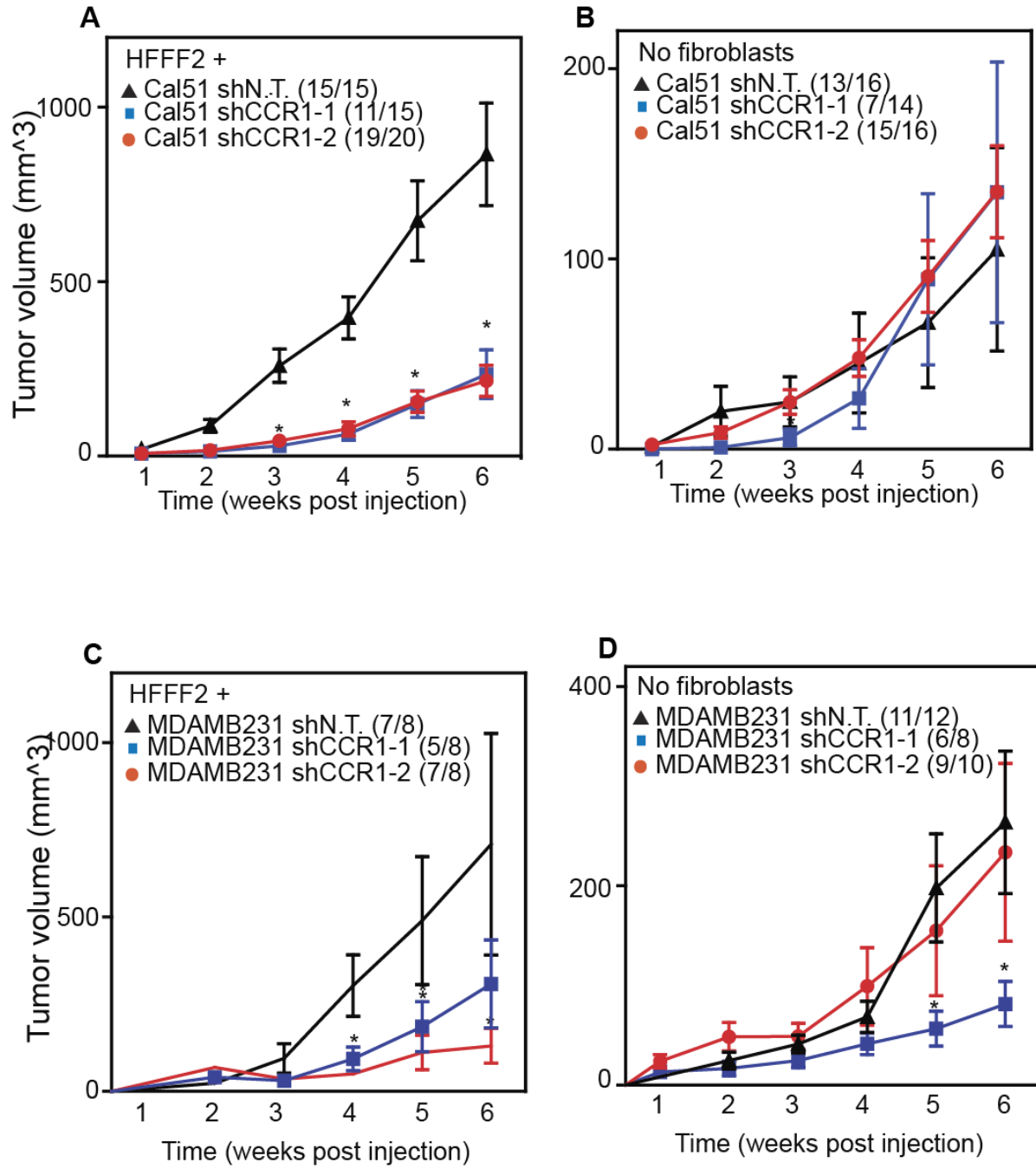


Figure 4.10: CCR1 silencing on breast cancer cells affects tumor growth in the presence of fibroblasts

A: Subcutaneous growth of Cal51 breast cancer cells stably expressing either control shRNA (shN.T.; black triangles), shRNA targeting CCR1 (shCCR1-1; blue squares or shCCR1-2; red circles) coinjected with admixed with HFFF2 fibroblasts. Tumor volumes were determined 1-6 weeks after injection. Tumor take rate/total injections for each group are indicated. Asterisks denote that the tumor group (shCCR1-1 or shCCR1-2) is significantly different than the control (shN.T). *P < 0.05. Error bars represent the mean \pm SEM.

B: Subcutaneous growth of Cal51 breast cancer cells stably expressing either control shRNA (shN.T.; black triangles), shRNA targeting CCR1 (shCCR1-1; blue squares or shCCR1-2; red circles). Tumor volumes were determined 1-6 weeks after injection. Tumor take rate/total injections for each group are indicated. Asterisks denote that the tumor group (shCCR1-1 or shCCR1-2) is significantly different than the control (shN.T). *P < 0.05. Error bars represent the mean \pm SEM.

C: Subcutaneous growth of MDAMB231 breast cancer cells stably expressing either control shRNA (shN.T.; black triangles), shRNA targeting CCR1 (shCCR1-1; blue squares or shCCR1-2; red circles) admixed with HFFF2 fibroblasts. Tumor volumes were determined 1-6 weeks after injection. Tumor take rate/total injections for each group are indicated. Asterisks denote that the tumor group (shCCR1-1 or shCCR1-2) is significantly different than the control (shN.T). *P < 0.05. Error bars represent the mean \pm SEM.

D: Subcutaneous growth of MDAMB231 breast cancer cells stably expressing either control shRNA (shN.T.; black triangles), shRNA targeting CCR1 (shCCR1-1; blue squares or shCCR1-2; red circles). Tumor volumes were determined 1-6 weeks after injection. Tumor take rate/total injections for each group are indicated. Asterisks denote that the tumor group (shCCR1-1 or shCCR1-2) is significantly different than the control (shN.T). *P < 0.05. Error bars represent the mean \pm SEM.

Figure 4.11

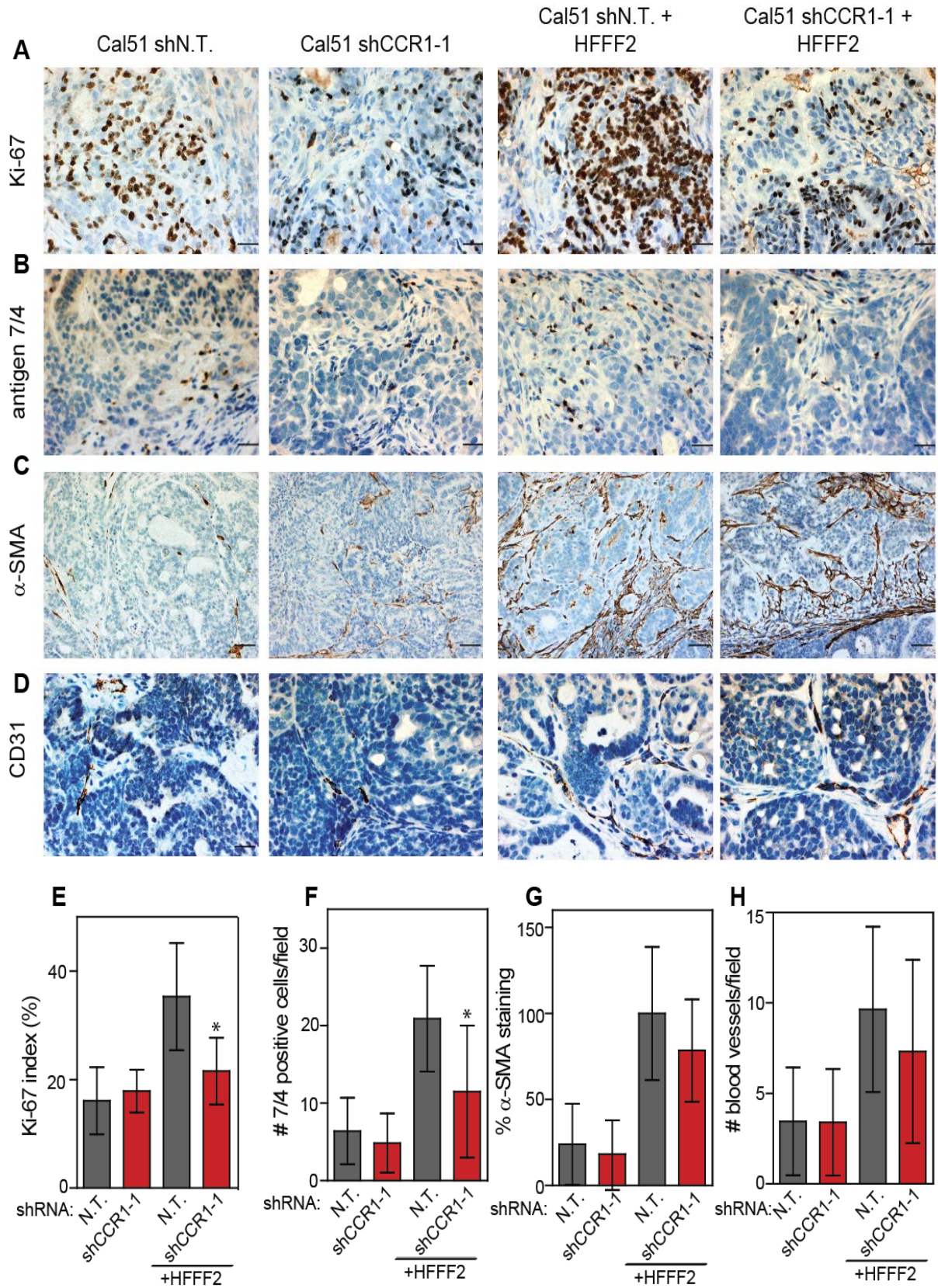


Figure 4.11: Silencing CCR1 on breast cancer cells affects recruitment of immune cells and proliferation

A: Immunostaining of proliferative cells in (from left to right) Cal51shN.T.+HFFF2 (control), Cal51shCCR1-1+HFFF2; Cal51shN.T.(control) and Cal51shCCR-1 using an antibody to Ki-67. Panels are representative of multiple fields of tumor sections from three tumors per group.

B: Immunostaining as in A, but of neutrophils and inflammatory monocytes using an antibody 7-4. Panels are representative of multiple fields of tumor sections from three tumors per group.

C: Immunostaining as in A, but of reactive fibroblasts and pericytes using an antibody to α -SMA. Panels are representative of multiple fields of tumor sections from three tumors per group.

D: Immunostaining as in A, but of blood vessels using an antibody to CD31. Panels are representative of multiple fields of tumor sections from three tumors per group.

E: Quantification of Ki-67 positive cells in Cal51 cells stably expressing either control shRNA (shN.T.) or shRNA targeting CCR1 (shCCR1-1) in tumors with (+HFFF2) or without HFFF2 fibroblasts. The number of Ki-67 positive cells was calculated as a percentage of total number of cells from five different fields of three different tumors per group. Bars represent the mean \pm SD. Asterisk indicates a significant difference between control (shN.T.) and experimental groups (shCCR-1) *P < 0.05.

F: Quantification as in E, but of 7/4 positive cells. Bars represent the mean \pm SD. Asterisk indicates a significant difference between control (shN.T.) and experimental groups (shCCR-1) *P < 0.05.

G: Quantification as in E, but of α -SMA staining

H: Quantification as in E, but of blood vessels

Discussion

Chemokines actively recruit immune cells and induce tumor cell proliferation, angiogenesis and metastasis (Qian et al., 2011; Robinson et al., 2003; Soria et al., 2011). Carcinoma associated fibroblasts are potent secretors of chemokines thereby contributing to tumor promotion (Erez et al., 2010; Mishra et al., 2011). Actions of chemokines result in cancer associated inflammation. Non-resolving, chronic inflammation is a vital feature of premalignant and malignant microenvironments thereby emphasizing the role of proinflammatory chemokines in tumor progression (Balkwill and Mantovani, 2011).

In this study, I show that stromal fibroblast produced CCL2, 7 and 8 have non-redundant roles in tumor progression. Silencing the expression of either one restricts the ability of the protumorigenic fibroblasts to cooperate with breast cancer cells. RNAi mediated silencing of CCL2 negatively affects growth *in vivo*, and is accompanied by a significant reduction in the recruitment of neutrophils and inflammatory monocytes. This is consistent with previous studies reporting the effects of silencing CCL2 on tumor growth (Granot et al., 2011). Silencing CCL2 also reduces the number of blood vessels in tumors. At this point, it is not clear if this effect is mediated through a direct action of CCL2 on endothelial cells or indirectly through recruitment other pro angiogenic immune cells. For example, CCL2 actively recruits tumor associated macrophages that promote angiogenesis (Mishra et al., 2011). It remains to be seen if RNAi suppression of CCL2 in this system can abrogate the tumor-promoting effects of TAMs by blocking their recruitment to the tumor site.

Functional roles for CCL7 in the tumor microenvironment are not well characterized. I demonstrate that silencing CCL7 expression in the fibroblasts results in a significant reduction in tumor growth. Silencing of fibroblast produced CCL7 reduces tumor cell proliferation *in vivo*.

However, there was no effect on the proliferation of breast cancer cells *in vitro* upon the addition of recombinant CCL7. This suggests that the pro-proliferative effect of CCL7 is tumor-microenvironment dependent requiring the presence of additional factors. In addition, CCL7 is shown to induce migration and invasion in oral squamous carcinoma cells (Jung et al., 2010). It is interesting to speculate that CCL7 mediates invasion in breast cancer cells as well. Further investigation will clarify this point. Even though CCL7 is known to recruit monocytes to the tumor site upon injury (Coussens and Werb, 2002), there was no difference in CD4 positive cells recruited to the tumor site between the control and CCL7 silenced groups. This does not preclude the possibility that silencing CCL7 affects the recruitment of different types of immune cells to the tumor site or that the effect is at a different stage in tumor progression (Dahinden et al., 1994). Extensive characterization of recruited immune cells in CCL7 silenced tumors is likely to provide clues into the specific actions of CCL7 in immune cell recruitment. Even though the effect of silencing fibroblast secreted CCL8 on tumor growth is minor compared to CCL2 and CCL7, it has an effect on the recruitment of neutrophils and monocytes. At this point, it is not clear if silencing CCL8 affects recruitment of other immune cells. For example, CCL8 was shown to be a potent attractor of eosinophils and Th₂ T-cells (Islam et al., 2011; Weber et al., 1995) and the effects of CCL8 silencing could be mediated in part by aberrant recruitment of these tumor-promoting cells (Balkwill and Mantovani, 2012; Coussens and Pollard, 2011).

Since there was coordinated upregulation of CCR1 receptor expression on breast cancer cells upon co-culture with TSFs, I hypothesized that silencing CCR1 would abrogate some of the effects of the stromal fibroblasts as well. Moreover, one of the chemokine candidates CCL7 has a direct pro-proliferative effect that may be mediated by CCL7 binding to CCR1 on the breast cancer cells. Indeed silencing CCR1 on breast cancer cells resulted in the loss of tumor growth in

the presence of co-injected fibroblasts. Though there were no differences in tumor growth of CCR1 silenced breast cancer cells in the absence of co-injected fibroblasts, tumor-take rates were significantly reduced.

Tumor proliferation and recruitment of neutrophils are reduced in tumors resulting from CCR1 silenced breast cancer cells and TSFs. Previous studies have demonstrated a role for cancer-cell expressed CCR1 in proliferation and recruitment of monocytes (Robinson et al., 2003). Other studies have also suggested a role for CCR1 in invasion and it remains to be seen whether silencing CCR1 in this system contributes to the invasiveness of the breast cancer cells (Wang et al., 2009).

Taking the actions of all the genes tested together, I found that while some of these effects are directly on the tumor cells, others are mediated indirectly affecting other components of the microenvironment like blood vessels and immune cells instead. Blocking the receptor CCR1 on the cancer cells results in immune cell blockade (indirect effect) and tumor cell proliferation (direct effect). The induction of CCR1 in co-cultured cancer cells occurs concomitantly with the upregulation of two ligands of CCR1: CCL7 and CCL8 in the tumor supportive fibroblasts. The ligands are then able to act tumor cells affecting proliferation (CCL7; direct effect) or affecting the recruitment of immune cells (CCL8; indirect effect). Finally, although CCL2 is not a major ligand for CCR1, it is induced in co-cultured tumor-supportive fibroblasts. It acts on blood vessels and immune cells (indirect) thereby contributing to tumor progression. One might speculate that CCL2 is coinduced along with CCL7 and CCL8 but may not act through CCR1 on the cancer cells acting instead on immune cells that express its primary receptor, CCR2. Both direct and indirect effects act together to contribute to tumor progression. A table summarizing the effects of silencing these genes is shown in Table 4.1.

Inhibitors of chemokines and their receptors are currently being tested as potential drug targets. For example, anti-CCL2 antibodies have been tested in pre-clinical models of prostate cancer (Zhang et al., 2010). Blockade of CCL2 signaling results in reduced metastasis and increased survival in mouse models of breast cancer (Qian et al., 2011). Similarly, abrogating CXCR4/CXCL12 signaling reduces metastasis in mouse models of lung cancer (Kim et al., 2008). Targeting chemokine receptor CCR1 results in blockade of immune cell recruitment and invasion in pre-clinical mouse models of breast, colon and lung cancer (Kitamura et al., 2010; Robinson et al., 2003; Wang et al., 2009). Based on this, clinical trials of CCR1 antagonists are underway for treatment for rheumatoid arthritis and may hold promise for the cancer therapy as well (Gladue et al., 2010).

Chemokines and their receptors are highly attractive drug targets (Balkwill and Mantovani, 2012). However, targeting specific chemokines still remains a challenge because of the diverse roles they mediate. Moreover, chemokine signaling is highly stage- and type-specific in cancer development (Balkwill, 2012). Therefore, systematic in-depth analysis of chemokines will contribute greatly to our understanding of their functions and present targets for therapeutic intervention.

Table 4.1: Effects of silencing CCL2, CCL7, CCL8 and CCR1 on the tumor microenvironment

shRNA	Process	Proliferation	Immune cells	Blood vessels	Fibroblasts
targeting	Marker	Ki-67	7-4	CD31	α -sma
CCL2		No	Yes	Yes	No
CCL7		Yes	No	No	No
CCL8		No	Yes	No	No
CCR1		Yes	Yes	No	No

Chapter V

Future Perspectives and Conclusions

Future Perspectives

The interaction between tumor cells and carcinoma associated fibroblasts is vital to the tumor progression (Orimo and Weinberg, 2006). Although some molecules mediating this molecular crosstalk have been identified, the scope of all relevant interactions still remains unclear (Polyak and Kalluri, 2010). One of the major goals of this study was to identify a more complete catalog of these mediators and to determine how many of the interactions were functionally important to mediate tumor progression in a co-xenograft based model. Functional analyses of cancer cells and tumor-supportive fibroblasts combined with extensive bioinformic analysis has identified potentially important genes mediating diverse processes in the tumor microenvironment. In addition, this study has provided an excellent opportunity for the development of a model system relevant to human cancer and concepts that can be readily extended to future studies.

Firstly, tumor supportive and non-supportive fibroblasts were identified exclusively in relation to basal breast cancer cell lines. However, the composition and features of tumor microenvironments of different cancer types are likely to be distinct from one another. The co-xenograft, co-culture method developed here could be easily applied to identify specific factors that mediate functionally relevant interactions in the different types of tumor microenvironments. Secondly, the system of cells composed of cancer cells and fibroblasts could be easily expanded

to include other cell types. For example, the modified co-culture and co-xenografting system could include endothelial cells in addition to cancer cells and fibroblasts. This system can be used for studying the interactions of three cell types in relation to each other, reflecting the complexity of the *in vivo* tumor microenvironment more accurately. Thirdly, the genomic analyses were focused on identifying secreted factors whose expression was upregulated in co-cultured tumor supportive fibroblasts. However, different criteria could be applied to identify genes important in mediating other aspects of tumor-stromal interactions. For example, one could focus their efforts exclusively on identifying transport proteins, structural proteins, proteases or phosphorylated proteins instead of secreted factors.

The experimental workflow used in this study identifies 58 secreted factors that are induced in co-cultured, tumor-supportive fibroblasts. These genes are also upregulated in primary human breast stroma, making them attractive candidates for functional analysis. The functional analysis for each of the candidates tested was performed using co-xenografting assays of cancer cells and tumor supportive fibroblasts in which candidate genes had been silenced using RNAi. This was followed by extensive characterization of the tumor microenvironment using immunohistochemistry. As a result of the time consuming nature of these analyses, only five of the 58 genes were selected for further validation. However, it would be extremely interesting to systematically analyze the functional roles of the remaining 53 candidates in mediating breast-stromal fibroblast interactions and modulating the tumor microenvironment.

Furthermore, my results indicate that several genes play non-redundant, important roles in mediating interactions between tumor cells and stromal fibroblasts. Therefore, I would like to test the hypothesis that silencing two or more of these genes at the same time would lead to additional tumor suppressive effects. For example, silencing AREG in the fibroblasts causes a

reduction in EGFR phosphorylation and α -sma positive cells whereas CCL2 silencing affects recruitment of blood vessels and 7/4 positive immune cells. Silencing AREG and CCL2 simultaneously may further restrict the ability of HFFF2 fibroblasts to cooperate with breast cancer cells than silencing either AREG or CCL2 alone. If this is indeed the case, then this would support the idea that targeting many points in the stromal microenvironment along with conventional chemotherapy would provide survival benefit to patients.

I used immunohistochemistry to evaluate if silencing candidate mediators affected processes like proliferation (using Ki-67), number of blood vessels (using CD31), number of reactive fibroblasts and pericytes (using α -sma) and neutrophils and monocytes (using 7/4). Although this analysis is quantitative, it is not comprehensive as it doesn't include all components of the microenvironment. Moving forward, I would like to perform more analysis using a larger set of markers. Alternatively, I would like to use single-cell RNA sequencing of individual cells from the tumors in which the candidate mediators have been silenced to identify both qualitative and quantitative changes in the composition of the tumor microenvironment.

A majority of breast cancer patients die of metastases to the bone, brain and lungs. Metastasis is the systematic dissemination of tumor sites distinct from the primary lesion. It is becoming clear that the stromal microenvironment plays a crucial role in engaging the tumor cells and causing them to metastasize. Previous studies have shown that stromally secreted factors are involved in promoting breast cancer metastasis (Karnoub et al, 2007). Similarly, one of the candidate mediators tested in this study, CCL2, has previously been reported to promote breast cancer metastasis to the lungs (Qian et al, 2011). I would like to test the effects of silencing the candidate genes on breast cancer metastasis. To perform these experiments, I would

like to use a spontaneously metastasizing model of breast cancer since in addition to the co-culture, co-xenografting model to validate my findings.

Clinical implications

Tumor promoting activities of the microenvironment include proliferative signals, evading growth suppression, resisting cell death, inducing angiogenesis, creating a proinflammatory milieu and promoting metastasis (Hanahan and Coussens, 2012). Because of the multitude of functions mediated by the microenvironment, agents inhibiting collaborative interactions between tumor cells and components of the stroma are actively being pursued as potential cancer treatments (Anton and Glod, 2009).

Blocking angiogenesis cuts off the blood supply to the tumor, thereby severely restricting tumor growth. Anti-angiogenic drugs were the first class of drugs targeting cellular components other than cancer cells. An anti-VEGFA antibody, Bevacicumab (Avastin ®) is FDA approved for use in colorectal, lung, breast and brain cancer in combination with conventional chemotherapy (Verheul and Pinedo, 2003). A number of antiangiogenic drugs like sorafenib (Nexavar®), sunitinib (Sutent®), pazopanib (Votrient®) and everolimus (Afinitor®) targeting receptor tyrosine kinases have been approved subsequently (Shojaei, 2012).

Based on their tumor promoting and inhibiting roles, immune cells can be targeted effectively to achieve tumor suppression. For example, the blockade of a molecule CTLA-4 expressed on the surface of T-cells stimulates anti-tumor immunity. An antibody targeting CTLA-4 (Ipilimumab; Yervoy ®) was recently approved for use in melanoma (Hodi et al., 2010). Similarly, blockade of Colony Stimulating Factor-1 Receptor (CSF-1R) increases anti-

tumor immunity and response to chemotherapy in preclinical models of breast cancer by abrogation of macrophage recruitment (Denardo et al., 2011).

Carcinoma associated fibroblasts are a potent source of CXCL12 in the tumor microenvironment (Orimo et al., 2005). CXCL12 promotes angiogenesis, tumor cell proliferation and confers resistance to chemotherapy. Inhibitors of CXCL12 are currently being tested for their ability to sensitize patients to chemotherapy (Duda et al., 2011).

Although targeting the microenvironment is an attractive strategy to restrict the growth of the tumors, development of resistance to therapy presents a truly challenging obstacle (Casanovas, 2011). In one example, the lack of recruited macrophages was fully compensated by neutrophils to promote tumor growth (Pahler et al., 2008). This underscores the complex nature of interactions in the tumor microenvironment (Hanahan and Coussens, 2012). But at the same time, it presents multiple opportunities for therapeutic intervention. Through this study, it is evident that several fibroblast secreted proteins have non-redundant functional roles in tumor promotion that could be potentially targeted for treatment. However, it is important to note that stromal gene expression patterns of individual patients are strikingly diverse (Finak et al., 2008; Ma et al., 2009) and may consequently affect the patient's response to microenvironment based therapy.

Conclusion

It is important to elucidate and functionally characterize the contributions of specific components of the tumor microenvironment in order to envisage effective therapies that prolong patient survival. Most stromal cell based treatments are currently used in combination with conventional chemotherapy regimens (De Palma and Hanahan, 2012). Identifying combinations

that target multiple stromal components in addition to the cancer cells may vastly improve patient survival. The rapid improvements in imaging and sequencing technology give us a unique opportunity to personalize these treatments so that they provide the maximum benefit to patients (De Palma and Hanahan, 2012).

CHAPTER VI

Materials and methods

Cell lines and tissue culture

Breast carcinoma cell lines Cal51, MDAMB231, JIMT-1 and HCC1954 were obtained from American Type Culture Collection (ATCC; Manassas, VA). The cell lines were maintained in Dulbecco's Modified Eagle Medium (DMEM) + 10% Fetal Bovine Serum (FBS). Human fetal foreskin fibroblast strain HFFF2 was obtained from Sigma Aldrich (St. Louis, MO). Human newborn foreskin fibroblasts HFF1 and CCD1112Sk and human fetal lung fibroblasts Wi38 were obtained from ATCC. All fibroblasts were maintained in DMEM+10%FBS. Bing cells and 293T cells were obtained from ATCC and used as packaging cells for retroviral and lentiviral infections, respectively. The cell lines were maintained in Dulbecco's Modified Eagle Medium (DMEM) + 10% Fetal Bovine Serum (FBS). All cancer cell lines, fibroblasts and packaging cell lines were maintained under standard tissue culture conditions at 37⁰C and 5% CO₂.

Subcutaneous injections in nude mice

All studies utilizing human xenograft experiments in nude mice were approved by Cold Spring Harbor's Institutional Animal Care and Use Committee. Five-six week old female nude mice (NCR nu/nu) were purchased from Charles River Inc. (Wilmington, MA) and were irradiated at 400cGy 24-36 hours prior to injections. For cell line only injections, one million breast cancer cells were trypsinized, washed, counted and resuspended in 100ul of DMEM

without serum. Cells were placed on ice until they were injected in nude mice. For cell line and fibroblast admixing experiments, one million breast cancer cells and one and half million human fibroblasts were trypsinized, washed, counted separately and admixed in 100ul of DMEM without serum just before injections and injected subcutaneously into left and right flanks of nude mice. Tumor were measured weekly by calipers and volume (TV) was calculated as $TV = 0.523 \times X \times Y^2$ where X=larger diameter and Y=smaller diameter.

Tumor extraction, immunohistochemistry and microscopy

Tumors were excised at indicated time points post injections or when one of the measurements reached 2cm. The animals were sacrificed using CO₂ following which tumors were removed and washed in saline before storage in 10% buffered Formalin solution. The formalin fixed tumors were embedded in paraffin and cut into 10 micron thick sections for histology and immunohistochemistry. The tumors for immunofluorescence were excised and cryoembedded in Tissue-tek O.C.T. embedding compound (Electron Microscopy Sciences).

Immunohistochemistry was performed as follows: Tissue sections were de-parafinized in xylene, followed by rehydration using series of alcohol dilutions from 100% to 50%. Antigen retrieval was done using 1% Sodium citrate 10 mM, pH 6.0 solution in a pressure cooker for 20 minutes. DNase digestion was used in the case of nuclear antigens. Following quenching of endogenous peroxidase activity and blocking using 10% normal goat serum (NGS), the sections were incubated in the primary antibody at 4⁰C overnight. HRP conjugated secondary antibodies (Vector Labs) were used for paraffin sections and were developed using a DAB substrate (Vector Labs, CA). The nuclei were stained with hematoxylin (Sigma Aldrich, MO). The sections were dehydrated and mounted using H1000 hardset medium (Vector Labs). For immunofluorescence,

the same sequence was followed except deparafinization and rehydration were omitted; instead the sections were fixed in acetone for 20 minutes. There was no step to quench endogenous peroxidase. The secondary antibodies used were AlexaFluor488 and AlexaFluor568 (Invitrogen). A list of primary antibodies used for immunohistochemistry and their respective dilutions is shown in Table 6.1

Retrovirus production and transduction

For DsRed and GFP tagging of breast cancer cells and fibroblasts respectively, retroviral vector expressing DsRed (Clontech) or GFP was used (MLP-GFP were provided by Dr.S.Lowe, MSKCC). Plasmid DNA was amplified using Endofree Maxiprep kit (Qiagen). 1 million Bing cells were plated for 24 hours in a 10cm dish to achieve approximately 30% confluence at the time of transfection. They were transfected with 12ug of the target plasmid DNA and 8ug of amphotrophic helper DNA plasmid (provided by Dr. D. Mu, Penn State) using the calcium phosphate transfection (Promega). Precipitates were allowed to form overnight and culture medium was replaced the following morning. About 16 hours after transfection, efficiency was measured using fluorescence microscopy. Plates with >50% efficiency were discarded. Plates with successful transfections were allowed to incubate for ~48 hours post transfections. Viral particles were collected by harvesting supernatants from the packagers and filtered through a 0.45 μ M membrane (Millipore). Unconcentrated virus with polybrene (5ug/ml; Millipore) was used to infect 500,000 breast cancer cells or fibroblasts overnight. The medium was replaced the following morning and cells were monitored for DsRed or GFP expression ~48 hours post viral infection through fluorescence microscopy. The cells were selected in Puromycin (3ug/ml;Sigma) for a period of 72 hours.

Co-culture of breast cancer cells and fibroblasts

One and a half million GFP tagged human fibroblasts (HFFF2, HFF1, CCD1112Sk or Wi38) were plated in 10 cm dishes and allowed to attach overnight. The following morning, one million DsRed tagged Cal51 or MDAMB231 were plated on top of the fibroblasts. the co-culture was allowed to incubate for six days following which the cells were washed, trypsinized, collected and resuspended in PBS+1% FBS for FACS sorting. Monocultures of breast cancer cells or fibroblasts were also plated at the same time as co-cultures to be used as controls.

Flow Cytometry

Cell suspensions were sorted into DsRed⁺ Cal51 or MDAMB231 cells or GFP⁺ fibroblasts using the ARIA II cell sorter (Beckton Dickenson). Compensation for two-color experiments was performed with FACS Diva software (Becton Dickinson Immunocytometry Systems, Franklin Lakes, New Jersey, USA). Flow cytometry analysis was performed with controls: unstained samples, single color controls and double-color admixed mock co-cultures for determining appropriate gates, voltages and compensations. Monocultures of DsRed⁺ Cal51 or MDAMB231 cells or GFP⁺ fibroblasts were also passed through the ARIA II cell sorter to reduce experimental variation.

RNA isolation, transcriptional profiling and data analysis

Cells sorted from flow cytometry were immediately processed for RNA isolation. Total RNA was isolated using RNeasy kit (Qiagen). RNA was quantified using Nanodrop (Thermo Scientific) and 1ug RNA was used for Microarray Analysis. Microarrays were performed by on Affymetrix Gene 1.0 ST array. This array contains 1 million 25-mer probes covering ~29000

genes in the human genome. Data was extracted and used for background correction, normalization and summarization of the probes using the AROMA package.

shRNA targeting and lentiviral transduction

shRNAs targeting candidate genes were obtained from The RNAi Consortium of the Broad Institute library (Sigma Aldrich). The shRNAs were obtained as lentiviral constructs in the pLKO.1 vector and were obtained as bacterial stocks. The stocks were streaked on LB-Amp plates and incubated overnight at 37⁰C. Individual bacterial colonies were amplified and plasmid DNA was prepared using Endofree Maxiprep kit (Qiagen).

293T packaging cells were plated at a density of 1x10⁶ cells/10 cm dish. 24 hours post plating, the medium was replaced with OptiMEM (low serum) medium. 18µl of transfection agent Fugene6 (Roche) was mixed with OptiMEM, 12 µg of plasmid DNA (from shRNAs) and 20µl of Lentiviral mix (Sigma). The cells were incubated with the mix overnight following which the medium was replaced. Viral supernatants were harvested 36 hours and 72 hours post transfection. Viral supernatants with Polybrene (5ug/ml; Millipore) were used to infect 1x10⁶ recipient cells for 12 hours. Cells were selected in 3ug/ml puromycin (Sigma) for 72 hours. Knockdown efficiency was quantified using qRT-PCR analysis and/or Western blot. A list of shRNA sequences used for targeting candidate genes can be found in Table 6.2.

cDNA synthesis quantitative RT-PCR

1µg of total RNA was used to make cDNA using the qScript cDNA SuperMix (Quanta Biosciences). Briefly, the RNA was mixed with Supermix consisting of randomers and oligo (dT) primers, buffers and RNaseH enzyme and nuclease free water for a reaction volume of

20 μ l. The mix was incubated at 25⁰C for 5 minutes followed by 30 minutes at 42⁰C and 15 minutes at 85⁰C. The resultant cDNA was stored at -20⁰C and used for qRT-PCR. 0.5 μ l (of 20 μ l) of the cDNA was used for each reaction of a qRT-PCR. Each 20 μ l reaction was made up as follows: 10 μ l PerfeCTa® SYBR® Green FastMix, ROX™ (Quanta Biosciences), 1 μ l each of forward and reverse primer (50nM final concentration), 0.5 μ l cDNA template and 7.5 μ l nuclease free water. The reactions were set up in 384 well-plates (Applied Biosystems) and run on the Applied Biosystems 7900HT (Applied Biosystems) Real Time-PCR system. Data were processed and analyzed using 7900HT Software (Applied Biosystems). Primer sequences used are as follows: AREG 5'-TGGAAGCAGTAACATGCAAATGTC-3' and 5'-GGCTGCTAATGCAATTTTTGATAA-3'; CCL2 5'-GATCTCAGTGCAGAGGCTCG-3' and 5'-TGCTTGTCCAGGTGGTCCA-3'; CCL7 5'-TGATTCATCCTCTCTGCTTCC-3' and 5'-GATTGGTCCAGGATAACCCA-3'.

Western blotting

Cells were grown in 10 cm plates until they reached confluency. For generating protein lysates, cells were washed and incubated in RIPA buffer (Sigma Aldrich) containing protease inhibitor cocktail (Roche) for 10 minutes on ice. Subsequently, cells were scraped using a sterile scraper and protein fraction was isolated by centrifugation at 14000 rpm for 30 minutes at 4 degrees celcius. Protein was quantified using Bradford assay (Biorad) following which it was denatured by boiling in 6X Lamelli buffer (Biorad) containing 5% β -mercaptoethanol for 5 minutes at 95 degree celcius. Equal amounts of protein were loaded in 4-20% Tris-Glycine gradient gels (Invitrogen) and run in Tris-Glycine buffer (Biorad) at 90V for 2 hours. Proteins were transferred to a nitrocellulose membrane using Tris-Glycine buffer containing 20%

methanol. Membranes were blocked with 5% bovine serum albumin (Sigma) for 1 hour and incubated with primary antibodies overnight at 4 degree celcius. Fluorescent secondary antibodies (IR700 or IR800; Licor Biosciences) were used to detect the primary antibody signal and membranes were scanned using the Odyssey scanner (Licor Biosciences). A list of antibodies can be found in Table 6.1

Cell viability assays (MTT assays)

Relative viability was quantified by using the Cell Proliferation kit (Roche). 1000 cells were plated in 96 well plated and allowed to grow for 72 hours. Then they were incubated with the MTT (3-(4,5-Dimethylthiazol-2-yl)-2,5-diphenyltetrazolium bromide) solution for 4 hours. The viable cells reduce the MTT to formazan. This is followed by solubilization of the formazan dye overnight. The absorbance was read at 595nm in a spectrophotometer and quantified. The experiments were performed in triplicate.

Boyden Migration assay

Subconfluent WT-MEFs were incubated in DMEM+1% FBS overnight. 50,000 Wi38, CCD1112Sk, HFF1, HFFF2 fibroblasts or HFFF2 fibroblasts expressing control shRNA (shN.T.) or shRNA targeting amphiregulin (shAREG) were plated in triplicate in 24-well plates and allowed to incubate in DMEM+1% FBS overnight. The next morning, WT-MEFs were washed with PBS, trypsinized, counted and resuspended at a concentration of 500,000 cells/ml in DMEM. Medium was replaced 24-well plate with the fibroblasts. Chemotactic agents were added to the wells in 0.5ml DMEM at desired concentrations. Triplicate wells with DMEM and DMEM +10% were included as controls. Each 24-well plate was then fitted with Boyden

migration plate (Cytoselect, Cell Biolabs Inc.) and 300ul of DMEM containing WT-MEFs was added on the upper chamber (150,000 cells). The plates were incubated at 37⁰C for 5 hours. Post incubation, the upper chamber was transferred to an empty 24-well plate. The wells were washed in PBS and the non-migratory on the membrane were wiped off with a Q-tip several times. The migratory cells on the underside of the membrane were fixed with 100% methanol for 10 minutes after which they were stained using 0.5% crystal violet solution for 15 minutes. The membranes were washed in distilled water for 10 minutes, dried and examined under a microscope. Membranes were examined under high power objective on the Olympus IX70 microscope. Migratory cells from five different fields from each well were counted and averaged over three independent experiments. The results were presented as number of migratory cells/high power field.

Wound healing scratch migration assay

50,000 HFFF2 fibroblasts expressing control shRNA (shN.T.) or shRNA targeting amphiregulin (shAREG) were plated in triplicate in 24-well plates and allowed to incubate in DMEM+1% FBS overnight. Conditioned medium was collected 24 hours later and spun at 1000rpm for 5 minutes to remove any cells. 100,000 Wild type-MEFs were plated in 24-well plates in DMEM+1%FBS and allowed to adhere overnight. The following morning, medium was aspirated and cells were washed with PBS. A scratch wound was made using a clean, sterile plastic pipette tip in each well. Conditioned medium, DMEM or DMEM+10% FBS was added to the wells in triplicate. The plate was then imaged using low magnification (4X and 10X) on an Olympus microscope 0hr and 16 hours post scratch. The plate was incubated at 37 degrees/5%CO₂ during the course of the assay. Images collected from 0 and 16 hour timepoints

were imported into ImageJ software (NIH). Area of the scratch was calculated using the free-hand area tool. The difference in the area between 0 or 16 hours was calculated for each well and averaged over replicates. The area was normalized to DMEM and expressed as a percentage.

Table 6.1: List of antibodies used in this study

Antibody	Source	Purpose	Dilution
α -SMA	Sigma (A2547)	Immunohistochemistry	1:5000
7-4	Cedarlane (CL8993AP)	Immunohistochemistry	1:200
Ki-67	Dako (MIB5)	Immunohistochemistry	1:4000
CD31	Abcam (ab28364)	Immunohistochemistry	1:200
pEGFR	Epitomics (EP774Y)	Immunohistochemistry	1:400
CCR1	Abcam (ab89257)	Western blot	1:1000
Amphiregulin	Abcam (ab89119)	Western blot	1:500
CCL2	Abcam (ab9669)	Western blot	1:500
CCL7	Abcam (ab18694)	Western blot	1:200

Table 6.2: shRNA targeting sequences used in this study

Symbol	Accession number	Designation	TRC Number	Targeting sequence
AREG	NM_001657.2	shAREG-1	TRCN0000117994	CCGGCTGGCTATATTGTCGATGATCTCGAGATCATCGACAATATAGCCAGGTTTTTG
		shAREG-2	TRCN0000117995	CCGGAAACGAAAGAAACTTCGAACTCGAGTTCGAAAGTTCTTTCGGTCTTTTTG
		shAREG-3	TRCN0000117993	CCGGCACTGCCAAGTCATAGCCATACTCGAGTATGGCTATGACTTGGCAGTGTTTTG
		shAREG-4	TRCN0000117996	CCGGAAACCCACAAATACCTGGCTATCTCGAGATAGCCAGGTATTTGTGGTCTTTTTG
CCL2	NM_002982	shCCL2-1	TRCN0000338418	CCGGCCAGTCACCTGCTGTATAAECTCGAGTTATAACAGCAGGTGACTGGGTTTTTG
		shCCL2-2	TRCN000006283	CCGGCCAGTCACCTGCTGTATAAECTCGAGTTATAACAGCAGGTGACTGGGTTTTT
CCL7	NM_006273	shCCL7-1	TRCN0000057893	CCGGGTGCTACAGATTTATCAATACTCGAGTATTGATAAATCTGTAGCAGCTTTTTG
		shCCL7-2	TRCN0000057894	CCGGCCAGGACTTATGAAGCACCTCTCGAGAGGTGCTTCATAAAGTCTGGTTTTTG
CCL8	NM_005623	shCCL8-1	TRCN0000057948	CCGGGTGGAGAGCTACACAAGAATCTCGAGATTCCTGTAGCTCTCCAGCTTTTTG
		shCCL8-2	TRCN0000057949	CCGGGTGCTTTAACGTGATCAATACTCGAGTATTGATCACGTTAAAGCAGCTTTTTG
		shCCL8-3	TRCN0000057952	CCGGCCATGAAGCATCTGGACCAAACTCGAGTTTGGTCCAGATGCTTCATGGTTTTTG
STC1	NM_003155	shSTC1-1	TRCN0000151758	CCGGCTAAATTTGACACTCAGGGAACCTCGAGTTCCTGAGTGTCAAATTTAGTTTTTG
		shSTC1-2	TRCN0000154599	CCGGATGGGATGTATGACATCTGTCTCGAGACAGATGTACATCCCATCTTTTTTG
		shSTC1-3	TRCN0000155141	CCGGCATTCTGTCAAAGAGAGGCTTACTCGAGTAAGCTCTTTTGACGAATGCTTTTTG
		shSTC1-4	TRCN0000156272	CCGGCCAAAGGATGATTGCTGAGGTCGAGACCTCGAGACCTCAGCAATCATCCTTTGGTTTTTG
		shSTC1-5	TRCN0000157907	CCGGCACATCCCATGAGAGTGCATACTCGAGTATGCACCTCTCATGGGATGTGTTTTTG
CCR1	NM_001295	shCCR1-1	TRCN0000008186	CCGGCCTACAATTTGACTATACCTTCGAGAAGTATAGTCAAATGTAGGGTTTTT
		shCCR1-2	TRCN0000008188	CCGGGCTCTGAAACTGAACCTCTTTCTCGAGAAAAGAGTTTCAGTTCAGAGCTTTTT

Bibliography

Adam, L., Crepin, M., Lelong, J.C., Spanakis, E., and Israel, L. (1994). Selective interactions between mammary epithelial cells and fibroblasts in co-culture. *Int J Cancer* 59, 262-268.

Ala-aho, R., and Kahari, V.M. (2005). Collagenases in cancer. *Biochimie* 87, 273-286.

Alam, R., Forsythe, P., Stafford, S., Proost, P., and Vandamme, J. (1994). Monocyte Chemotactic Peptide-3 (Mcp-3), a New C-C Chemokine, Is the 2nd Most Potent Histamine-Releasing Factor for Basophils. *Faseb J* 8, A480-A480.

Alam, R., Lett-Brown, M.A., Forsythe, P.A., Anderson-Walters, D.J., Kenamore, C., Kormos, C., and Grant, J.A. (1992). Monocyte chemotactic and activating factor is a potent histamine-releasing factor for basophils. *The Journal of clinical investigation* 89, 723-728.

Allinen, M., Beroukhi, R., Cai, L., Brennan, C., Lahti-Domenici, J., Huang, H., Porter, D., Hu, M., Chin, L., Richardson, A., et al. (2004). Molecular characterization of the tumor microenvironment in breast cancer. *Cancer Cell* 6, 17-32.

Ankrapp, D.P., and Bevan, D.R. (1993). Insulin-like growth factor-I and human lung fibroblast-derived insulin-like growth factor-I stimulate the proliferation of human lung carcinoma cells in vitro. *Cancer Res* 53, 3399-3404.

Ashley, R.L., Antoniazzi, A.Q., Anthony, R.V., and Hansen, T.R. (2011). The chemokine receptor CXCR4 and its ligand CXCL12 are activated during implantation and placentation in sheep. *Reprod Biol Endocrinol* 9, 148.

Balkwill, F. (2004). Cancer and the chemokine network. *Nat Rev Cancer* 4, 540-550.

Balkwill, F.R. (2012). The chemokine system and cancer. *J Pathol* 226, 148-157.

Balkwill, F.R., and Mantovani, A. (2012). Cancer-related inflammation: common themes and therapeutic opportunities. *Semin Cancer Biol* 22, 33-40.

Barbieri, F., Bajetto, A., and Florio, T. (2010). Role of chemokine network in the development and progression of ovarian cancer: a potential novel pharmacological target. *J Oncol* 2010, 426956.

Basset, P., Bellocq, J.P., Wolf, C., Stoll, I., Hutin, P., Limacher, J.M., Podhajcer, O.L., Chenard, M.P., Rio, M.C., and Chambon, P. (1990). A novel metalloproteinase gene specifically expressed in stromal cells of breast carcinomas. *Nature* 348, 699-704.

Bauer, M., Su, G., Casper, C., He, R., Rehrauer, W., and Friedl, A. (2010). Heterogeneity of gene expression in stromal fibroblasts of human breast carcinomas and normal breast. *Oncogene* 29, 1732-1740.

Begley, L., Monteleon, C., Shah, R.B., Macdonald, J.W., and Macoska, J.A. (2005). CXCL12 overexpression and secretion by aging fibroblasts enhance human prostate epithelial proliferation in vitro. *Aging Cell* 4, 291-298.

Bhowmick, N.A., Neilson, E.G., and Moses, H.L. (2004). Stromal fibroblasts in cancer initiation and progression. *Nature* 432, 332-337.

Bianchi-Frias, D., Vakar-Lopez, F., Coleman, I.M., Plymate, S.R., Reed, M.J., and Nelson, P.S. (2010). The effects of aging on the molecular and cellular composition of the prostate microenvironment. *PLoS One* 5.

Bierie, B., and Moses, H.L. (2009). Gain or loss of TGFbeta signaling in mammary carcinoma cells can promote metastasis. *Cell Cycle* 8, 3319-3327.

Bissell, M.J., and Hines, W.C. (2011). Why don't we get more cancer? A proposed role of the microenvironment in restraining cancer progression. *Nat Med* 17, 320-329.

Bisson, C., Blacher, S., Polette, M., Blanc, J.F., Kebers, F., Desreux, J., Tetu, B., Rosenbaum, J., Foidart, J.M., Birembaut, P., et al. (2003). Restricted expression of membrane type 1-matrix metalloproteinase by myofibroblasts adjacent to human breast cancer cells. *Int J Cancer* 105, 7-13.

Blanchet, S., Ramgolam, K., Baulig, A., Marano, F., and Baeza-Squiban, A. (2004). Fine particulate matter induces amphiregulin secretion by bronchial epithelial cells. *Am J Respir Cell Mol Biol* 30, 421-427.

Buess, M., Nuyten, D.S., Hastie, T., Nielsen, T., Pesich, R., and Brown, P.O. (2007). Characterization of heterotypic interaction effects in vitro to deconvolute global gene expression profiles in cancer. *Genome Biol* 8, R191.

Busser, B., Sancey, L., Brambilla, E., Coll, J.L., and Hurbin, A. (2011). The multiple roles of amphiregulin in human cancer. *Biochim Biophys Acta* 1816, 119-131.

Busser, B., Sancey, L., Josserand, V., Niang, C., Favrot, M.C., Coll, J.L., and Hurbin, A. (2010). Amphiregulin promotes BAX inhibition and resistance to gefitinib in non-small-cell lung cancers. *Mol Ther* 18, 528-535.

Campbell, I., Polyak, K., and Haviv, I. (2009a). Clonal mutations in the cancer-associated fibroblasts: the case against genetic coevolution. *Cancer Res* 69, 6765-6768; discussion 6769.

Campbell, I., Polyak, K., and Haviv, I. (2009b). Genomic Alterations in Tumor Stroma Response. *Cancer Res* 69, 6764-6764.

- Camps, J.L., Chang, S.M., Hsu, T.C., Freeman, M.R., Hong, S.J., Zhau, H.E., von Eschenbach, A.C., and Chung, L.W. (1990). Fibroblast-mediated acceleration of human epithelial tumor growth in vivo. *Proc Natl Acad Sci U S A* 87, 75-79.
- Casey, T., Bond, J., Tighe, S., Hunter, T., Lintault, L., Patel, O., Eneman, J., Crocker, A., White, J., Tessitore, J., et al. (2009). Molecular signatures suggest a major role for stromal cells in development of invasive breast cancer. *Breast Cancer Res Treat* 114, 47-62.
- Chang, H.Y., Sneddon, J.B., Alizadeh, A.A., Sood, R., West, R.B., Montgomery, K., Chi, J.T., van de Rijn, M., Botstein, D., and Brown, P.O. (2004). Gene expression signature of fibroblast serum response predicts human cancer progression: similarities between tumors and wounds. *PLoS Biol* 2, E7.
- Cheng, N., Chytil, A., Shyr, Y., Joly, A., and Moses, H.L. (2007). Enhanced hepatocyte growth factor signaling by type II transforming growth factor-beta receptor knockout fibroblasts promotes mammary tumorigenesis. *Cancer Res* 67, 4869-4877.
- Chokki, M., Mitsuhashi, H., and Kamimura, T. (2006). Metalloprotease-dependent amphiregulin release mediates tumor necrosis factor-alpha-induced IL-8 secretion in the human airway epithelial cell line NCI-H292. *Life Sci* 78, 3051-3057.
- Coffey, R.J., Hawkey, C.J., Damstrup, L., Graves-Deal, R., Daniel, V.C., Dempsey, P.J., Chinery, R., Kirkland, S.C., DuBois, R.N., Jetton, T.L., et al. (1997). Epidermal growth factor receptor activation induces nuclear targeting of cyclooxygenase-2, basolateral release of prostaglandins, and mitogenesis in polarizing colon cancer cells. *Proc Natl Acad Sci U S A* 94, 657-662.
- Condeelis, J., and Pollard, J.W. (2006). Macrophages: obligate partners for tumor cell migration, invasion, and metastasis. *Cell* 124, 263-266.
- Coussens, L.M., and Pollard, J.W. (2011). Leukocytes in mammary development and cancer. *Cold Spring Harb Perspect Biol* 3.
- Coussens, L.M., and Werb, Z. (2002). Inflammation and cancer. *Nature* 420, 860-867.
- Crawford, Y., Kasman, I., Yu, L., Zhong, C., Wu, X., Modrusan, Z., Kaminker, J., and Ferrara, N. (2009). PDGF-C mediates the angiogenic and tumorigenic properties of fibroblasts associated with tumors refractory to anti-VEGF treatment. *Cancer Cell* 15, 21-34.
- Dagouassat, M., Suffee, N., Hlawaty, H., Haddad, O., Charni, F., Laguillier, C., Vassy, R., Martin, L., Schischmanoff, P.O., Gattegno, L., et al. (2010). Monocyte chemoattractant protein-1 (MCP-1)/CCL2 secreted by hepatic myofibroblasts promotes migration and invasion of human hepatoma cells. *Int J Cancer* 126, 1095-1108.

Dahinden, C.A., Geiser, T., Brunner, T., von Tscherner, V., Caput, D., Ferrara, P., Minty, A., and Baggiolini, M. (1994). Monocyte chemotactic protein 3 is a most effective basophil- and eosinophil-activating chemokine. *J Exp Med* 179, 751-756.

Daly, A.J., McIlreavey, L., and Irwin, C.R. (2008). Regulation of HGF and SDF-1 expression by oral fibroblasts--implications for invasion of oral cancer. *Oral Oncol* 44, 646-651.

Das, S.K., Chakraborty, I., Paria, B.C., Wang, X.N., Plowman, G., and Dey, S.K. (1995). Amphiregulin is an implantation-specific and progesterone-regulated gene in the mouse uterus. *Mol Endocrinol* 9, 691-705.

de Visser, K.E., Korets, L.V., and Coussens, L.M. (2005). De novo carcinogenesis promoted by chronic inflammation is B lymphocyte dependent. *Cancer Cell* 7, 411-423.

De Wever, O., Nguyen, Q.D., Van Hoorde, L., Bracke, M., Bruyneel, E., Gespach, C., and Mareel, M. (2004). Tenascin-C and SF/HGF produced by myofibroblasts in vitro provide convergent pro-invasive signals to human colon cancer cells through RhoA and Rac. *FASEB journal : official publication of the Federation of American Societies for Experimental Biology* 18, 1016-1018.

Debenzon, E.G. (1951). [Sarcomatous modification of the stroma in transplanted mice adenocarcinoma]. *Arkh Patol* 13, 23-28.

Decock, B., Conings, R., Lenaerts, J.P., Billiau, A., and Van Damme, J. (1990). Identification of the monocyte chemotactic protein from human osteosarcoma cells and monocytes: detection of a novel N-terminally processed form. *Biochem Biophys Res Commun* 167, 904-909.

DeCosse, J.J., Gossens, C., Kuzma, J.F., and Unsworth, B.R. (1975). Embryonic inductive tissues that cause histologic differentiation of murine mammary carcinoma in vitro. *J Natl Cancer Inst* 54, 913-922.

Denardo, D.G., Brennan, D.J., Rexhepaj, E., Ruffell, B., Shiao, S.L., Madden, S.F., Gallagher, W.M., Wadhvani, N., Keil, S.D., Junaid, S.A., et al. (2011). Leukocyte Complexity Predicts Breast Cancer Survival and Functionally Regulates Response to Chemotherapy. *Cancer Discov* 1, 54-67.

Dolberg, D.S., and Bissell, M.J. (1984). Inability of Rous sarcoma virus to cause sarcomas in the avian embryo. *Nature* 309, 552-556.

Dolberg, D.S., Hollingsworth, R., Hertle, M., and Bissell, M.J. (1985). Wounding and its role in RSV-mediated tumor formation. *Science* 230, 676-678.

Dudas, J., Bitsche, M., Schartinger, V., Falkeis, C., Sprinzl, G.M., and Riechelmann, H. (2011). Fibroblasts produce brain-derived neurotrophic factor and induce mesenchymal transition of oral tumor cells. *Oral Oncol* 47, 98-103.

Dwyer, R.M., Potter-Beirne, S.M., Harrington, K.A., Lowery, A.J., Hennessy, E., Murphy, J.M., Barry, F.P., O'Brien, T., and Kerin, M.J. (2007). Monocyte chemotactic protein-1 secreted by primary breast tumors stimulates migration of mesenchymal stem cells. *Clin Cancer Res* 13, 5020-5027.

Egeblad, M., and Werb, Z. (2002). New functions for the matrix metalloproteinases in cancer progression. *Nat Rev Cancer* 2, 161-174.

Egeblad, M., Littlepage, L.E., and Werb, Z. (2005). The fibroblastic coconspirator in cancer progression. *Cold Spring Harb Symp Quant Biol* 70, 383-388.

Egeblad, M., Nakasone, E.S., and Werb, Z. (2010). Tumors as organs: complex tissues that interface with the entire organism. *Dev Cell* 18, 884-901.

Erez, N., Truitt, M., Olson, P., Arron, S.T., and Hanahan, D. (2010). Cancer-Associated Fibroblasts Are Activated in Incipient Neoplasia to Orchestrate Tumor-Promoting Inflammation in an NF-kappaB-Dependent Manner. *Cancer Cell* 17, 135-147.

Faget, J., Biota, C., Bachelot, T., Gobert, M., Treilleux, I., Goutagny, N., Durand, I., Leon-Goddard, S., Blay, J.Y., Caux, C., et al. (2011). Early detection of tumor cells by innate immune cells leads to T(reg) recruitment through CCL22 production by tumor cells. *Cancer Res* 71, 6143-6152.

Fakhrejehani, E., and Toi, M. (2012). Tumor angiogenesis: pericytes and maturation are not to be ignored. *J Oncol* 2012, 261750.

Farmer, P., Bonnefoi, H., Anderle, P., Cameron, D., Wirapati, P., Becette, V., Andre, S., Piccart, M., Campone, M., Brain, E., et al. (2009). A stroma-related gene signature predicts resistance to neoadjuvant chemotherapy in breast cancer. *Nat Med* 15, 68-74.

Fernandes, A.M., Hamburger, A.W., and Gerwin, B.I. (1999). Production of epidermal growth factor related ligands in tumorigenic and benign human lung epithelial cells. *Cancer Lett* 142, 55-63.

Fernandez, E.J., and Lolis, E. (2002). Structure, function, and inhibition of chemokines. *Annu Rev Pharmacol Toxicol* 42, 469-499.

Ferrara, N., Hillan, K.J., Gerber, H.P., and Novotny, W. (2004). Discovery and development of bevacizumab, an anti-VEGF antibody for treating cancer. *Nat Rev Drug Discov* 3, 391-400.

Finak, G., Bertos, N., Pepin, F., Sadekova, S., Souleimanova, M., Zhao, H., Chen, H., Omeroglu, G., Meterissian, S., Omeroglu, A., et al. (2008). Stromal gene expression predicts clinical outcome in breast cancer. *Nat Med* 14, 518-527.

Folkman, J., Merler, E., Abernathy, C., and Williams, G. (1971). Isolation of a tumor factor responsible for angiogenesis. *J Exp Med* 133, 275-288.

Fromigue, O., Louis, K., Dayem, M., Milanini, J., Pages, G., Tartare-Deckert, S., Ponzio, G., Hofman, P., Barbry, P., Auburger, P., et al. (2003). Gene expression profiling of normal human pulmonary fibroblasts following coculture with non-small-cell lung cancer cells reveals alterations related to matrix degradation, angiogenesis, cell growth and survival. *Oncogene* 22, 8487-8497.

Fu, L., Zhang, C., Zhang, L.Y., Dong, S.S., Lu, L.H., Chen, J., Dai, Y., Li, Y., Kong, K.L., Kwong, D.L., et al. (2011). Wnt2 secreted by tumour fibroblasts promotes tumour progression in oesophageal cancer by activation of the Wnt/beta-catenin signalling pathway. *Gut* 60, 1635-1643.

Fukumura, D., Xavier, R., Sugiura, T., Chen, Y., Park, E.C., Lu, N., Selig, M., Nielsen, G., Taksir, T., Jain, R.K., et al. (1998). Tumor induction of VEGF promoter activity in stromal cells. *Cell* 94, 715-725.

Gao, D., Joshi, N., Choi, H., Ryu, S., Hahn, M., Catena, R., Sadik, H., Argani, P., Wagner, P., Vahdat, L.T., et al. (2012). Myeloid progenitor cells in the premetastatic lung promote metastases by inducing mesenchymal to epithelial transition. *Cancer Res* 72, 1384-1394.

Ghabrial, A.S., Levi, B.P., and Krasnow, M.A. (2011). A systematic screen for tube morphogenesis and branching genes in the *Drosophila* tracheal system. *PLoS Genet* 7, e1002087.

Giusti, C., Desruisseau, S., Ma, L., Calvo, F., Martin, P.M., and Berthois, Y. (2003). Transforming growth factor beta-1 and amphiregulin act in synergy to increase the production of urokinase-type plasminogen activator in transformed breast epithelial cells. *Int J Cancer* 105, 769-778.

Gladue, R.P., Brown, M.F., and Zwillich, S.H. (2010). CCR1 antagonists: what have we learned from clinical trials. *Curr Top Med Chem* 10, 1268-1277.

- Goede, V., Brogelli, L., Ziche, M., and Augustin, H.G. (1999). Induction of inflammatory angiogenesis by monocyte chemoattractant protein-1. *Int J Cancer* 82, 765-770.
- Graeber, T.G., and Eisenberg, D. (2001). Bioinformatic identification of potential autocrine signaling loops in cancers from gene expression profiles. *Nat Genet* 29, 295-300.
- Granot, Z., Henke, E., Comen, E.A., King, T.A., Norton, L., and Benezra, R. (2011). Tumor entrained neutrophils inhibit seeding in the premetastatic lung. *Cancer Cell* 20, 300-314.
- Grugan, K.D., Miller, C.G., Yao, Y., Michaylira, C.Z., Ohashi, S., Klein-Szanto, A.J., Diehl, J.A., Herlyn, M., Han, M., Nakagawa, H., et al. (2010). Fibroblast-secreted hepatocyte growth factor plays a functional role in esophageal squamous cell carcinoma invasion. *Proc Natl Acad Sci U S A* 107, 11026-11031.
- Haller, C. (1951). [Infrared studies of the vascularization of the stroma as an indication of the reaction to carcinoma]. *Med Klin* 46, 892-894.
- Hanahan, D., and Coussens, L.M. (2012). Accessories to the crime: functions of cells recruited to the tumor microenvironment. *Cancer Cell* 21, 309-322.
- Hembruff, S.L., Jokar, I., Yang, L., and Cheng, N. (2010). Loss of transforming growth factor-beta signaling in mammary fibroblasts enhances CCL2 secretion to promote mammary tumor progression through macrophage-dependent and -independent mechanisms. *Neoplasia* 12, 425-433.
- Hicks, J., Krasnitz, A., Lakshmi, B., Navin, N.E., Riggs, M., Leib, E., Esposito, D., Alexander, J., Troge, J., Gruber, V., et al. (2006). Novel patterns of genome rearrangement and their association with survival in breast cancer. *Genome Res* 16, 1465-1479.
- Himelstein, B.P., and Muschel, R.J. (1996). Induction of matrix metalloproteinase 9 expression in breast carcinoma cells by a soluble factor from fibroblasts. *Clin Exp Metastasis* 14, 197-208.
- Hirota, N., Risse, P.A., Novali, M., McGovern, T., Al-Alwan, L., McCuaig, S., Proud, D., Hayden, P., Hamid, Q., and Martin, J.G. (2012). Histamine may induce airway remodeling through release of epidermal growth factor receptor ligands from bronchial epithelial cells. *The FASEB journal : official publication of the Federation of American Societies for Experimental Biology*.
- Hodi, F.S., O'Day, S.J., McDermott, D.F., Weber, R.W., Sosman, J.A., Haanen, J.B., Gonzalez, R., Robert, C., Schadendorf, D., Hassel, J.C., et al. (2010). Improved survival with ipilimumab in patients with metastatic melanoma. *N Engl J Med* 363, 711-723.

- Hosein, A.N., Wu, M., Arcand, S.L., Lavallee, S., Hebert, J., Tonin, P.N., and Basik, M. (2010). Breast Carcinoma-Associated Fibroblasts Rarely Contain p53 Mutations or Chromosomal Aberrations. *Cancer Res* 70, 5770-5777.
- Hu, M., and Polyak, K. (2008a). Microenvironmental regulation of cancer development. *Curr Opin Genet Dev* 18, 27-34.
- Hu, M., and Polyak, K. (2008b). Molecular characterisation of the tumour microenvironment in breast cancer. *Eur J Cancer* 44, 2760-2765. Epub 2008 Nov 2719.
- Hu, M., Peluffo, G., Chen, H., Gelman, R., Schnitt, S., and Polyak, K. (2009). Role of COX-2 in epithelial-stromal cell interactions and progression of ductal carcinoma in situ of the breast. *Proc Natl Acad Sci U S A* 106, 3372-3377.
- Hu, M., Yao, J., Cai, L., Bachman, K.E., van den Brule, F., Velculescu, V., and Polyak, K. (2005). Distinct epigenetic changes in the stromal cells of breast cancers. *Nat Genet* 37, 899-905.
- Ishikawa, F., Yasukawa, M., Lyons, B., Yoshida, S., Miyamoto, T., Yoshimoto, G., Watanabe, T., Akashi, K., Shultz, L.D., and Harada, M. (2005). Development of functional human blood and immune systems in NOD/SCID/IL2 receptor (Faget et al.) chain(null) mice. *Blood* 106, 1565-1573.
- Ishikawa, N., Daigo, Y., Takano, A., Taniwaki, M., Kato, T., Hayama, S., Murakami, H., Takeshima, Y., Inai, K., Nishimura, H., et al. (2005). Increases of amphiregulin and transforming growth factor-alpha in serum as predictors of poor response to gefitinib among patients with advanced non-small cell lung cancers. *Cancer Res* 65, 9176-9184.
- Islam, S.A., Chang, D.S., Colvin, R.A., Byrne, M.H., McCully, M.L., Moser, B., Lira, S.A., Charo, I.F., and Luster, A.D. (2011). Mouse CCL8, a CCR8 agonist, promotes atopic dermatitis by recruiting IL-5+ T(H)2 cells. *Nat Immunol* 12, 167-177.
- Ito, A., Nakajima, S., Sasaguri, Y., Nagase, H., and Mori, Y. (1995). Co-culture of human breast adenocarcinoma MCF-7 cells and human dermal fibroblasts enhances the production of matrix metalloproteinases 1, 2 and 3 in fibroblasts. *Br J Cancer* 71, 1039-1045.
- Joesting, M.S., Perrin, S., Elenbaas, B., Fawell, S.E., Rubin, J.S., Franco, O.E., Hayward, S.W., Cunha, G.R., and Marker, P.C. (2005). Identification of SFRP1 as a candidate mediator of stromal-to-epithelial signaling in prostate cancer. *Cancer Res* 65, 10423-10430.
- Joyce, J.A., Pollard, J.W. (2009) Microenvironmental Regulation of Metastasis. *Nat Rev Cancer*.9, 239-252.

Jung, D.W., Che, Z.M., Kim, J., Kim, K., Kim, K.Y., and Williams, D. (2010). Tumor-stromal crosstalk in invasion of oral squamous cell carcinoma: a pivotal role of CCL7. *Int J Cancer* 127, 332-344.

Kalluri, R., and Weinberg, R.A. (2009). The basics of epithelial-mesenchymal transition. *J Clin Invest* 119, 1420-1428.

Kalluri, R., and Zeisberg, M. (2006). Fibroblasts in cancer. *Nat Rev Cancer* 6, 392-401.

Karnoub, A.E., Dash, A.B., Vo, A.P., Sullivan, A., Brooks, M.W., Bell, G.W., Richardson, A.L., Polyak, K., Tubo, R., and Weinberg, R.A. (2007). Mesenchymal stem cells within tumour stroma promote breast cancer metastasis. *Nature* 449, 557-563.

Kim, K.J., Li, B., Winer, J., Armanini, M., Gillett, N., Phillips, H.S., and Ferrara, N. (1993). Inhibition of vascular endothelial growth factor-induced angiogenesis suppresses tumour growth in vivo. *Nature* 362, 841-844.

Kim, S.Y., Lee, C.H., Midura, B.V., Yeung, C., Mendoza, A., Hong, S.H., Ren, L., Wong, D., Korz, W., Merzouk, A., et al. (2008). Inhibition of the CXCR4/CXCL12 chemokine pathway reduces the development of murine pulmonary metastases. *Clin Exp Metastasis* 25, 201-211.

Kitamura, T., Fujishita, T., Loetscher, P., Revesz, L., Hashida, H., Kizaka-Kondoh, S., Aoki, M., and Taketo, M.M. (2010). Inactivation of chemokine (C-C motif) receptor 1 (CCR1) suppresses colon cancer liver metastasis by blocking accumulation of immature myeloid cells in a mouse model. *Proc Natl Acad Sci U S A* 107, 13063-13068.

Kojima, Y., Acar, A., Eaton, E.N., Mellody, K.T., Scheel, C., Ben-Porath, I., Onder, T.T., Wang, Z.C., Richardson, A.L., Weinberg, R.A., et al. (2010). Autocrine TGF-beta and stromal cell-derived factor-1 (SDF-1) signaling drives the evolution of tumor-promoting mammary stromal myofibroblasts. *Proc Natl Acad Sci U S A* 107, 20009-20014.

Ksiazkiewicz, M., Gottfried, E., Kreutz, M., Mack, M., Hofstaedter, F., and Kunz-Schughart, L.A. (2010). Importance of CCL2-CCR2A/2B signaling for monocyte migration into spheroids of breast cancer-derived fibroblasts. *Immunobiology* 215, 737-747.

Kuperwasser, C., Chavarria, T., Wu, M., Magrane, G., Gray, J.W., Carey, L., Richardson, A., and Weinberg, R.A. (2004). Reconstruction of functionally normal and malignant human breast tissues in mice. *Proc Natl Acad Sci U S A* 101, 4966-4971.

Kurose, K., Gilley, K., Matsumoto, S., Watson, P.H., Zhou, X.P., and Eng, C. (2002). Frequent somatic mutations in PTEN and TP53 are mutually exclusive in the stroma of breast carcinomas. *Nat Genet* 32, 355-357.

- Laing, K.J., and Secombes, C.J. (2004). Chemokines. *Dev Comp Immunol* 28, 443-460.
- Larsen, C.G., Zachariae, C.O., Oppenheim, J.J., and Matsushima, K. (1989). Production of monocyte chemotactic and activating factor (MCAF) by human dermal fibroblasts in response to interleukin 1 or tumor necrosis factor. *Biochem Biophys Res Commun* 160, 1403-1408.
- Le Melletier, J., Daumet, and Paillas, J. (1952). [Intrinsic epistoma (bronchial epithelioma with altered stroma) and bronchial tuberculosis]. *J Fr Med Chir Thorac* 6, 441-445.
- Lebrecht, A., Grimm, C., Lantsch, T., Ludwig, E., Hefler, L., Ulbrich, E., and Koelbl, H. (2004). Monocyte chemoattractant protein-1 serum levels in patients with breast cancer. *Tumour Biol* 25, 14-17.
- Lederle, W., Hartenstein, B., Meides, A., Kunzelmann, H., Werb, Z., Angel, P., and Mueller, M.M. (2010). MMP13 as a stromal mediator in controlling persistent angiogenesis in skin carcinoma. *Carcinogenesis* 31, 1175-1184.
- LeJeune, S., Leek, R., Horak, E., Plowman, G., Greenall, M., and Harris, A.L. (1993). Amphiregulin, epidermal growth factor receptor, and estrogen receptor expression in human primary breast cancer. *Cancer Res* 53, 3597-3602.
- Leung, D.W., Cachianes, G., Kuang, W.J., Goeddel, D.V., and Ferrara, N. (1989). Vascular endothelial growth factor is a secreted angiogenic mitogen. *Science* 246, 1306-1309.
- Liles, J.S., Arnoletti, J.P., Kossenkov, A.V., Mikhaylina, A., Frost, A.R., Kulesza, P., Heslin, M.J., and Frolov, A. (2011). Targeting ErbB3-mediated stromal-epithelial interactions in pancreatic ductal adenocarcinoma. *Br J Cancer* 105, 523-533.
- Lin, E.Y., and Pollard, J.W. (2004). Macrophages: modulators of breast cancer progression. *Novartis Found Symp* 256, 158-168; discussion 168-172, 259-169.
- Lin, J., Liu, C., Ge, L., Gao, Q., He, X., Liu, Y., Li, S., Zhou, M., Chen, Q., and Zhou, H. (2011). Carcinoma-associated fibroblasts promotes the proliferation of a lingual carcinoma cell line by secreting keratinocyte growth factor. *Tumour Biol* 32, 597-602.
- Lin, S., Wan, S., Sun, L., Hu, J., Fang, D., Zhao, R., Yuan, S., and Zhang, L. (2012). Chemokine C-C motif receptor 5 and C-C motif ligand 5 promote cancer cell migration under hypoxia. *Cancer Sci*.

Liu, G., Yang, G., Chang, B., Mercado-Uribe, I., Huang, M., Zheng, J., Bast, R.C., Lin, S.H., and Liu, J. (2010). Stanniocalcin 1 and ovarian tumorigenesis. *J Natl Cancer Inst* 102, 812-827.

Locati, M., Zhou, D., Luini, W., Evangelista, V., Mantovani, A., and Sozzani, S. (1994). Rapid induction of arachidonic acid release by monocyte chemotactic protein-1 and related chemokines. Role of Ca²⁺ influx, synergism with platelet-activating factor and significance for chemotaxis. *J Biol Chem* 269, 4746-4753.

Lu, P., Weaver, V.M., and Werb, Z. (2012). The extracellular matrix: a dynamic niche in cancer progression. *J Cell Biol* 196, 395-406.

Lu, X., and Kang, Y. (2009). Chemokine (C-C motif) ligand 2 engages CCR2⁺ stromal cells of monocytic origin to promote breast cancer metastasis to lung and bone. *J Biol Chem* 284, 29087-29096.

Lu, X., Wang, Q., Hu, G., Van Poznak, C., Fleisher, M., Reiss, M., Massague, J., and Kang, Y. (2009). ADAMTS1 and MMP1 proteolytically engage EGF-like ligands in an osteolytic signaling cascade for bone metastasis. *Genes Dev* 23, 1882-1894.

Luo, X., Ruhland, M.K., Pazolli, E., Lind, A.C., and Stewart, S.A. (2011). Osteopontin stimulates preneoplastic cellular proliferation through activation of the MAPK pathway. *Mol Cancer Res* 9, 1018-1029.

Ma, L., Gauville, C., Berthois, Y., Millot, G., Johnson, G.R., and Calvo, F. (1999). Antisense expression for amphiregulin suppresses tumorigenicity of a transformed human breast epithelial cell line. *Oncogene* 18, 6513-6520.

Ma, L., de Roquancourt, A., Bertheau, P., Chevret, S., Millot, G., Sastre-Garau, X., Espie, M., Marty, M., Janin, A., and Calvo, F. (2001). Expression of amphiregulin and epidermal growth factor receptor in human breast cancer: analysis of autocriny and stromal-epithelial interactions. *J Pathol* 194, 413-419.

Ma, X.J., Dahiya, S., Richardson, E., Erlander, M., and Sgroi, D.C. (2009). Gene expression profiling of the tumor microenvironment during breast cancer progression. *Breast Cancer Res* 11, R7.

Maeda, T., Desouky, J., and Friedl, A. (2006). Syndecan-1 expression by stromal fibroblasts promotes breast carcinoma growth in vivo and stimulates tumor angiogenesis. *Oncogene* 25, 1408-1412.

Mahtouk, K., Hose, D., Reme, T., De Vos, J., Jourdan, M., Moreaux, J., Fiol, G., Raab, M., Jourdan, E., Grau, V., et al. (2005). Expression of EGF-family receptors and amphiregulin in multiple myeloma. Amphiregulin is a growth factor for myeloma cells. *Oncogene* 24, 3512-3524.

Mari, B.P., Anderson, I.C., Mari, S.E., Ning, Y., Lutz, Y., Kobzik, L., and Shipp, M.A. (1998). Stromelysin-3 is induced in tumor/stroma cocultures and inactivated via a tumor-specific and basic fibroblast growth factor-dependent mechanism. *J Biol Chem* 273, 618-626.

Masson, R., Lefebvre, O., Noel, A., Fahime, M.E., Chenard, M.P., Wendling, C., Kebers, F., LeMeur, M., Dierich, A., Foidart, J.M., et al. (1998). In vivo evidence that the stromelysin-3 metalloproteinase contributes in a paracrine manner to epithelial cell malignancy. *J Cell Biol* 140, 1535-1541.

Matsuo, Y., Ochi, N., Sawai, H., Yasuda, A., Takahashi, H., Funahashi, H., Takeyama, H., Tong, Z., and Guha, S. (2009). CXCL8/IL-8 and CXCL12/SDF-1alpha co-operatively promote invasiveness and angiogenesis in pancreatic cancer. *Int J Cancer* 124, 853-861.

McBryan, J., Howlin, J., Napoletano, S., and Martin, F. (2008). Amphiregulin: role in mammary gland development and breast cancer. *J Mammary Gland Biol Neoplasia* 13, 159-169.

Menon, L.G., Picinich, S., Koneru, R., Gao, H., Lin, S.Y., Koneru, M., Mayer-Kuckuk, P., Glod, J., and Banerjee, D. (2007). Differential gene expression associated with migration of mesenchymal stem cells to conditioned medium from tumor cells or bone marrow cells. *Stem Cells* 25, 520-528.

Mintz, B., and Illmensee, K. (1975). Normal genetically mosaic mice produced from malignant teratocarcinoma cells. *Proc Natl Acad Sci U S A* 72, 3585-3589.

Mishra, P., Banerjee, D., and Ben-Baruch, A. (2011). Chemokines at the crossroads of tumor-fibroblast interactions that promote malignancy. *J Leukocyte Biol* 89, 31-39.

Mishra, P.J., Humeniuk, R., Medina, D.J., Alexe, G., Mesirov, J.P., Ganesan, S., Glod, J.W., and Banerjee, D. (2008). Carcinoma-associated fibroblast-like differentiation of human mesenchymal stem cells. *Cancer Res* 68, 4331-4339.

Moinfar, F., Man, Y.G., Arnould, L., Bratthauer, G.L., Ratschek, M., and Tavassoli, F.A. (2000). Concurrent and independent genetic alterations in the stromal and epithelial cells of mammary carcinoma: implications for tumorigenesis. *Cancer Res* 60, 2562-2566.

Mueller, L., Goumas, F.A., Affeldt, M., Sandtner, S., Gehling, U.M., Brilloff, S., Walter, J., Karnatz, N., Lamszus, K., Rogiers, X., et al. (2007). Stromal fibroblasts in colorectal liver

metastases originate from resident fibroblasts and generate an inflammatory microenvironment. *Am J Pathol* 171, 1608-1618.

Mueller, M.M., and Fusenig, N.E. (2004). Friends or foes - bipolar effects of the tumour stroma in cancer. *Nat Rev Cancer* 4, 839-849.

Murata, T., Mizushima, H., Chinen, I., Moribe, H., Yagi, S., Hoffman, R.M., Kimura, T., Yoshino, K., Ueda, Y., Enomoto, T., et al. (2011). HB-EGF and PDGF mediate reciprocal interactions of carcinoma cells with cancer-associated fibroblasts to support progression of uterine cervical cancers. *Cancer Res* 71, 6633-6642.

Murdoch, C., and Finn, A. (2000). Chemokine receptors and their role in inflammation and infectious diseases. *Blood* 95, 3032-3043.

Nakagome, K., and Nagata, M. (2011). Pathogenesis of airway inflammation in bronchial asthma. *Auris Nasus Larynx* 38, 555-563.

Nakamura, T., Matsumoto, K., Kiritoshi, A., and Tano, Y. (1997). Induction of hepatocyte growth factor in fibroblasts by tumor-derived factors affects invasive growth of tumor cells: in vitro analysis of tumor-stromal interactions. *Cancer Res* 57, 3305-3313.

Nam, J.S., Kang, M.J., Suchar, A.M., Shimamura, T., Kohn, E.A., Michalowska, A.M., Jordan, V.C., Hirohashi, S., and Wakefield, L.M. (2006). Chemokine (C-C motif) ligand 2 mediates the prometastatic effect of dysadherin in human breast cancer cells. *Cancer Res* 66, 7176-7184.

Navolanic, P.M., Steelman, L.S., and McCubrey, J.A. (2003). EGFR family signaling and its association with breast cancer development and resistance to chemotherapy (Review). *Int J Oncol* 22, 237-252.

Neote, K., DiGregorio, D., Mak, J.Y., Horuk, R., and Schall, T.J. (1993). Molecular cloning, functional expression, and signaling characteristics of a C-C chemokine receptor. *Cell* 72, 415-425.

Nielsen, B.S., Egeblad, M., Rank, F., Askautrud, H.A., Pennington, C.J., Pedersen, T.X., Christensen, I.J., Edwards, D.R., Werb, Z., and Lund, L.R. (2008). Matrix metalloproteinase 13 is induced in fibroblasts in polyomavirus middle T antigen-driven mammary carcinoma without influencing tumor progression. *PLoS One* 3, e2959.

Noel, A., De Pauw-Gillet, M.C., Purnell, G., Nusgens, B., Lapiere, C.M., and Foidart, J.M. (1993). Enhancement of tumorigenicity of human breast adenocarcinoma cells in nude mice by matrigel and fibroblasts. *Br J Cancer* 68, 909-915.

Noel, A., Hajitou, A., L'Hoir, C., Maquoi, E., Baramova, E., Lewalle, J.M., Remacle, A., Kebers, F., Brown, P., Calberg-Bacq, C.M., et al. (1998). Inhibition of stromal matrix metalloproteinases: effects on breast-tumor promotion by fibroblasts. *Int J Cancer* 76, 267-273.

Noël A, Jost M, Maquoi E. (2008). Matrix metalloproteinases at cancer tumor-host interface. *Semin Cell Dev Biol.* 2008 Feb;19(1):52-60.

Noso, N., Proost, P., Van Damme, J., and Schroder, J.M. (1994). Human monocyte chemotactic proteins-2 and 3 (MCP-2 and MCP-3) attract human eosinophils and desensitize the chemotactic responses towards RANTES. *Biochem Biophys Res Commun* 200, 1470-1476.

Nyberg, P., Salo, T., and Kalluri, R. (2008). Tumor microenvironment and angiogenesis. *Front Biosci* 13, 6537-6553.

Okada, M., Saio, M., Kito, Y., Ohe, N., Yano, H., Yoshimura, S., Iwama, T., and Takami, T. (2009). Tumor-associated macrophage/microglia infiltration in human gliomas is correlated with MCP-3, but not MCP-1. *Int J Oncol* 34, 1621-1627.

Olumi, A.F., Grossfeld, G.D., Hayward, S.W., Carroll, P.R., Tlsty, T.D., and Cunha, G.R. (1999). Carcinoma-associated fibroblasts direct tumor progression of initiated human prostatic epithelium. *Cancer Res* 59, 5002-5011.

Orimo, A., and Weinberg, R.A. (2006). Stromal fibroblasts in cancer: a novel tumor-promoting cell type. *Cell Cycle* 5, 1597-1601.

Orimo, A., Gupta, P.B., Sgroi, D.C., Arenzana-Seisdedos, F., Delaunay, T., Naeem, R., Carey, V.J., Richardson, A.L., and Weinberg, R.A. (2005). Stromal fibroblasts present in invasive human breast carcinomas promote tumor growth and angiogenesis through elevated SDF-1/CXCL12 secretion. *Cell* 121, 335-348.

Ostman, A., and Augsten, M. (2009). Cancer-associated fibroblasts and tumor growth - bystanders turning into key players. *Curr Opin Genet Dev* 19, 67-73.

Overall, C.M., and Kleinfeld, O. (2006). Tumour microenvironment - opinion: validating matrix metalloproteinases as drug targets and anti-targets for cancer therapy. *Nat Rev Cancer* 6, 227-239.

Panos, R.J., Rubin, J.S., Csaky, K.G., Aaronson, S.A., and Mason, R.J. (1993). Keratinocyte growth factor and hepatocyte growth factor/scatter factor are heparin-binding growth factors for alveolar type II cells in fibroblast-conditioned medium. *J Clin Invest* 92, 969-977.

Paris, A.L., Meissner, W.A., and McDermott, W.V., Jr. (1982). Histologic changes seen in the hepatic parenchyma and in metastatic nodules following hepatic dearterialization. *J Surg Oncol* 19, 114-118.

Patel, Z.S., Grugan, K.D., Rustgi, A.K., Cucinotta, F.A., and Huff, J.L. (2012). Ionizing radiation enhances esophageal epithelial cell migration and invasion through a paracrine mechanism involving stromal-derived hepatocyte growth factor. *Radiat Res* 177, 200-208.

Pegram, M.D., Konecny, G., and Slamon, D.J. (2000). The molecular and cellular biology of HER2/neu gene amplification/overexpression and the clinical development of herceptin (trastuzumab) therapy for breast cancer. *Cancer Treat Res* 103, 57-75.

Peppercorn, J., Perou, C.M., and Carey, L.A. (2008). Molecular subtypes in breast cancer evaluation and management: divide and conquer. *Cancer Invest* 26, 1-10.

Perou, C.M., Sorlie, T., Eisen, M.B., van de Rijn, M., Jeffrey, S.S., Rees, C.A., Pollack, J.R., Ross, D.T., Johnsen, H., Akslen, L.A., et al. (2000). Molecular portraits of human breast tumours. *Nature* 406, 747-752.

Petersen, O.W., Nielsen, H.L., Gudjonsson, T., Villadsen, R., Rank, F., Niebuhr, E., Bissell, M.J., and Ronnov-Jessen, L. (2003). Epithelial to mesenchymal transition in human breast cancer can provide a nonmalignant stroma. *Am J Pathol* 162, 391-402.

Pietras, K., Pahler, J., Bergers, G., and Hanahan, D. (2008). Functions of paracrine PDGF signaling in the proangiogenic tumor stroma revealed by pharmacological targeting. *PLoS Med* 5, e19.

Plowman, G.D., Green, J.M., McDonald, V.L., Neubauer, M.G., Distech, C.M., Todaro, G.J., and Shoyab, M. (1990). The amphiregulin gene encodes a novel epidermal growth factor-related protein with tumor-inhibitory activity. *Mol Cell Biol* 10, 1969-1981.

Polanska, U.M., Acar, A., and Orimo, A. (2011). Experimental generation of carcinoma-associated fibroblasts (CAFs) from human mammary fibroblasts. *J Vis Exp*, e3201.

Polyak, K., and Kalluri, R. (2010). The role of the microenvironment in mammary gland development and cancer. *Cold Spring Harb Perspect Biol* 2, a003244.

Potter, S.M., Dwyer, R.M., Hartmann, M.C., Khan, S., Boyle, M.P., Curran, C.E., and Kerin, M.J. (2012). Influence of stromal-epithelial interactions on breast cancer in vitro and in vivo. *Breast Cancer Res Treat* 131, 401-411.

Proost, P., Wuyts, A., and Van Damme, J. (1996). Human monocyte chemotactic proteins-2 and -3: structural and functional comparison with MCP-1. *J Leukocyte Biol* 59, 67-74.

Qian, B.Z., Li, J., Zhang, H., Kitamura, T., Zhang, J., Campion, L.R., Kaiser, E.A., Snyder, L.A., and Pollard, J.W. (2011). CCL2 recruits inflammatory monocytes to facilitate breast-tumour metastasis. *Nature* 475, 222-225.

Qin, L., Tamasi, J., Raggatt, L., Li, X., Feyen, J.H., Lee, D.C., Dicicco-Bloom, E., and Partridge, N.C. (2005). Amphiregulin is a novel growth factor involved in normal bone development and in the cellular response to parathyroid hormone stimulation. *J Biol Chem* 280, 3974-3981.

Quante, M., Tu, S.P., Tomita, H., Gonda, T., Wang, S.S., Takashi, S., Baik, G.H., Shibata, W., Diprete, B., Betz, K.S., et al. (2011). Bone marrow-derived myofibroblasts contribute to the mesenchymal stem cell niche and promote tumor growth. *Cancer Cell* 19, 257-272.

Rezzoug, F., Seelan, R.S., Bhattacharjee, V., Greene, R.M., and Pisano, M.M. (2011). Chemokine-mediated migration of mesencephalic neural crest cells. *Cytokine* 56, 760-768.

Robinson, S.C., Scott, K.A., Wilson, J.L., Thompson, R.G., Proudfoot, A.E., and Balkwill, F.R. (2003). A chemokine receptor antagonist inhibits experimental breast tumor growth. *Cancer Res* 63, 8360-8365.

Rollins, B.J., Morrison, E.D., and Stiles, C.D. (1988). Cloning and expression of JE, a gene inducible by platelet-derived growth factor and whose product has cytokine-like properties. *Proc Natl Acad Sci U S A* 85, 3738-3742.

Rollins, B.J., Walz, A., and Baggiolini, M. (1991). Recombinant human MCP-1/JE induces chemotaxis, calcium flux, and the respiratory burst in human monocytes. *Blood* 78, 1112-1116.

Ronnov-Jessen, L., Van Deurs, B., Nielsen, M., and Petersen, O.W. (1992). Identification, paracrine generation, and possible function of human breast carcinoma myofibroblasts in culture. *In Vitro Cell Dev Biol* 28A, 273-283.

Rosas, M., Thomas, B., Stacey, M., Gordon, S., and Taylor, P.R. (2010). The myeloid 7/4-antigen defines recently generated inflammatory macrophages and is synonymous with Ly-6B. *J Leukoc Biol* 88, 169-180.

Rossi, D., and Zlotnik, A. (2000). The biology of chemokines and their receptors. *Annu Rev Immunol* 18, 217-242.

Rozenchan, P.B., Carraro, D.M., Brentani, H., de Carvalho Mota, L.D., Bastos, E.P., e Ferreira, E.N., Torres, C.H., Katayama, M.L., Roela, R.A., Lyra, E.C., et al. (2009). Reciprocal changes in gene expression profiles of cocultured breast epithelial cells and primary fibroblasts. *Int J Cancer* 125, 2767-2777.

Rudnick, J.A., Arendt, L.M., Klebba, I., Hinds, J.W., Iyer, V., Gupta, P.B., Naber, S.P., and Kuperwasser, C. (2011). Functional heterogeneity of breast fibroblasts is defined by a prostaglandin secretory phenotype that promotes expansion of cancer-stem like cells. *PLoS One* 6, e24605.

Saijo, Y., Tanaka, M., Miki, M., Usui, K., Suzuki, T., Maemondo, M., Hong, X., Tazawa, R., Kikuchi, T., Matsushima, K., et al. (2002). Proinflammatory cytokine IL-1 beta promotes tumor growth of Lewis lung carcinoma by induction of angiogenic factors: in vivo analysis of tumor-stromal interaction. *J Immunol* 169, 469-475.

Saji, H., Koike, M., Yamori, T., Saji, S., Seiki, M., Matsushima, K., and Toi, M. (2001). Significant correlation of monocyte chemoattractant protein-1 expression with neovascularization and progression of breast carcinoma. *Cancer* 92, 1085-1091.

Santos, R.P., Benvenuti, T.T., Honda, S.T., Del Valle, P.R., Katayama, M.L., Brentani, H.P., Carraro, D.M., Rozenchan, P.B., Brentani, M.M., de Lyra, E.C., et al. (2011). Influence of the interaction between nodal fibroblast and breast cancer cells on gene expression. *Tumour Biol* 32, 145-157.

Sanz-Moreno, V., Gadea, G., Ahn, J., Paterson, H., Marra, P., Pinner, S., Sahai, E., and Marshall, C.J. (2008). Rac activation and inactivation control plasticity of tumor cell movement. *Cell* 135, 510-523.

Sato, N., Maehara, N., and Goggins, M. (2004). Gene expression profiling of tumor-stromal interactions between pancreatic cancer cells and stromal fibroblasts. *Cancer Res* 64, 6950-6956.

Sawyers, C.L. (2005). Making progress through molecular attacks on cancer. *Cold Spring Harb Symp Quant Biol* 70, 479-482.

Schmid, S.A., Gaumann, A., Wondrak, M., Eckermann, C., Schulte, S., Mueller-Klieser, W., Wheatley, D.N., and Kunz-Schughart, L.A. (2007). Lactate adversely affects the in vitro formation of endothelial cell tubular structures through the action of TGF-beta1. *Exp Cell Res* 313, 2531-2549.

Schor, A.M., Rushton, G., Ferguson, J.E., Howell, A., Redford, J., and Schor, S.L. (1994). Phenotypic heterogeneity in breast fibroblasts: functional anomaly in fibroblasts from histologically normal tissue adjacent to carcinoma. *Int J Cancer* 59, 25-32.

Seemayer, T.A., Lagace, R., Schurch, W., and Tremblay, G. (1979). Myofibroblasts in the stroma of invasive and metastatic carcinoma: a possible host response to neoplasia. *Am J Surg Pathol* 3, 525-533.

Semov, A., Moreno, M.J., Onichtchenko, A., Abulrob, A., Ball, M., Ekiel, I., Pietrzynski, G., Stanimirovic, D., and Alakhov, V. (2005). Metastasis-associated protein S100A4 induces angiogenesis through interaction with Annexin II and accelerated plasmin formation. *J Biol Chem* 280, 20833-20841.

Shimoda, M., Mellody, K.T., and Orimo, A. (2010). Carcinoma-associated fibroblasts are a rate-limiting determinant for tumour progression. *Semin Cell Dev Biol* 21, 19-25.

Shojaei, F. (2012). Anti-angiogenesis therapy in cancer: Current challenges and future perspectives. *Cancer Lett.*

Shoyab, M., McDonald, V.L., Bradley, J.G., and Todaro, G.J. (1988). Amphiregulin: a bifunctional growth-modulating glycoprotein produced by the phorbol 12-myristate 13-acetate-treated human breast adenocarcinoma cell line MCF-7. *Proc Natl Acad Sci U S A* 85, 6528-6532.

Shoyab, M., Plowman, G.D., McDonald, V.L., Bradley, J.G., and Todaro, G.J. (1989). Structure and function of human amphiregulin: a member of the epidermal growth factor family. *Science* 243, 1074-1076.

Sica, A., Wang, J.M., Colotta, F., Dejana, E., Mantovani, A., Oppenheim, J.J., Larsen, C.G., Zachariae, C.O., and Matsushima, K. (1990). Monocyte chemotactic and activating factor gene expression induced in endothelial cells by IL-1 and tumor necrosis factor. *J Immunol* 144, 3034-3038.

Sieweke, M.H., Thompson, N.L., Sporn, M.B., and Bissell, M.J. (1990). Mediation of wound-related Rous sarcoma virus tumorigenesis by TGF-beta. *Science* 248, 1656-1660.

Silvy, M., Giusti, C., Martin, P.M., and Berthois, Y. (2001). Differential regulation of cell proliferation and protease secretion by epidermal growth factor and amphiregulin in tumoral versus normal breast epithelial cells. *Br J Cancer* 84, 936-945.

Simian, M., Hirai, Y., Navre, M., Werb, Z., Lochter, A., and Bissell, M.J. (2001). The interplay of matrix metalloproteinases, morphogens and growth factors is necessary for branching of mammary epithelial cells. *Development* 128, 3117-3131.

Simpson, P.T., Reis-Filho, J.S., Gale, T., and Lakhani, S.R. (2005). Molecular evolution of breast cancer. *J Pathol* 205, 248-254.

Slamon, D.J., Godolphin, W., Jones, L.A., Holt, J.A., Wong, S.G., Keith, D.E., Levin, W.J., Stuart, S.G., Udove, J., Ullrich, A., et al. (1989). Studies of the HER-2/neu proto-oncogene in human breast and ovarian cancer. *Science* 244, 707-712.

Smith, G.M., and Hale, J.H. (1997). Macrophage/Microglia regulation of astrocytic tenascin: synergistic action of transforming growth factor-beta and basic fibroblast growth factor. *J Neurosci* 17, 9624-9633.

Soria, G., Ofri-Shahak, M., Haas, I., Yaal-Hahoshen, N., Leider-Trejo, L., Leibovich-Rivkin, T., Weitzenfeld, P., Meshel, T., Shabtai, E., Gutman, M., et al. (2011). Inflammatory mediators in breast cancer: coordinated expression of TNFalpha & IL-1beta with CCL2 & CCL5 and effects on epithelial-to-mesenchymal transition. *BMC Cancer* 11, 130.

Sorlie, T., Perou, C.M., Tibshirani, R., Aas, T., Geisler, S., Johnsen, H., Hastie, T., Eisen, M.B., van de Rijn, M., Jeffrey, S.S., et al. (2001). Gene expression patterns of breast carcinomas distinguish tumor subclasses with clinical implications. *Proc Natl Acad Sci U S A* 98, 10869-10874.

Sorlie, T., Tibshirani, R., Parker, J., Hastie, T., Marron, J.S., Nobel, A., Deng, S., Johnsen, H., Pesich, R., Geisler, S., et al. (2003). Repeated observation of breast tumor subtypes in independent gene expression data sets. *Proc Natl Acad Sci U S A* 100, 8418-8423.

Sottile, J. (2004). Regulation of angiogenesis by extracellular matrix. *Biochim Biophys Acta* 1654, 13-22.

Sozzani, S., Locati, M., Zhou, D., Rieppi, M., Luini, W., Lamorte, G., Bianchi, G., Polentarutti, N., Allavena, P., and Mantovani, A. (1995). Receptors, signal transduction, and spectrum of action of monocyte chemotactic protein-1 and related chemokines. *J Leukocyte Biol* 57, 788-794.

Steffensen, B., Hakkinen, L., and Larjava, H. (2001). Proteolytic events of wound-healing--coordinated interactions among matrix metalloproteinases (MMPs), integrins, and extracellular matrix molecules. *Crit Rev Oral Biol Med* 12, 373-398.

Sternlicht, M.D., Lochter, A., Sympon, C.J., Huey, B., Rougier, J.P., Gray, J.W., Pinkel, D., Bissell, M.J., and Werb, Z. (1999). The stromal proteinase MMP3/stromelysin-1 promotes mammary carcinogenesis. *Cell* 98, 137-146.

Streicher, K.L., Willmarth, N.E., Garcia, J., Boerner, J.L., Dewey, T.G., and Ethier, S.P. (2007). Activation of a nuclear factor kappaB/interleukin-1 positive feedback loop by amphiregulin in human breast cancer cells. *Mol Cancer Res* 5, 847-861.

Strieter, R.M., Wiggins, R., Phan, S.H., Wharram, B.L., Showell, H.J., Remick, D.G., Chensue, S.W., and Kunkel, S.L. (1989). Monocyte chemotactic protein gene expression by cytokine-treated human fibroblasts and endothelial cells. *Biochem Biophys Res Commun* 162, 694-700.

Stuelten, C.H., DaCosta Byfield, S., Arany, P.R., Karpova, T.S., Stetler-Stevenson, W.G., and Roberts, A.B. (2005). Breast cancer cells induce stromal fibroblasts to express MMP-9 via secretion of TNF-alpha and TGF-beta. *J Cell Sci* 118, 2143-2153.

Tamura, S., Oshima, T., Yoshihara, K., Kanazawa, A., Yamada, T., Inagaki, D., Sato, T., Yamamoto, N., Shiozawa, M., Morinaga, S., et al. (2011). Clinical significance of STC1 gene expression in patients with colorectal cancer. *Anticancer Res* 31, 325-329.

Tarin, D., and Croft, C.B. (1969). Ultrastructural features of wound healing in mouse skin. *J Anat* 105, 189-190.

Taub, D.D., Proost, P., Murphy, W.J., Anver, M., Longo, D.L., van Damme, J., and Oppenheim, J.J. (1995). Monocyte chemotactic protein-1 (MCP-1), -2, and -3 are chemotactic for human T lymphocytes. *The Journal of clinical investigation* 95, 1370-1376.

Thelen, M. (2001). Dancing to the tune of chemokines. *Nat Immunol* 2, 129-134.

Tlsty, T.D., and Hein, P.W. (2001). Know thy neighbor: stromal cells can contribute oncogenic signals. *Curr Opin Genet Dev* 11, 54-59.

Todorutiu, C., and Simu, G. (1965). Aspects of the Stroma during Genesis of Experimental Hepatoma Induced by P-Dab. *Oncology* 19, 43-54.

Trimboli, A.J., Cantemir-Stone, C.Z., Li, F., Wallace, J.A., Merchant, A., Creasap, N., Thompson, J.C., Caserta, E., Wang, H., Chong, J.L., et al. (2009). Pten in stromal fibroblasts suppresses mammary epithelial tumours. *Nature* 461, 1084-1091.

Tsai, S.T., Yang, K.Y., Jin, Y.T., Lin, Y.C., Chang, M.T., and Wu, L.W. (2006). Amphiregulin as a tumor promoter for oral squamous cell carcinoma: involvement of cyclooxygenase 2. *Oral Oncol* 42, 381-390.

Tyan, S.W., Kuo, W.H., Huang, C.K., Pan, C.C., Shew, J.Y., Chang, K.J., Lee, E.Y., and Lee, W.H. (2011). Breast cancer cells induce cancer-associated fibroblasts to secrete hepatocyte growth factor to enhance breast tumorigenesis. *PLoS One* 6, e15313.

Ueno, T., Toi, M., Saji, H., Muta, M., Bando, H., Kuroi, K., Koike, M., Inadera, H., and Matsushima, K. (2000). Significance of macrophage chemoattractant protein-1 in macrophage recruitment, angiogenesis, and survival in human breast cancer. *Clin Cancer Res* 6, 3282-3289.

Uguccioni, M., D'Apuzzo, M., Loetscher, M., Dewald, B., and Baggiolini, M. (1995). Actions of the chemotactic cytokines MCP-1, MCP-2, MCP-3, RANTES, MIP-1 alpha and MIP-1 beta on human monocytes. *Eur J Immunol* 25, 64-68.

Valkovic, T., Lucin, K., Krstulja, M., Dobi-Babic, R., and Jonjic, N. (1998). Expression of monocyte chemotactic protein-1 in human invasive ductal breast cancer. *Pathol Res Pract* 194, 335-340.

Van Damme, J., Proost, P., Lenaerts, J.P., and Opdenakker, G. (1992). Structural and functional identification of two human, tumor-derived monocyte chemotactic proteins (MCP-2 and MCP-3) belonging to the chemokine family. *J Exp Med* 176, 59-65.

van de Vijver, M.J., He, Y.D., van't Veer, L.J., Dai, H., Hart, A.A., Voskuil, D.W., Schreiber, G.J., Peterse, J.L., Roberts, C., Marton, M.J., et al. (2002). A gene-expression signature as a predictor of survival in breast cancer. *N Engl J Med* 347, 1999-2009.

van't Veer, L.J., Dai, H., van de Vijver, M.J., He, Y.D., Hart, A.A., Mao, M., Peterse, H.L., van der Kooy, K., Marton, M.J., Witteveen, A.T., et al. (2002). Gene expression profiling predicts clinical outcome of breast cancer. *Nature* 415, 530-536.

Vandamme, J., Proost, P., Put, W., Arens, S., Lenaerts, J.P., Conings, R., Opdenakker, G., Heremans, H., and Billiau, A. (1994). Induction of Monocyte Chemotactic Proteins Mcp-1 and Mcp-2 in Human Fibroblasts and Leukocytes by Cytokines and Cytokine Inducers - Chemical Synthesis of Mcp-2 and Development of a Specific Ria. *J Immunol* 152, 5495-5502.

Varmus, H.E., Stavnezer, J., Medeiros, E., and Bishop, J.M. (1975). Detection and characterization of RNA tumor virus-specific DNA in cells. *Bibl Haematol*, 451-461.

Velazquez, O.C., Snyder, R., Liu, Z.J., Fairman, R.M., and Herlyn, M. (2002). Fibroblast-dependent differentiation of human microvascular endothelial cells into capillary-like 3-dimensional networks. *FASEB journal : official publication of the Federation of American Societies for Experimental Biology* 16, 1316-1318.

Verheul, H.M., and Pinedo, H.M. (2003). Vascular endothelial growth factor and its inhibitors. *Drugs Today (Barc)* 39 Suppl C, 81-93.

Visscher, D.W., Sarkar, F.H., Kasunic, T.C., and Reddy, K.B. (1997). Clinicopathologic analysis of amphiregulin and heregulin immunostaining in breast neoplasia. *Breast Cancer Res Treat* 45, 75-80.

Von Numers, C. (1953). The mode of stroma formation in transplanted mouse carcinoma. *Ann Med Exp Biol Fenn* 31(3), 327-337.

Vrana, J.A., Stang, M.T., Grande, J.P., and Getz, M.J. (1996). Expression of tissue factor in tumor stroma correlates with progression to invasive human breast cancer: paracrine regulation by carcinoma cell-derived members of the transforming growth factor beta family. *Cancer Res* 56, 5063-5070.

Wadlow, R.C., Wittner, B.S., Finley, S.A., Bergquist, H., Upadhyay, R., Finn, S., Loda, M., Mahmood, U., and Ramaswamy, S. (2009). Systems-level modeling of cancer-fibroblast interaction. *PLoS One* 4, e6888.

Wang, C.L., Sun, B.S., Tang, Y., Zhuang, H.Q., and Cao, W.Z. (2009). CCR1 knockdown suppresses human non-small cell lung cancer cell invasion. *J Cancer Res Clin Oncol* 135, 695-701.

Wang, C.S., and Tetu, B. (2002). Stromelysin-3 expression by mammary tumor-associated fibroblasts under in vitro breast cancer cell induction. *Int J Cancer* 99, 792-799.

Wang, T.N., Albo, D., and Tuszynski, G.P. (2002). Fibroblasts promote breast cancer cell invasion by upregulating tumor matrix metalloproteinase-9 production. *Surgery* 132, 220-225.

Weaver, V.M., Petersen, O.W., Wang, F., Larabell, C.A., Briand, P., Damsky, C., and Bissell, M.J. (1997). Reversion of the malignant phenotype of human breast cells in three-dimensional culture and in vivo by integrin blocking antibodies. *J Cell Biol* 137, 231-245.

Weber, M., Uguccioni, M., Ochensberger, B., Baggiolini, M., Clark-Lewis, I., and Dahinden, C.A. (1995). Monocyte chemotactic protein MCP-2 activates human basophil and eosinophil leukocytes similar to MCP-3. *J Immunol* 154, 4166-4172.

Willmarth, N.E., and Ethier, S.P. (2008). Amphiregulin as a novel target for breast cancer therapy. *J Mammary Gland Biol Neoplasia* 13, 171-179.

Yasumoto, K., Yamada, T., Kawashima, A., Wang, W., Li, Q., Donev, I.S., Tacheuchi, S., Mouri, H., Yamashita, K., Ohtsubo, K., et al. (2011). The EGFR ligands amphiregulin and heparin-binding egf-like growth factor promote peritoneal carcinomatosis in CXCR4-expressing gastric cancer. *Clin Cancer Res* 17, 3619-3630.

Zeisberg, E.M., Potenta, S., Xie, L., Zeisberg, M., and Kalluri, R. (2007). Discovery of endothelial to mesenchymal transition as a source for carcinoma-associated fibroblasts. *Cancer Res* 67, 10123-10128.

Zeisberg, M., Strutz, F., and Muller, G.A. (2000). Role of fibroblast activation in inducing interstitial fibrosis. *J Nephrol* 13 Suppl 3, S111-120.

Zhang, J., Patel, L., and Pienta, K.J. (2010). CC chemokine ligand 2 (CCL2) promotes prostate cancer tumorigenesis and metastasis. *Cytokine Growth Factor Rev* 21, 41-48.

Zhang, W., Matrisian, L.M., Holmbeck, K., Vick, C.C., and Rosenthal, E.L. (2006). Fibroblast-derived MT1-MMP promotes tumor progression in vitro and in vivo. *BMC Cancer* 6, 52.

Zhu, C.Q., Popova, S.N., Brown, E.R., Barsyte-Lovejoy, D., Navab, R., Shih, W., Li, M., Lu, M., Jurisica, I., Penn, L.Z., et al. (2007). Integrin alpha 11 regulates IGF2 expression in fibroblasts to enhance tumorigenicity of human non-small-cell lung cancer cells. *Proc Natl Acad Sci U S A* 104, 11754-11759.

Zigrino, P., Kuhn, I., Bauerle, T., Zamek, J., Fox, J.W., Neumann, S., Licht, A., Schorpp-Kistner, M., Angel, P., and Mauch, C. (2009). Stromal expression of MMP-13 is required for melanoma invasion and metastasis. *J Invest Dermatol* 129, 2686-2693.

Zlotnik, A., Burkhardt, A.M., and Homey, B. (2011). Homeostatic chemokine receptors and organ-specific metastasis. *Nat Rev Immunol* 11, 597-606.

Zutter, M.M., Painter, A.A., Stataz, W.D., and Tsung, Y.L. (1995). Regulation of alpha 2 integrin gene expression in cells with megakaryocytic features: a common theme of three necessary elements. *Blood* 86, 3006-3014.

Appendix

Role of Stanniocalcin-1 (STC-1) in breast tumor-stromal fibroblast interaction

Introduction

Stanniocalcin-1 (STC1) is a glycoprotein hormone functioning as a regulator of calcium homeostasis (Nelson et al., 1996). Mammalian STC1 maps to Chromosome 8p and described has 247 amino acids producing a ~50Kd glycoprotein (Chang et al., 1995; Paciga et al., 2005). STC1 is expressed in kidneys, prostate, ovaries and bones (Chang et al., 2003) mediating functions like wound healing, chemotaxis, angiogenesis and protection from apoptosis (Filvaroff et al., 2002; Kahn et al., 2000; Kanellis et al., 2004; McCudden et al., 2002; Yoshiko and Aubin, 2004; Zhang et al., 2000).

STC1 was implicated in cancer progression because of elevated levels of STC1 in hepatocellular, breast, ovarian, prostate and colorectal cancers (Chang et al., 2003; Tamura et al., 2011). Liu and colleagues conducted the first detailed study into the functional roles of STC1 in ovarian carcinoma. The authors concluded that STC1 transformed immortalized ovarian surface cells resulting in the formation of tumors in mice and played a role in the cell (Liu et al., 2010). Other studies have identified STC1 expression being regulated positively by BRCA1 and negatively by hypoxia, Sp1 and PKC α (Chang et al., 2003; Cornmark et al., 2011; Law et al., 2011). STC-1 binds receptors on the plasma membrane though the expression, distribution, identity and mechanism of action of these receptors is debated (Luo et al., 2004; Yeung et al., 2012). STC1 is overexpressed in cancer associated fibroblasts of prostate cancers compared to normal adjacent fibroblasts (Orr et al., 2012). However, it is not clear if STC1 overexpression in CAFs has functional consequences to tumor progression.

I selected STC1 for functional characterization because it is selectively induced in co-cultured, tumor-supportive fibroblasts and also upregulated in primary human stroma. I silenced STC1 expression in HFFF2 tumor-supportive fibroblasts using shRNAs targeting STC1 and used them in co-injection assays with Cal51 breast cancer cell line. Additionally, I treated Cal51 and MDAMB231 cell lines with recombinant STC1 to test its effect on proliferation.

Results

RNAi suppression of STC1 does not restrict the ability of tumor-supportive fibroblasts to promote tumorigenicity

I generated HFFF2 cells stably expressing shRNA targeting STC1 by lentiviral infections. shRNA containing a non-targeting sequence was used as the control. Of the five shRNAs tested, four efficiently reduced STC1 expression below 70% of control (Figure A.1.A). However, 2/4 shRNAs also had adverse effects on HFFF2 cell viability (Figure A.1.B). I used 1.5×10^6 HFFF2 cells stably expressing shRNAs towards STC1 (shSTC1-2 and shSTC1-4) or non-targeting sequence (shN.T) in a co-injection assay with 1×10^6 Cal51 cells in 5-6 week old irradiated female nude mice. Tumor volumes were not significantly different between the experimental and control groups 6 weeks post injections (Figure A.1.C).

Effects of recombinant STC1 on proliferation

STC1 has been shown to increase proliferation in ovarian carcinoma cells (Liu et al., 2010). So I wanted to test if STC1 could promote proliferation or viability in Cal51 and MDAMB231 cells. Doses of up to 500ng/ml did not increase proliferation and viability 72 hours post treatment. In fact, Cal51 cells are significantly less viable in the presence of 25,50,100 and 500ng/ml of STC1 compared to the control (0 ng/ml) (Figure A.1.D)

Discussion

The functional role of STC1 in breast cancer progression is not clear. In this model, silencing STC1 in co-injected tumor-supportive fibroblasts had no effect on tumor volume six weeks post injections. Recombinant STC1 did not increase proliferation of breast cancer cell lines Cal51 and MDAMB231 in agreement with studies (Nguyen et al., 2009). The lack of a functional role for STC1 despite being induced in co-cultured tumor-supportive fibroblasts and in breast cancer stroma is not surprising. A number of molecules are often upregulated during cancer progression without effects on tumor volume (Nielsen et al., 2008). These molecules nevertheless serve as spatial and temporal molecular markers. It is possible that STC1 is in fact functionally important but this particular model system is not suited for its characterization. For example, HFFF2 cells may express STC1 at low basal levels making the relatively robust induction ineffective. Another possibility is that STC1 causes changes to tumor architecture which has no outcome on tumor volume but is important nonetheless. Studies have ranged from detailing crucial roles for STC-1 to showing that it has no functional consequences (Chang et al., 2008; Liu et al., 2010). Using the most appropriate model and physiological context is the key to include or exclude STC-1 as a functional player in breast tumor-fibroblast interactions.

Figure A.1

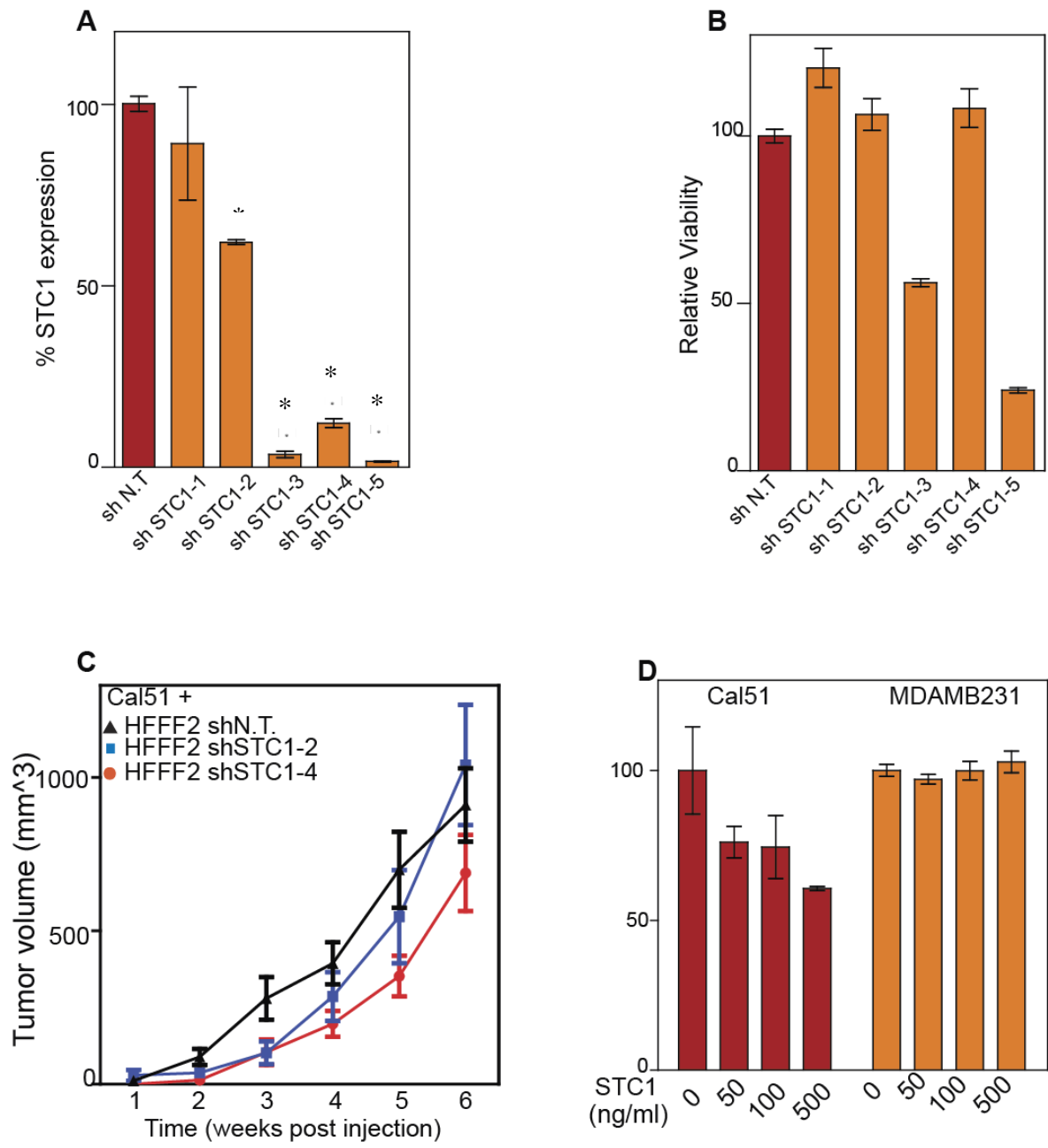


Figure A.1: Fibroblast secreted STC1 does not have a functional role in tumor promoting ability of tumor-supportive fibroblasts

A: qRT-PCR analysis of STC1 knockdown in HFFF2 fibroblasts. STC1 expression in HFFF2 cells expressing either non-target shRNA (shN.T.) or shRNA targeting STC1 (shSTC1-5)) was calculated as a ratio of STC1/GAPDH and expressed as a percentage of shN.T. n= 3, Error bars= +/- SD. Asterisks indicate that the expression of STC1 is significantly different between the control (shN.T.) and the indicated group (shCCL8-1 and shCCL8-2). * p<0.01.

B: Relative viability of HFFF2 fibroblasts expressing shRNA towards STC1 (shSTC1-5) compared to HFFF2 cells expressing non-target shRNA (shN.T) was quantified using a 72-hour MTT assay. n=4; Error bars represent mean +/-SD.

C: Subcutaneous growth of Cal51 breast cancer cells co-injected with HFFF2 cells stably expressing either with control shRNA (shN.T.; black triangles), shRNA targeting STC1 (shSTC1-2; blue squares or shSTC1-4; red circles). Tumor volumes were determined 1-6 weeks after injection. Error represent denote mean ±SEM.

D: Relative viability of Cal51 and MDAMB231 breast cancer cells treated with indicated dose of recombinant STC1 (STC1-0,50,100 or 500 ng/ml) was calculated using MTT assay 72-hour post treatment. Relative viability is expressed as a percentage of the untreated group (0 ng/ml) for each cell line. n=4; Error bars represent mean +/- SD.

References:

- Chang, A.C., Hook, J., Lemckert, F.A., McDonald, M.M., Nguyen, M.A., Hardeman, E.C., Little, D.G., Gunning, P.W., and Reddel, R.R. (2008). The murine stanniocalcin 2 gene is a negative regulator of postnatal growth. *Endocrinology* *149*, 2403-2410.
- Chang, A.C., Janosi, J., Hulsbeek, M., de Jong, D., Jeffrey, K.J., Noble, J.R., and Reddel, R.R. (1995). A novel human cDNA highly homologous to the fish hormone stanniocalcin. *Mol Cell Endocrinol* *112*, 241-247.
- Chang, A.C., Jellinek, D.A., and Reddel, R.R. (2003). Mammalian stanniocalcins and cancer. *Endocr Relat Cancer* *10*, 359-373.
- Cornmark, L., Lonne, G.K., Jogi, A., and Larsson, C. (2011). Protein kinase Calpha suppresses the expression of STC1 in MDA-MB-231 breast cancer cells. *Tumour Biol* *32*, 1023-1030.
- Filvaroff, E.H., Guillet, S., Zlot, C., Bao, M., Ingle, G., Steinmetz, H., Hoeffel, J., Bunting, S., Ross, J., Carano, R.A., *et al.* (2002). Stanniocalcin 1 alters muscle and bone structure and function in transgenic mice. *Endocrinology* *143*, 3681-3690.
- Kahn, J., Mehraban, F., Ingle, G., Xin, X., Bryant, J.E., Vehar, G., Schoenfeld, J., Grimaldi, C.J., Peale, F., Draksharapu, A., *et al.* (2000). Gene expression profiling in an in vitro model of angiogenesis. *Am J Pathol* *156*, 1887-1900.
- Kanellis, J., Bick, R., Garcia, G., Truong, L., Tsao, C.C., Etemadmoghadam, D., Poindexter, B., Feng, L., Johnson, R.J., and Sheikh-Hamad, D. (2004). Stanniocalcin-1, an inhibitor of macrophage chemotaxis and chemokinesis. *Am J Physiol Renal Physiol* *286*, F356-362.
- Law, A.Y., Yeung, B.H., Ching, L.Y., and Wong, C.K. (2011). Sp1 is a transcription repressor to stanniocalcin-1 expression in TSA-treated human colon cancer cells, HT29. *J Cell Biochem* *112*, 2089-2096.
- Liu, G., Yang, G., Chang, B., Mercado-Uribe, I., Huang, M., Zheng, J., Bast, R.C., Lin, S.H., and Liu, J. (2010). Stanniocalcin 1 and ovarian tumorigenesis. *J Natl Cancer Inst* *102*, 812-827.
- Luo, C.W., Kawamura, K., Klein, C., and Hsueh, A.J. (2004). Paracrine regulation of ovarian granulosa cell differentiation by stanniocalcin (STC) 1: mediation through specific STC1 receptors. *Mol Endocrinol* *18*, 2085-2096.

McCudden, C.R., James, K.A., Hasilo, C., and Wagner, G.F. (2002). Characterization of mammalian stanniocalcin receptors. Mitochondrial targeting of ligand and receptor for regulation of cellular metabolism. *J Biol Chem* 277, 45249-45258.

Nelson, A.E., Namkung, H.J., Patava, J., Wilkinson, M.R., Chang, A.C., Reddel, R.R., Robinson, B.G., and Mason, R.S. (1996). Characteristics of tumor cell bioactivity in oncogenic osteomalacia. *Mol Cell Endocrinol* 124, 17-23.

Nguyen, A., Chang, A.C., and Reddel, R.R. (2009). Stanniocalcin-1 acts in a negative feedback loop in the prosurvival ERK1/2 signaling pathway during oxidative stress. *Oncogene* 28, 1982-1992.

Nielsen, B.S., Egeblad, M., Rank, F., Askautrud, H.A., Pennington, C.J., Pedersen, T.X., Christensen, I.J., Edwards, D.R., Werb, Z., and Lund, L.R. (2008). Matrix metalloproteinase 13 is induced in fibroblasts in polyomavirus middle T antigen-driven mammary carcinoma without influencing tumor progression. *PLoS One* 3, e2959.

Orr, B., Riddick, A.C., Stewart, G.D., Anderson, R.A., Franco, O.E., Hayward, S.W., and Thomson, A.A. (2012). Identification of stromally expressed molecules in the prostate by tag-profiling of cancer-associated fibroblasts, normal fibroblasts and fetal prostate. *Oncogene* 31, 1130-1142.

Paciga, M., James, K., Gillespie, J.R., and Wagner, G.F. (2005). Evidence for cross-talk between stanniocalcins. *Can J Physiol Pharmacol* 83, 953-956.

Tamura, S., Oshima, T., Yoshihara, K., Kanazawa, A., Yamada, T., Inagaki, D., Sato, T., Yamamoto, N., Shiozawa, M., Morinaga, S., *et al.* (2011). Clinical significance of STC1 gene expression in patients with colorectal cancer. *Anticancer Res* 31, 325-329.

Yeung, B.H., Law, A.Y., and Wong, C.K. (2012). Evolution and roles of stanniocalcin. *Mol Cell Endocrinol* 349, 272-280.

Yoshiko, Y., and Aubin, J.E. (2004). Stanniocalcin 1 as a pleiotropic factor in mammals. *Peptides* 25, 1663-1669.

Zhang, K., Lindsberg, P.J., Tatlisumak, T., Kaste, M., Olsen, H.S., and Andersson, L.C. (2000). Stanniocalcin: A molecular guard of neurons during cerebral ischemia. *Proc Natl Acad Sci U S A* 97, 3637-3642.